

COMPARISON OF NUMERICAL AND HYDRAULIC
OCEANOGRAPHIC PREDICTION MODELS

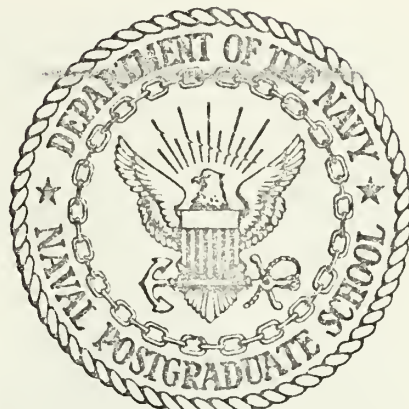
Leopoldo Salas Römer

Library

Naval Postgraduate School
Monterey, California 93940

NAVAL POSTGRADUATE SCHOOL

Monterey, California



THESIS

COMPARISON OF NUMERICAL AND HYDRAULIC
OCEANOGRAPHIC PREDICTION MODELS

by

Leopoldo Salas Römer

Thesis Advisor:

E. B. Thornton

September 1972

Approved for public release; distribution unlimited.

T152287

Comparison of Numerical and Hydraulic
Oceanographic Prediction Models

by

Leopoldo Salas Römer
Commander, Venezuelan Navy

Submitted in partial fulfillment of the
requirements for the degree of

MASTER OF SCIENCE IN OCEANOGRAPHY

from the

NAVAL POSTGRADUATE SCHOOL
September 1972

ABSTRACT

The Hydro-Numerical Prediction Model developed by Hansen is applied to San Diego Bay, and the results compared both with the hydraulic model and the real data obtained by field measurements. This allows one of the few good comparisons between numerical and hydraulic models for the prediction of actual conditions.

The bay was divided into two sections that were run separately in order to obtain the desirable spatial resolution. This division required solving the problems of proper tuning and matching techniques between both portions. The solution involved the addition of an appended pseudo-bay to the first section of the model in order to compensate for the correct tidal prism. The effects of a proposed second open entrance in the southern part of the bay were studied. This resulted in an increase of flushing in the southern portion of the bay but caused the currents in the center of the bay to be small which decreased dispersion in the central portion of the bay. In general, both models produced similar and reliable results, but there was a considerable reduction of cost and time with the numerical model.

TABLE OF CONTENTS

I.	INTRODUCTION -----	11
A.	REVIEW -----	11
B.	OBJECTIVES -----	12
II.	HYDRAULIC MODEL OF SAN DIEGO BAY -----	14
A.	DESCRIPTION OF SAN DIEGO BAY -----	14
B.	PURPOSE OF THE U.S. CORPS OF ENGINEERS MODEL STUDY -----	16
C.	THE HYDRAULIC MODEL -----	16
D.	RESULTS OF THE HYDRAULIC MODEL -----	21
III.	THE HANSEN HYDRODYNAMICAL-NUMERICAL MODEL -----	27
A.	SELECTION OF THE GRID -----	35
B.	TIDE INPUT IN THE MODEL (1) -----	37
C.	ADDITION OF AN APPENDED PSEUDO-BAY-----	40
D.	MODEL (2) -----	54
E.	MODEL (3) -----	63
IV.	MERITS OF HYDRAULIC AND NUMERICAL MODELS -----	79
V.	CONCLUSIONS -----	83
	APPENDIX A. NUMERICAL PROGRAMS -----	87
	BIBLIOGRAPHY -----	133
	INITIAL DISTRIBUTION LIST -----	135
	FORM DD 1473 -----	140

LIST OF FIGURES

1.	SAN DIEGO BAY -----	15
2-1.	HEIGHT IN THE PROTOTYPE AND IN THE HYDRAULIC MODEL -----	23
2.	A. CURRENT AT A-2 U.S. CORPS OF ENGINEER RESULTS -	25
	B. CUURENT AT B-2 U.S. CORPS OF ENGINEER RESULTS -	25
3.	A. CURRENT AT C-2 U.S. CORPS OF ENGINEER RESULTS -	26
	B. CURRENT AT D-2 U.S. CORPS OF ENGINEER RESULTS -	26
4.	A. SCHEME OF THE GRID NET -----	33
	B. COMPUTATION GRID -----	33
5.	A. INPUT BOUNDARY AND FREE BOUNDARY WITHOUT CONTINUATION -----	39
	B. LEVELING OF THE EDGES (LUBRICATED WALL) AT BOUNDARIES -----	39
	C. CONTINUATION OF CURRENT AT THE FREE OPEN BOUNDARY WITH THE GRADIENT CORRECTED BY A CONSTANT -----	39
6.	A. VALUES OF Z ALONG MODEL (1) FOR DIFFERENT CONSTANTS IN THE CONTINUATION OF THE FREE BOUNDARY AFTER 1 HOUR OF REAL TIME -----	41
7.	VALUES OF VELOCITY AT M-3 AND N-45 TO 53 IN THE FREE OPEN BOUNDARY FOR DIFFERENT CONSTANTS IN THE CONTINUATION AFTER 1 HOUR OF REAL TIME -----	41
8.	APPENDED AREAS IN MODEL (1) -----	42
9.	CIRCULATION IN MODEL (1) WITH THE APPENDED AREAS --	43
10.	A. HEIGHT AT NAVY PIER MODEL (1) FOR DIFFERENT APPENDED AREAS -----	45
	B. HEIGHT AT PIER N. 2 MODEL (1) FOR DIFFERENT APPENDED AREAS -----	45
11.	A. CURRENT AT A-2 MODEL (1) FOR DIFFERENT APPENDED AREAS -----	46

B.	CURRENT AT C-2 MODEL (1) FOR DIFFERENT APPENDED AREAS -----	46
12.	A. VOLUME TRANSPORT IN SECTION AA1 MODEL (1) -----	47
	B. VOLUME TRANSPORT IN SECTION AA2 MODEL (1) -----	47
13.	A. CURRENT AT A-2 MODEL (1) -----	48
	B. CURRENT AT B-1 MODEL (1) -----	48
14.	A. CURRENT AT C-2 MODEL (1) -----	49
	B. NET VOLUME TRANSPORT MODEL (1) -----	49
15.	A. HEIGHT AT NAVY PIER MODEL (1) -----	50
	B. HEIGHT AT PIER N. 2 MODEL (1) -----	50
16.	CURRENT DISTRIBUTION IN MODEL (1) AT TIME = 0 Hr ---	51
17.	CURRENT DISTRIBUTION IN MODEL (1) AT TIME = 3 Hr ---	52
18.	CURRENT DISTRIBUTION IN MODEL (1) AT TIME = 9 Hr ---	53
19.	A. CURRENT AT C-2 MODEL (2) FOR DIFFERENT VALUES OF R -----	55
	B. CURRENT AT D-2 MODEL (2) FOR DIFFERENT VALUES OF R -----	55
20.	A. HEIGHT AT PIER N. 2 MODEL (2) FOR DIFFERENT VALUES OF R -----	56
	B. HEIGHT AT SOUTH BAY MODEL (2) FOR DIFFERENT VALUES OF R -----	56
20-1.	ENERGY DENSITY SPECTRUM -----	58
21.	A. CURRENT AT C-2 FOR DIFFERENT MINIMUM DEPTHS -----	60
	B. HEIGHT AT PIER N. 2 FOR DIFFERENT MINIMUM DEPTHS -----	60
22.	A. CURRENT AT C-2 MODEL (2) -----	61
	B. CURRENT AT D-2 MODEL (2) -----	61
23.	A. HEIGHT AT PIER N. 2 MODEL (2) -----	62
	B. HEIGHT AT SOUTH BAY MODEL (2) -----	62

24.	CURRENT DISTRIBUTION IN MODEL (2) AT TIME = 3 Hr --	64
25.	CURRENT DISTRIBUTION IN MODEL (2) AT TIME = 9 Hr --	65
26.	CURRENT DISTRIBUTION IN MODELS (1) and (2) AT TIME = 9 Hr -----	66
27.	CURRENT DISTRIBUTION IN MODELS (1) and (2) AT TIME = 3 Hr -----	67
28.	CURRENT DISTRIBUTION IN MODELS (1) and (2) AT TIME = 15 Hr -----	68
29.	CURRENT DISTRIBUTION HYDRAULIC MODEL (BASE TEST) AT TIME = 12 Hr -----	70
30.	CURRENT DISTRIBUTION HYDRAULIC MODEL (BASE TEST) AT TIME = 18 Hr -----	71
31.	A. CURRENT AT C-2 MODEL (3) -----	72
	B. CURRENT AT D-2 MODEL (3) -----	72
32.	A. CURRENT AT CROWN CAVE MODEL (3) -----	73
	B. HEIGHT AT SOUTH BAY MODEL (3) -----	73
33.	NET VOLUME TRANSPORT MODEL (3) -----	74
34.	CURRENT DISTRIBUTION MODEL (3) -----	75
35.	CURRENT DISTRIBUTION MODEL (3) -----	76
36.	CURRENT DISTRIBUTION HYDRAULIC MODEL (PROPOSED SECOND ENTRANCE) AT TIME = 12 Hr -----	77
37.	CURRENT DISTRIBUTION HYDRAULIC MODEL (PROPOSED SECOND ENTRANCE) AT TIME = 18 Hr -----	78

TABLE OF SYMBOLS AND ABBREVIATIONS

c	Phase wave speed
c_m	Velocity in the model
c_p	Velocity in the prototype
d	Total difference
F	Friction force
f	Coriolis parameter
F_r	Froude number
g	Acceleration of gravity
g_m	Gravity in the model
g_p	Gravity in the prototype
H	Total depth ($h + \eta$)
h	Depth of the water at mean sea level
h_m	Depth in the model
h_p	Depth in the prototype
HTU	Depth at U and V grid points
HTV	Depth at V grid points
HTZ	Depth at Z grid points
J	Dimensionless constant
K	Coefficient of horizontal kinematic eddy viscosity
\vec{k}	Vertical unit vector
km	Kilometer
L	Characteristic length
L_m	Characteristic length in the model
L_p	Characteristic length in the prototype

ℓ	Length of mesh
M,N	Grid co-ordinates (also m,n)
m	Meter
cm	Centimeter
MEH NEH	Near border grid points
p	Hydrostatic pressure
R	Bottom roughness coefficient
R_g	Gravity ratio. Gravity scale
R_c	Velocity ratio. Velocity scale
R_h	Depth ratio. Vertical scale
R_L	Length ratio. Horizontal scale
R_t	Time ratio. Time scale
R_{vd}	Discharge ratio. Discharge scale
R_v	Volume ratio. Volume scale
r	Coefficient of friction
t	Time
u,v	Components of horizontal velocity
\vec{V}	Total velocity vector
V_c	Characteristic velocity
\bar{V}, \bar{U}	Mean u and v components
$W()$	Wind speed component
X,Y	Space co-ordinates
Z,U,V	Grid points
α	Smoothing parameter
β	$1 - \alpha$

δ	Partial difference
γ	Specific weight
λ	Drag coefficient
η	Sea level anomaly
ρ	Density of the fluid
τ	Wind stress
$\vec{\Omega}$	Earth angular velocity
∇	$\frac{\partial}{\partial x} + \frac{\partial}{\partial y}$
τ^b	Bottom stress
Δ	Difference

ACKNOWLEDGEMENTS

I wish to express my sincere thanks to everyone who has assisted in the preparation of this study. In particular, I extend my gratitude to Dr. T. Laevastu of the Environmental Prediction Research Facility, to Mr. Sheldon Lazanoff of Fleet Numerical Weather Central, and to Miss Sharon Raney of the Computer Center for their helpful suggestions, encouragement, and programming assistance. Finally to Dr. Edward B. Thornton, my thesis advisor, my sincere thanks for his patience, understanding, and constructive criticism that contributed greatly to the completion of this project.

I. INTRODUCTION

A. REVIEW

The study of bays, estuaries and other semi-restricted areas is difficult because these masses of water are subject to constant movement with short time irregular periodicities. The important mechanism driving the circulation in these areas generally is the tide. The water is partially renewed and mixed during each tidal cycle due to the interchange of water between such areas and the ocean. The shape and depth of the area governs the direction and speed of the currents generated during this interchange. The constant flow of water causes a constant state of non-equilibrium of constituents, temperature and potential energy inside the bays or estuaries.

The study of such areas by field observations is extremely laborious requiring large expenditures of manpower and money. Another approach to the solution of the problem is to reproduce the physical characteristics of these areas by the use of hydraulic models. Hydraulic models have been used for many decades and have proven to be a reliable method for studying an area although space and operating problems make them a relatively expensive tool of investigation.

With the advent of high speed computers, the numerical solution of the differential equations used to describe

flow was made possible. Oceans, seas, gulfs and other water masses have been described by the use of this technique. It transforms a physical model into a program which can be modified to simulate different conditions more easily, can be stored for future uses and alterations, is faster and allows solutions to be obtained at reasonable cost.

The U. S. Army Corps of Engineers made a study of San Diego Bay by means of a hydraulic model based on field measurements made in early 1967. The results have been reported in a Technical Report [10] and published in a paper [1] by the U. S. Corps of Engineers.

The Hydro-Numerical Prediction Model developed by Hansen is applied to San Diego Bay, and the results compared both with the hydraulic model and the data obtained by field measurements. This allows one of the few good comparisons between numerical and hydraulic models for the prediction of actual conditions.

B. OBJECTIVES

The objective of this thesis is to reproduce by means of the Hansen hydrodynamic-numerical model the existing conditions in San Diego Bay and compare them with conditions produced in the hydraulic model operated by the U. S. Corps of Engineers. This comparison will result in a proper evaluation of the merits and limitations of both models.

The division of the bay into two separate models is attempted in order to obtain comparable resolution in the numerical model. This division requires solving problems in the method of running numerical models in series and of transferring boundary conditions from one section to another.

II. HYDRAULIC MODEL OF SAN DIEGO BAY

A. DESCRIPTION OF SAN DIEGO BAY

San Diego Bay is located on the southern coast of California, U.S.A. The bay is long, curved, has an area of approximately 90 sq. km. and a maximum width of 3.1 km. [Fig. 1]. It is connected with the ocean by the narrow Zuniga Channel at its northern end.

The inflow of fresh water can be considered negligible except during local heavy rainfall. The circulation of the entire bay is driven by the tide at its unique entrance. The tidal circulation can be perturbed by local wind conditions.

The tide is of the mixed type with a period of 24.83 hours and maximum range of about 1.89 meters. Field measurements indicate that tidal variations become larger in the bay increasing to 1.98 meters at the center portion of the bay and 2.1 meters near the southern end. Currents have a maximum speed of about 0.7 meters/second in Zuiga Channel.

A channel is maintained for navigation starting at Zuniga Channel and continuing throughout San Diego Bay. The channel depth is 12.8 meters below MLLW from the ocean to the vicinity of the South Bay gage. Other channels of minor importance exist in the southern portion of the bay.

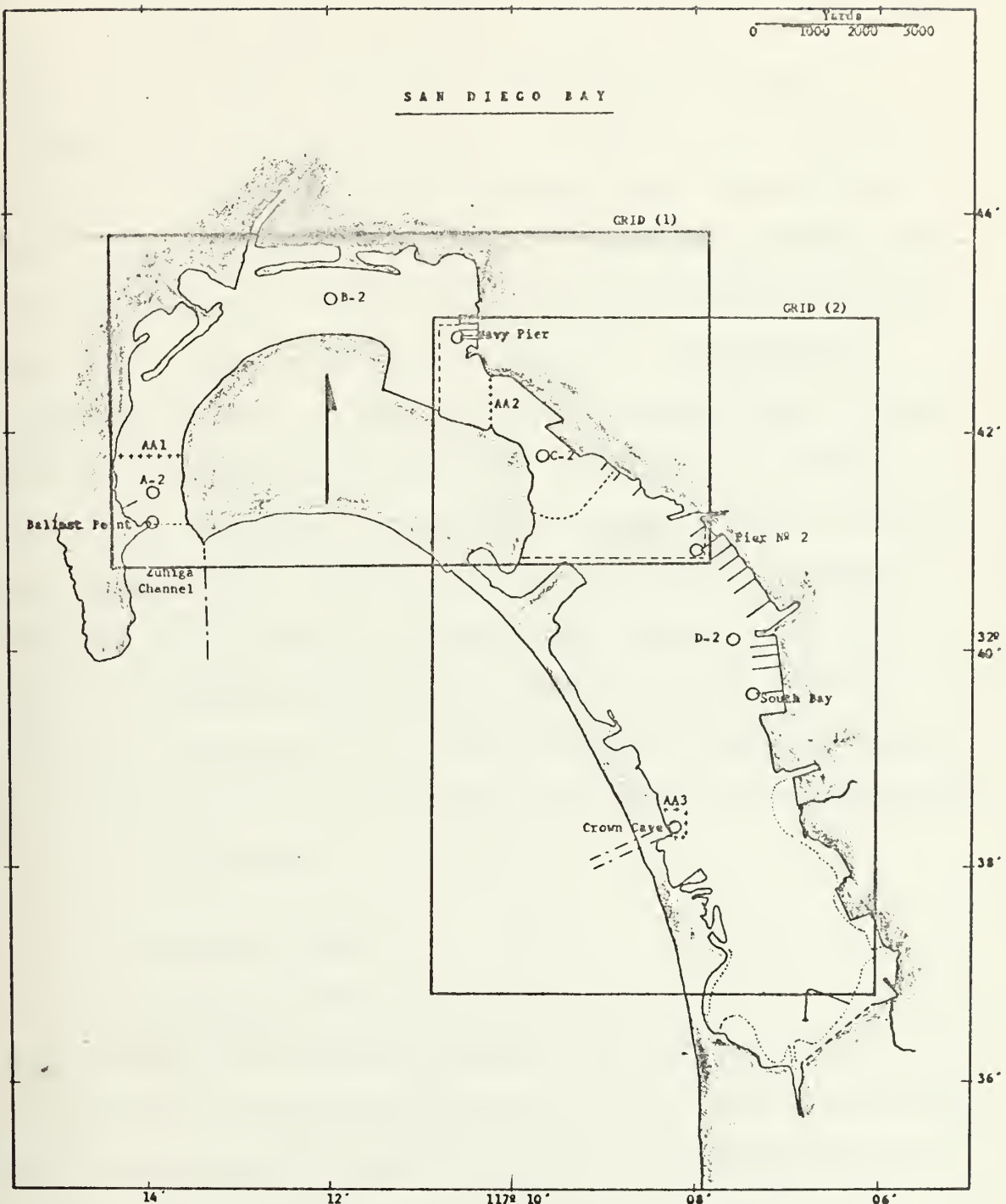


FIGURE 1

B. PURPOSE OF THE U.S. CORPS OF ENGINEERS MODEL STUDY

The natural shape of San Diego Bay and its only entrance at the northern end, its use as a Naval Base, and the influence of a large community surrounding the Bay, have brought into consideration the construction of a second navigation entrance somewhere along Silver Strand Beach. This second entrance is expected to cause decreasing ship traffic throughout Zuniga Channel and increasing flushing rate of the Bay, possibly improving the environmental conditions within the bay. A major consideration in evaluating the overall benefits of a second entrance depend heavily on assessing the extent to which it would increase the flushing rate. These effects could not be computed reliably by the available analytical methods [10], so a physical hydraulic model of the bay, in which several suggested locations for a second entrance could be tested, was constructed to investigate the effects of each proposed location, in detail.

C. THE HYDRAULIC MODEL

The dominant forces in rivers, narrow estuaries and some lakes, are pressure gradient forces driving circulations which are opposed by friction [12]. In large scales of circulations, the opposing forces are combinations of friction and Coriolis force, or Coriolis force alone.

Similarity can be considered as being graded from geometrical through kinematic to dynamic in the attempt to

reproduce the existing conditions in a scale model. A model has geometric similarity if the ratios of all homologous dimensions are equal. The model is said to have kinematic similarity if the paths and patterns of motion are geometrically similar to those of homologous occurrences in the prototype, and the ratios of homologous velocities are equal at all times. Dynamic similarity is achieved when the ratios of homologous masses and forces affecting motion are equal at all times. Complete dynamical similarity is difficult to achieve in fluid models and, kinematic similarity, of necessity, involves elements of dynamic similarity.

The general equation of motion can be written in the form:

$$\rho \frac{d\vec{V}}{dt} = -\rho 2\vec{\Omega} \times \vec{V} - \nabla p + \rho \vec{g} + F$$

Where:

$$\rho \frac{d\vec{V}}{dt} = \text{inertial force}$$

$$\rho 2\vec{\Omega} \times \vec{V} = \text{coriolis force}$$

$$\nabla p = \text{pressure gradient force}$$

$$\rho \vec{g} = \text{gravity force}$$

$$F = \text{friction force}$$

Each term of the equations of motion represents the forces present in a prototype and what is to be represented

in a model. Since the totality of forces cannot be easily reproduced in hydrodynamic models, a few important terms are usually singled out.

In scaling a model, each quantity and dimension of those particular terms of the equation of motion used to describe a flow must be reduced to the model scale. Dimensionless ratios of terms are used to achieve correct model scales. The numerical value of the dimensional ratio must be the same for the model as for the prototype for similiarity to prevail.

Several dimensionless ratios of terms are common to oceanographic modeling, and each one is used depending on the characteristics of the flow in the prototype. The Froude number is generally used in models of estuaries because it involve the ratio of inertial to gravity forces. These forces are, with friction, the dominant forces. The direction of flow is primarily down the gradient of pressure.

The Froude number is defined as:

$$Fr = \frac{\text{inertial term}}{\text{gravitational term}} = \frac{V_c}{(L\gamma/\rho)^{1/2}}$$

Where:

V_c = characteristic velocity

L = characteristic length

γ = specific weight

ρ = fluid density

As a preliminary step in scaling a phenomenon down to model size, it is useful to construct a ratio of units which by convention is:

$$R = \frac{A_m}{A_p}$$

where A_m is a number representing the dimensions of a certain property of the model and A_p the dimensions of the homologous property in the prototype.

The length ratio is fixed first in order to match the available space or equipment. The numerical value of each dimensionless group constant can be held altering the ratios of the other units included in a dimensionless group. By these procedures, time and other unit dimensions of other related properties may have to be altered to permit the fluid motion in the model to be regarded as behaving in the same physical manner as that in the prototype.

The ratio of inertial (velocity and length) and gravity is of concern for the Froude Number. Shallow-water gravity waves, such as tides, propagate at a speed $C = \sqrt{gh}$. The velocity ratio (R_c) is satisfied using the length ratio (R_L), where

$$R_c = \frac{C_m}{C_p} = \sqrt{\frac{g_m h_m}{g_p h_p}} = \sqrt{R_g R_h} \doteq \sqrt{R_h}$$

which assumes that the gravity ratio (R_g) is one. Therefore, the length ratio and velocity ratio are left as adjustable parameters

$$R_c = \sqrt{R_h} = \frac{R_L}{R_t}$$

It can be seen from this equation that R_t shortens with increasing R_h and lengthens with increasing R_L .

A distinction between the vertical length (h) and the horizontal length (L) is often made. If the Froude model is geometrically similar to its prototype, $R_h = R_L$.

The vertical scale (R_h) generally must be chosen so that the least depth of water in which the flow is to be studied is approximately one cm. to prevent capillary effects from being important. Then, it may be necessary to depart from similarity by distorting vertical dimensions such that $R_h > R_L$. One is led to a choice of scales by a path which touches first the minimum depth requirement and then an adjustment of the R_L and R_t such that either one becomes constant, leaving the others to be adjusted. The R_t (time ratio) is usually the most flexible parameter available and determines the frequencies of the simulated tides.

The effects of wind stress on the circulation in estuaries and bays are often important and sometimes dominate the tide. To scale it in a model requires more knowledge

of the dynamics of momentum transfer across the air-sea interface than is now available. Empirical procedures must be made to suffice.

For the U.S. Corps of Engineers hydraulic model, the following characteristics and scales were used:

Area: 280 sq. km.

Horizontal scale (R_L) = 1:500

Vertical scale (R_h) = 1:100

Velocity scale (R_c) = 1:10

Time scale (R_t) = 1:50

Discharge scale (R_{vd}) = 1:500 000

Volume scale (R_v) = 1:25 000 000

Physical dimensions = 35 x 40 meters

D. RESULTS OF THE HYDRAULIC MODEL

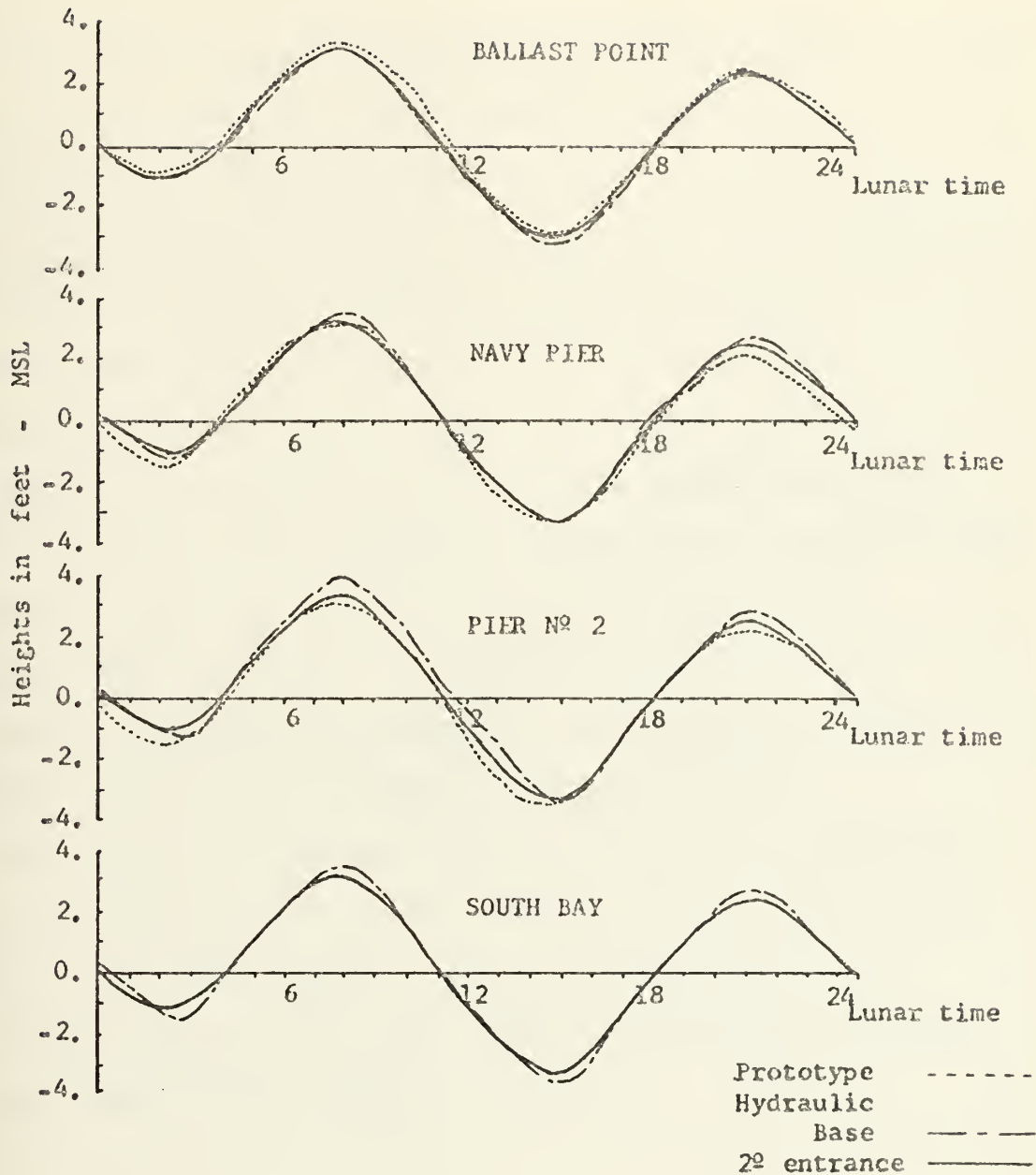
The type of flow being studied determines the predominant forces to consider for dynamic similarity. The San Diego Bay model used a Froude number scaling criteria. After determining the dynamic scaling, a hydraulic model is constructed to match the scaled geometry of the prototype. After reproducing the geometry as closely as possible, kinematic similarity must be obtained. This is accomplished by matching the hydraulic head and flow patterns at various locations in the model over the tidal cycle. This matching is generally accomplished by using roughness elements which can consist of concrete blocks or metal strips. The roughness elements have the effect of increasing turbulence and

changing mean flow patterns. This is a rather laborious and tedious procedure and usually is the most time consuming aspect of hydraulic model building. After the kinematic similarity is satisfactorily accomplished, the model is presumed to be calibrated.

Tests of existing conditions were made under carefully controlled conditions of tides, currents, and simulated pollution input [1]. The results of these calibration tests, called Base Tests, were used to evaluate the effects of navigation openings. Thus, any differences noted during the tests of the proposed second entrances were attributed to influences of the plan being tested and not to errors in the construction of the model.

The wind conditions on the day of observations can introduce large modifications to the normal surface and current characteristics in a bay such as San Diego Bay. Differences from day to day in the values of a mixed tide make a one-day observation a non-periodic function. Therefore, modifications of the field measurements were introduced in order to make them periodic and comparable to a non-wind situation.

The effects of the south entrance on tides throughout the bay are shown by comparative tide curves for measured, base and planned conditions in figure 2-1. The second entrance caused a reduction in the tide range at the southern



HEIGHTS IN THE PROTOTYPE AND IN
THE HYDRAULIC MODEL

FIGURE 2-1

end of the bay by lowering high water and raising low water. At the south bay gage, the reduction in tide range was about 15 cm.

The effects of the second entrance on mid-depth current velocity are shown in figures 2 and 3. The opening reduced the maximum mid-depth current velocities at all stations on gauges "A" through "D" by 15 to 75 cm./sec. The flushing of the southern portion of the bay became governed by the new entrance and there seemed to be little interchange of water between the northern and southern portion of the bay with the area in the vicinity of Pier No. 2 gauge having very small currents. Under those new conditions, the entire bay appears to have two completely different circulation systems driven by tides at Zuniga Channel and at the second entrance. The flushing appears to be increased in the southern portion by including a second entrance.

The pictorial representations of the flow in the bay under both conditions [1] are shown in figures 29, 30, 36 and 37. In these figures, the flow is represented at different stages of the tide, and its intensity is scaled by the length of the lines.

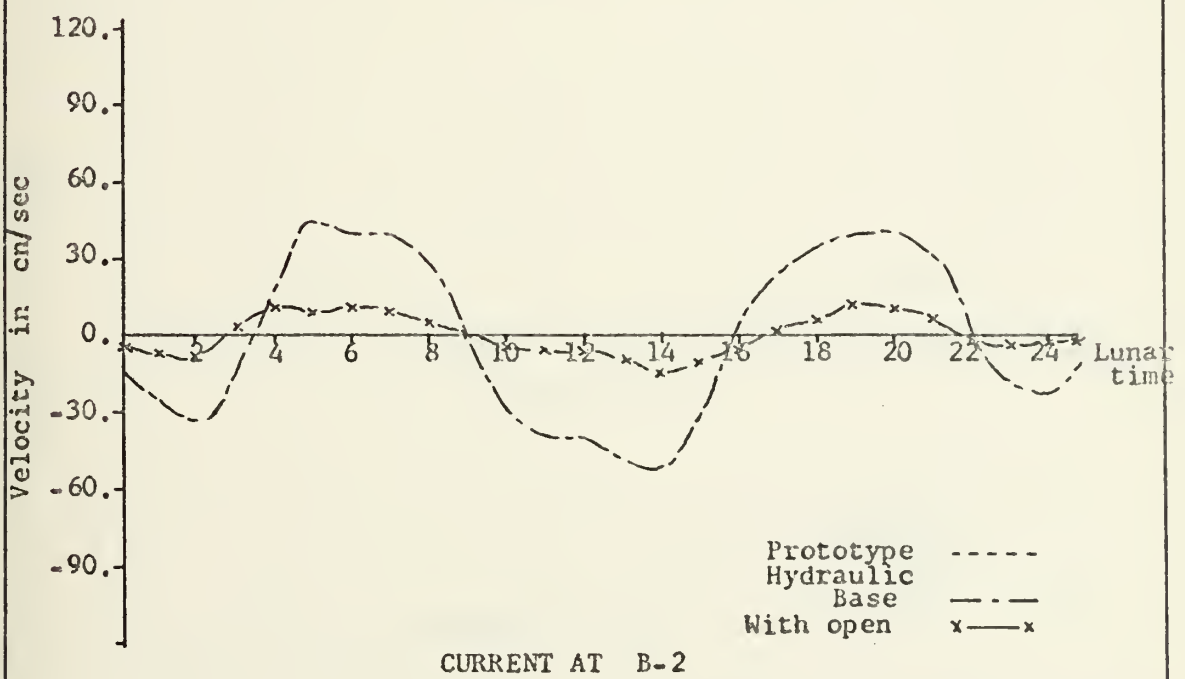
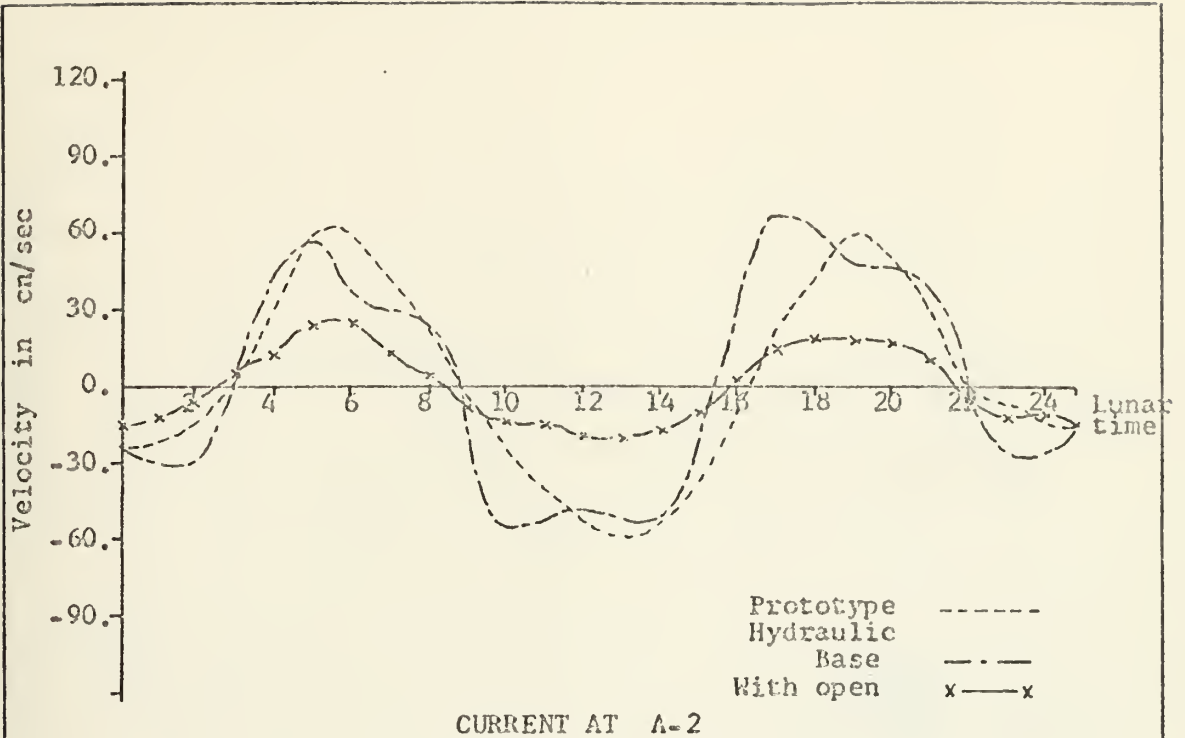


FIGURE 2

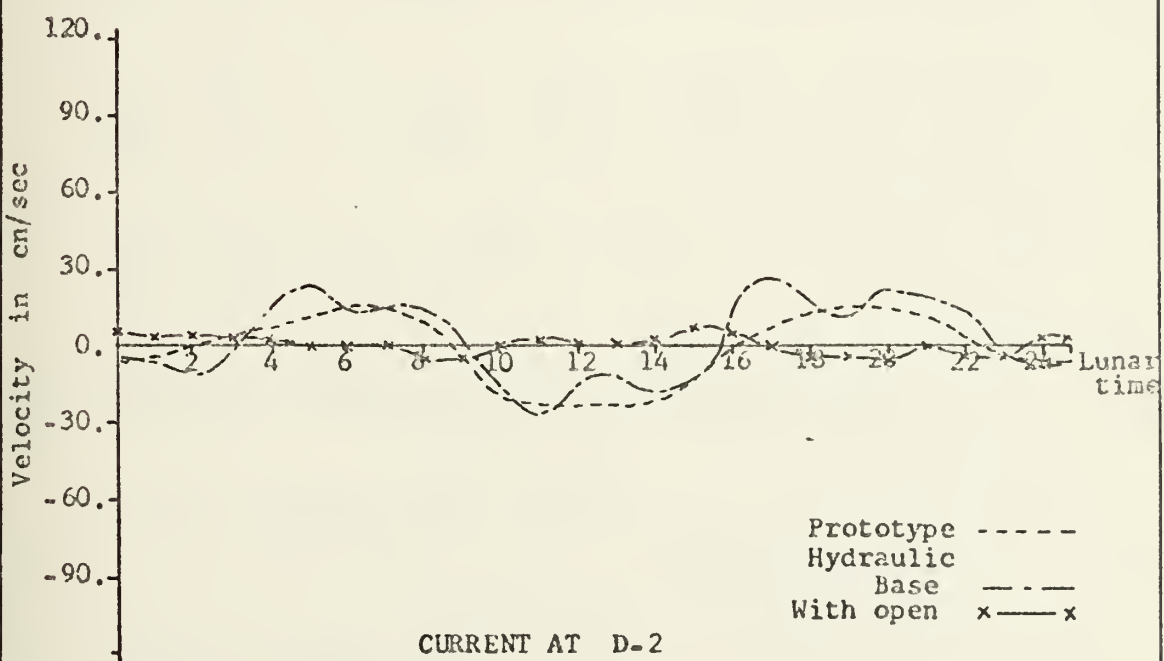
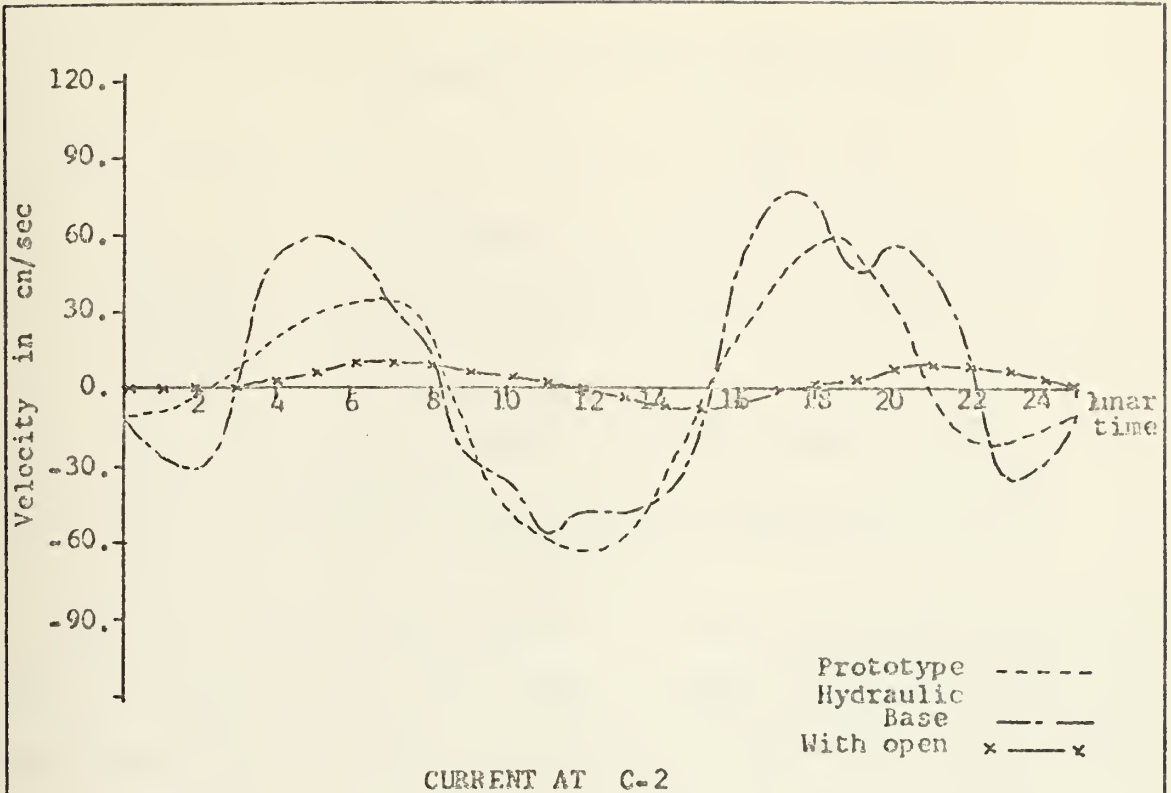


FIGURE 3

III. THE HANSEN HYDRODYNAMICAL MODEL

The assumptions of the numerical model are:

1. The fluid is homogeneous and incompressible.
2. Pressure is hydrostatic and thus, the changes in pressure are due solely to changes in water surface elevation.
3. Advection terms are ignored.
4. The fluid is in hydrostatic equilibrium in the vertical direction.
5. The geographical and vertical variations of the Coriolis force are neglected.

Applying these assumptions to the equations of conservation of momentum and mass, basic equations are obtained for the single-layer model developed by Hansen [6]. Horizontal momentum equations are integrated over depth to give

$$\frac{\partial u}{\partial t} - fv = -g \frac{\partial \eta}{\partial x} + K \nabla^2 u - \tau^b(x) + \tau(x)$$

$$\frac{\partial v}{\partial t} + fu = -g \frac{\partial \eta}{\partial y} + K \nabla^2 v - \tau^b(y) + \tau(y)$$

$$\frac{\partial \eta}{\partial t} + \frac{\partial}{\partial x} (Hu) + \frac{\partial}{\partial y} (Hv) = 0.$$

The wind stress components are represented by

$$\tau(x) = \frac{\lambda}{H} w_x \sqrt{w_x^2 + w_y^2},$$

$$\tau(y) = \frac{\lambda}{H} w_y \sqrt{w_x^2 + w_y^2}$$

and the bottom stress components are represented by

$$\tau^b(x) = \frac{r}{H} u \sqrt{u^2 + v^2} \quad \text{and}$$

$$\tau^b(y) = \frac{r}{H} v \sqrt{u^2 + v^2} .$$

The various terms of the equations are defined as:

K = coefficient of horizontal kinematic eddy viscosity

λ = drag coefficient

$w()$ = wind speed component

η = surface elevation

H = total depth = $h + \eta$

x, y = space coordinates

u, v = velocity components

g = acceleration of gravity

f = coriolis parameter

$\nabla = \frac{\partial}{\partial x} + \frac{\partial}{\partial y}$

Both the wind stress and bottom stress equations are empirically developed. The wind stress terms, as used in the model, are assumed to be a quadratic expression in wind speed, where λ is the wind drag coefficient with a typical value of 0.65. The bottom stress is assumed to be non-linearly dependent on u and v , and its formulation, like the wind stress, have been derived by empirical means. It was originally formulated for shallow water application. Over deep water, its value becomes small and its applicability is questionable.

An implicit central difference scheme is used for achieving time dependent solutions of the equations. At the boundaries, the values of η , u and v are taken at the actual points rather than from the surrounding points as shown in Figure 4.

The driving forces are tides input at the open boundaries, and wind at the surface over the entire grid. The tide values are computed at each time step and introduced as new values of η at each point of the boundaries.

The finite approximations are given below. The water surface elevations are first calculated using the conservation of mass equation.

$$\begin{aligned} \eta^{\frac{t+\Delta t}{2}}(n,m) &= \eta^{\frac{-t-\Delta t}{2}}(n,m) - \frac{\Delta t}{\Delta \rho} \{ H_u^t(n,m) U^t(n,m) \\ &\quad - H_u^t(n,m-1) U^t(n,m-1) + H_v^t(n-1,m) V^t(n-1,m) \\ &\quad - H_v^t(n,m) V^t(n,m) \} \end{aligned}$$

The horizontal and vertical velocity components are then determined from respective horizontal and vertical momentum equations.

$$U^{t+\Delta t}(n,m) = \{1 - [\Delta t \cdot r/H] U^{t+\Delta t}(n,m)\} \sqrt{\bar{U}^t(n,m)^2 + V^{*t}(n,m)} \bar{U}^t(n,m)$$

$$+ \Delta t \cdot f \cdot V^{*t}(n,m) - \frac{\Delta t / 2 g}{\Delta \ell} \{ n^{t+\frac{\Delta t}{2}}(n,m+1) \\ - n^{t+\frac{\Delta t}{2}}(n,m) \} + \Delta t \cdot X^{t+\Delta t}(n,m)$$

$$V^{t+\Delta t}(n,m) = \{1 - [\Delta t \cdot r/H] V^{t+\frac{\Delta t}{2}}(n,m)\} \sqrt{\bar{V}^t(n,m)^2 + U^{(t)}(n,m)} \bar{V}^t(n,m)$$

$$- \Delta t \cdot f \cdot U^{*t}(n,m) - \frac{\Delta t / 2 g}{\Delta \ell} \{ n^{t+\frac{\Delta t}{2}}(n,m) \\ - n^{t+\frac{\Delta t}{2}}(n+1,m) \} + \Delta t \cdot Y^{t+\Delta t}(n,m)$$

where

$$\bar{U}^t(n,m) = \alpha U^t(n,m) + \frac{1-\alpha}{4} \{ U^t(n-1,m) + U^t(n+1,m) + U^t(n,m+1) \\ + U^t(n,m-1) \} ,$$

$$\bar{V}^t(n,m) = \alpha V^t(n,m) + \frac{1-\alpha}{4} \{ V^t(n-1,m) + V^t(n+1,m) + V^t(n,m+1) \\ + V^t(n,m-1) \} ,$$

$$U^{*t}(n,m) = \frac{1}{4} \{ U^t(n,m-1) + U^t(n+1,m-1) + U^t(n,m) + U^t(n+1,m) \} , \text{ and}$$

$$V^{*t}(n,m) = \frac{1}{4} \{ V^t(n,m-1) + V^t(n+1,m-1) + V^t(n,m) + V^t(n+1,m) \} .$$

The factor α can be interpreted as related to the horizontal kinematic viscosity parameter. In the program it is treated as a tuning parameter and is related to the eddy viscosity coefficient by:

$$\frac{K\Delta t}{\Delta \ell^2} = \frac{1-\alpha}{4} = \frac{\beta}{4}$$

The total depth of water is calculated by:

$$Hu^{t+\Delta t}(n,m) = hu(n,m) + \frac{1}{2} \{ n^{t+\frac{\Delta t}{2}}(n,m) + n^{t+\frac{\Delta t}{2}}(n,m+1) \}$$

$$Hv^{t+\Delta t}(n,m) = hv(n,m) + \frac{1}{2} \{ n^{t+\frac{\Delta t}{2}}(n,m) + n^{t+\frac{\Delta t}{2}}(n,m+1) \}$$

The effects of wind are computed by:

$$X^t = \frac{\lambda w_x^t \sqrt{(w_x^t)^2 + (w_y^t)^2}}{H} - \frac{1}{\rho} \frac{\partial P_o}{\partial x} \quad \text{and}$$

$$Y^t = \frac{\lambda w_y^t \sqrt{(w_x^t)^2 + (w_y^t)^2}}{H} - \frac{1}{\rho} \frac{\partial P_o}{\partial y} .$$

where P_o is the barometric pressure. Its gradient is assumed to be zero for small areas and normal conditions.

The stability of the model is governed by the Courant-Friedrichs-Levy criterion which says that the maximum length of the time step is determined by the grid size and maximum depth in the area,

$$\Delta t \leq \frac{\ell}{\sqrt{2gH_{\max}}} .$$

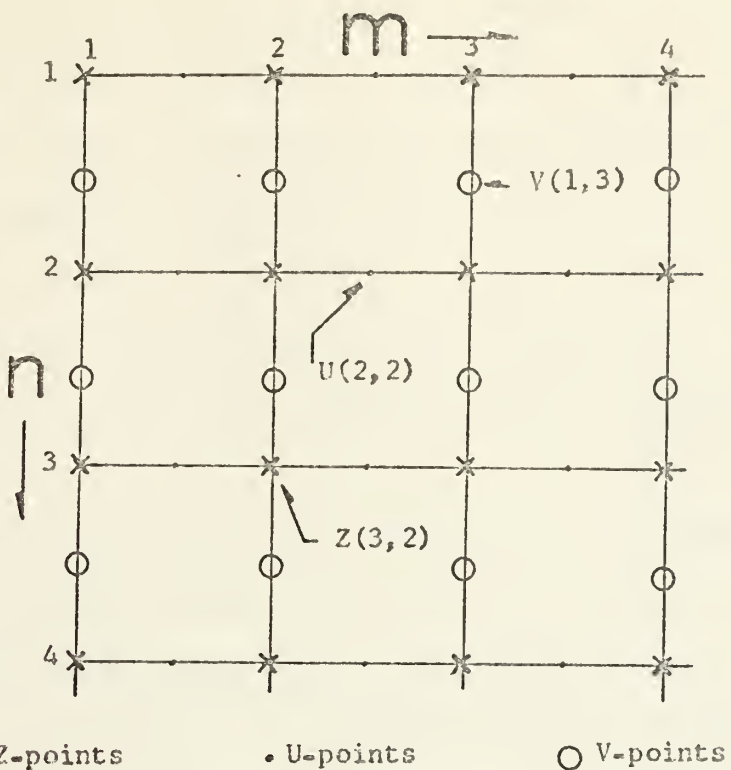
For this particular grid, a Δt (half-time step) of 5 seconds was adopted.

If the computational area contains small sections of greater depths [4], a "false bottom" can sometimes be assumed in these areas. (E.g., areas deeper than 500 meters can be assumed to be 500 meters deep.) This will often result in a considerable increase in the time step, or a decrease of the grid length if total computation time is a critical factor. Experiments have shown that the error introduced with the above procedure is acceptable in some cases for practical applications of the model.

The grid net consists of three different sets of grid points shown in Figure 4-a; the water elevation (z), the u -velocity component and the v -velocity component. Each of these three points have the same coordinate designation (n,m) . The coastline must pass through u and v points and not through z points and the values of depths at any of these particular points are read in the program as HTU and HTV.

The HTZ points act as water-coast-land designators having values of 1, -1, and 0 respectively. The HTU and HTV show the depth values (in cm.), the coastline as -1, and land as 0, depending on their location in the grid [Figure 4-b].

At the input open boundaries, HTZ points have values of -2 (and -3) for the first and second open boundaries (if applicable). Outside of the input boundaries, values of zero for HTZ are prescribed.



SCHEME OF THE GRID NET

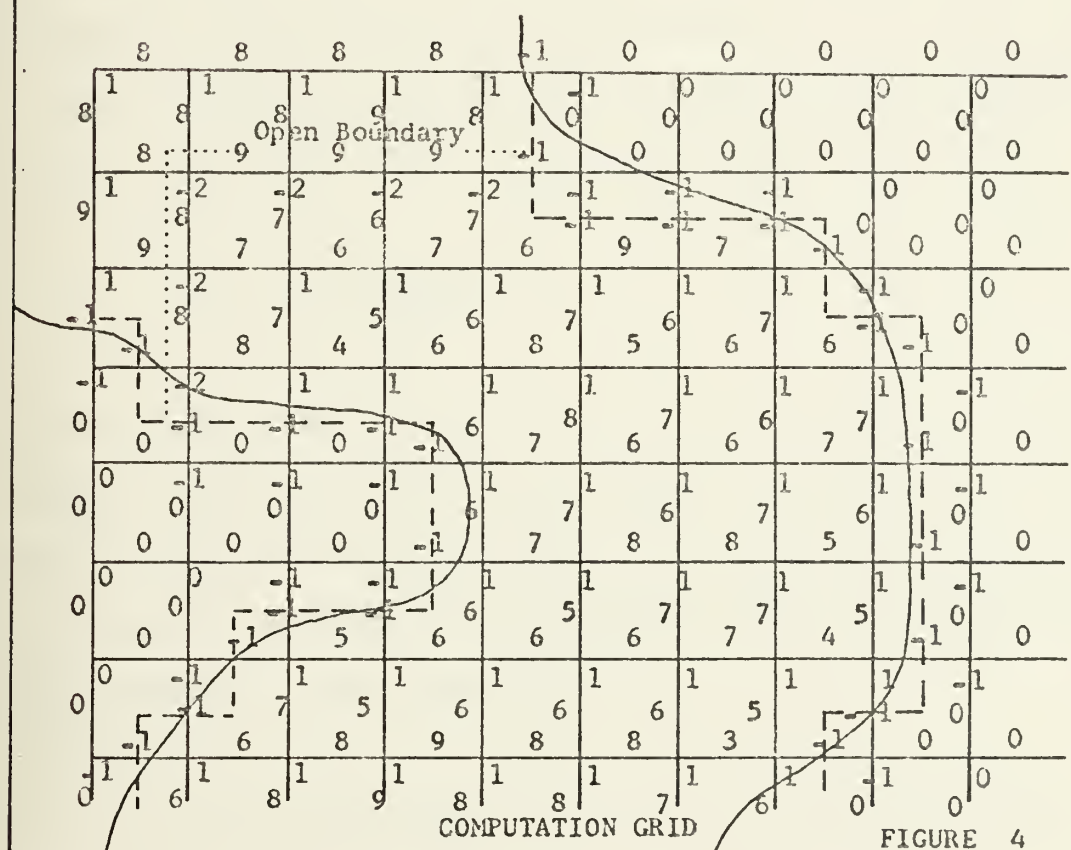


FIGURE 4

The coefficient of horizontal kinematic eddy viscosity is interpreted as related to the values of the u and v current components. Hansen states that the computations are always stable for values of Beta ($1-\alpha$) larger than zero and the normal value used is 0.01. However, this coefficient can also be used as a tuning factor. If a higher value is used, the current speed is generally decreased.

In areas where the depth distribution is irregular, accelerations and surface irregularities appear in the model. This abnormality can be solved by means of a proper smoothing of the bottom or the sea surface. This is accomplished in this model by the smoothing of the sea surface elevation which is a numerical artifact of the model. This is done to insure numerical convergence.

The coefficient of horizontal kinematic eddy viscosity in the finite solution, is represented by the relation

$$K = \frac{\Delta\ell^2(1-\alpha)}{4\Delta t}$$

For the values of $\Delta\ell$ (100 m), Δt (5 sec.) of this specific model, and alpha (0.992) recommended by Laevastu for estuaries (personal communication), K becomes $0.9 \times 10^5 \text{ cm}^2/\text{sec.}$

Bowden [2] suggests for estuaries with a tidal current amplitude of V and a depth of h,

$$K = 0.15 Vh$$

This relation gives a value of $K = 0.25 \times 10^5 \text{ cm}^2/\text{sec.}$ for the northern portion of San Diego Bay. This corresponds to an α value of 0.995. For the southern part, this equation gives a value of $K = 0.3 \times 10^4$ with a corresponding value of $\alpha = 0.999$.

The use of these high values for α must be done with caution because the low smoothing can allow undesirable oscillations in the model. If a too low value of α is used in order to obtain good smoothing, the resolution of current could be affected.

As was pointed out in the assumptions of the Hansen Model, the advection terms, $u_j \frac{\partial u_i}{\partial x_j}$ have been neglected. If a value of 50 cm/sec. (about one knot) is assumed for both u_j and u_i , and if the distance between grid points is 200 m, then, the advection terms are of the order of 10^{-2} cm/sec. A representative value of the local velocity change $\frac{\partial u_i}{\partial t}$, is calculated using a Δt of a quarter tidal cycle of 3 hours during which time the velocity changes from a maximum represented by 50 cm/sec. to zero. This term then is of the same order of magnitude as the advection terms. The coefficient of horizontal eddy viscosity (K) is deduced from the horizontal advection terms; then, in the model, what is partially done by the tuning process is accounted in K for the values of the neglected advection terms.

A. SELECTION OF THE GRID

The selection of the grid size is usually based on requirements of details and accuracy, and availability

of computer core memory and time. For open areas and round shaped smooth bays, where the expected velocities and direction fields are smooth, it is not necessary to use a fine mesh. In areas where topography is of primary importance a fine mesh is necessary for reliable results.

The flow in San Diego Bay is governed by the topography of the area; therefore, a small grid size must be introduced. To cover the entire area, a large array would be necessary which would require a large amount of core and computation time.

On the other hand, due to deficiencies in the boundary conditions of the model, inaccuracies of the computations are found near land grid points; therefore, if acceptable results are desirable in narrow channels, the grid must provide enough grid points across these areas.

A small grid of 100 x 100 array was lain over San Diego Bay. Because of the difficulty of handling by the computer, the area was divided in two regions with sufficient overlap to insure proper calibration.

The way the boundary conditions are set at the open boundaries produce errors which propagate throughout the adjacent grid points; therefore, the overlap area must be of considerable size in order that the match section be distant enough from both open boundaries that these influences are negligible. For this specific model, a long

and narrow portion of the bay in front of Coronado was chosen, assuming that in this area flow is parallel to the coastline and free of big eddies.

This division gives two grids: a northern grid of 53 x 30 designated as grid (1), and a second southern grid of 58 x 40 and designated as grid (2) [Figure 1].

The second portion of the bay was run under two different conditions: first under existing conditions (model (2)) and, secondly, with a second open boundary at Crown Cove (model (3)). The division of the bay into two different models will not allow for computation of velocity at the northern entrance for the case of the model (3), but it will give a good indication of what the future conditions will be in the northern channel as the point C-2 (see Fig. 1) will be computed in the second and third models.

B. TIDE INPUT IN THE MODEL (1)

In the northern model referred to as model (1) (the one with two open boundaries), tidal values at both openings was first introduced. The time inaccuracies of the prototype measurements forced water in and out of the bay at the two ends simultaneously. This procedure causes a non-equilibrium state in the bay with corresponding erroneous answers.

A new procedure was tried by leaving the second boundary open without a driving force, letting the water flow in and out according to the propagation of the tidal wave

from the first boundary. Continuation of the surface of the water and currents for each point in the free open boundary was prescribed to insure the flow of water throughout this end. For the values of height, this continuation was obtained by leveling the edges using the concept of a "lubricated wall",

$$Z(NEH,M) = Z(NEH-1,M)$$

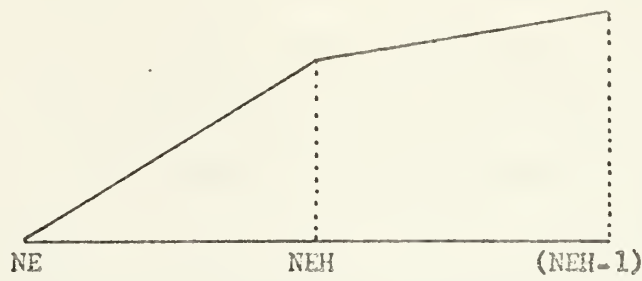
Attempts to continue the surface slope resulted in disturbances being generated in the model,

$$Z(NEH,M) = Z(NEH-1,M) + [Z(NEH-1,M) - Z(NEH-2,M)].$$

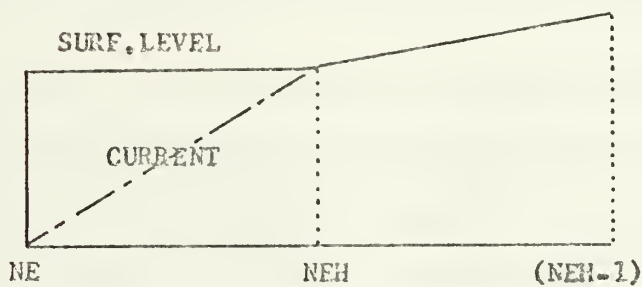
Leveling the edges and letting the model compute the values of currents itself resulted in too severe a decay of the values of velocity at the second boundary; this resulted in no flow through the free open boundary.

To obtain the correct flow of water throughout the free open boundary, a continuation of current (u and v) was prescribed with the assumption that calibration of the model could be obtained modifying the values of this slope by means of applying a smoothing constant (J) to its value [Figure 5],

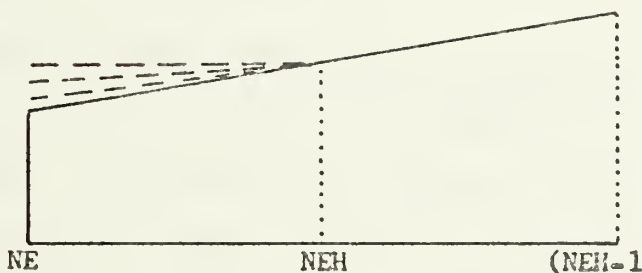
$$V(NEH,M) = V(NEH-1,M) + J[V(NEH-1,M) - V(NEH-2,M)].$$



INPUT BOUNDARY AND FREE BOUNDARY WITHOUT CONTINUATION



LEVELING OF THE EDGES(LUBRICATED WALL)AT BOUNDARIES



CONTINUATION OF CURRENT AT THE FREE OPEN BOUNDARY
WITH THE GRADIENT CORRECTED
BY A CONSTANT

FIGURE 5

Variations of the values of the currents in the entire model were obtained, but great disturbances in the water surface were introduced up to a point that back-flux was obtained. Figures 6 and 7 show different results obtained for different values of J in the continuation of current used at the free open boundary.

These disturbances in the surface can be reduced by applying an inverse correction to the slope of the surface at the edge

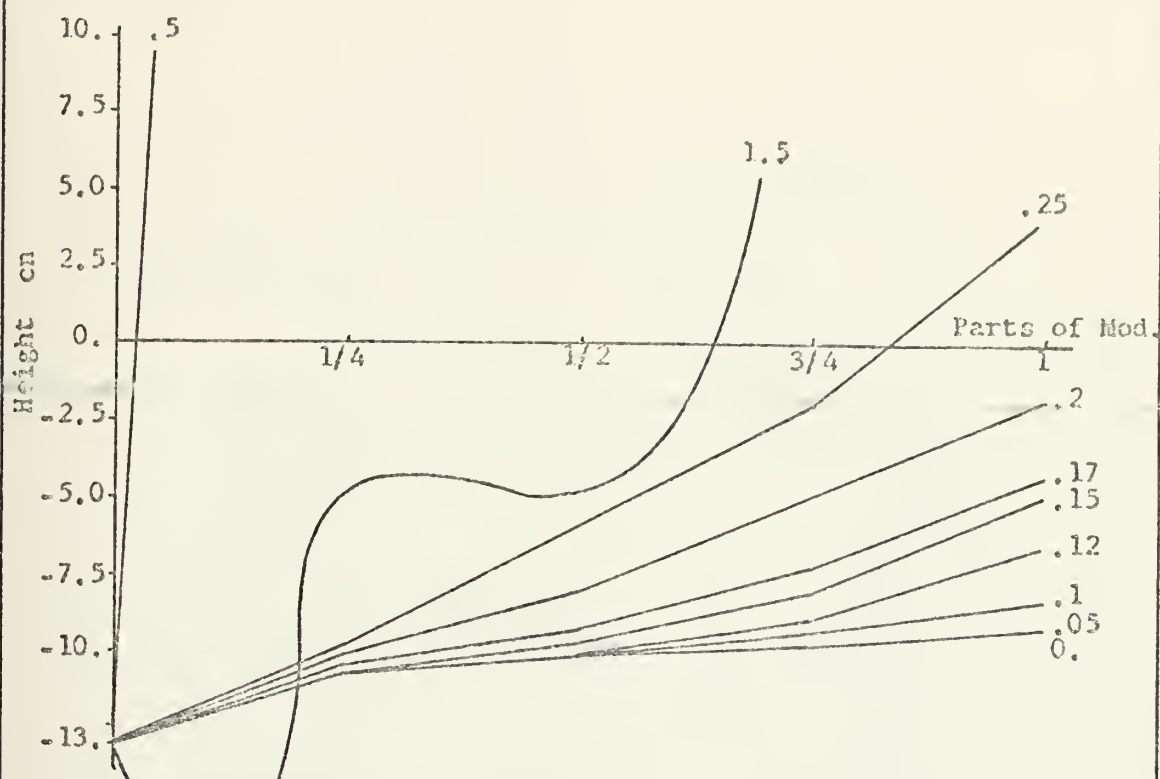
$$Z(\text{NEH}, M) = Z(\text{NEH}-1, M) - C(Z(\text{NEH}-1, M) - Z(\text{NEH}-2, M)).$$

No further calibration was attempted because this procedure is not realistic, but a proper calibration may give a good result with savings in computation time.

Because no satisfactory answer was obtained from a free open boundary, the idea was abandoned and the addition of an appended pseudo-bay was tried.

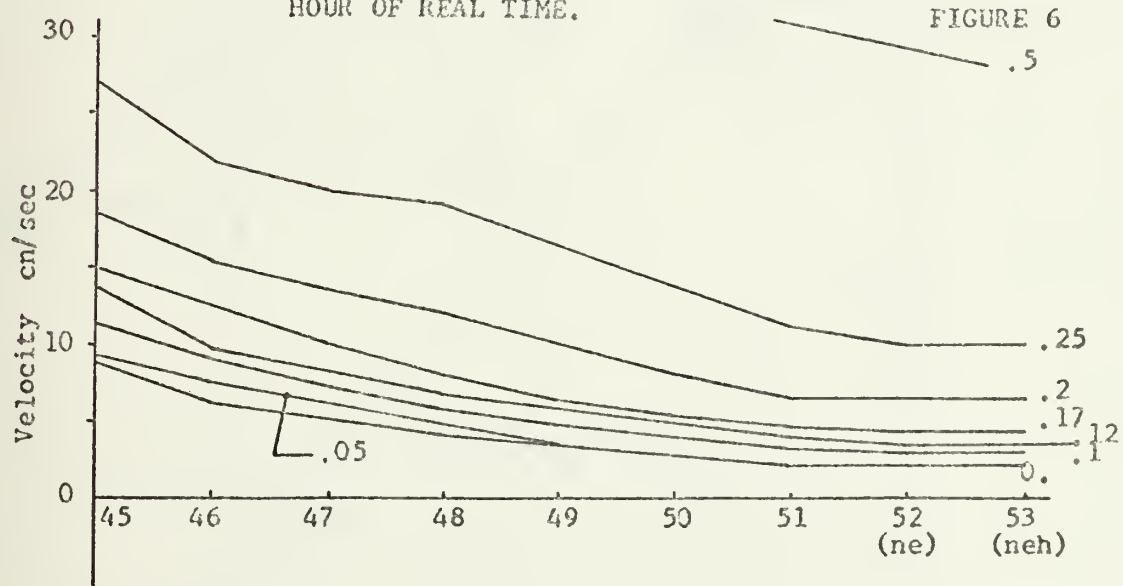
C. ADDITION OF AN APPENDED PSEUDO-BAY

The addition of an appended area at the end of the model (1) creates an additional tidal prism which will force the volume of water passing throughout the first model to increase. This new area, Figures 8 and 9, was obtained by filling the empty spaces of the grid and connecting them to the end of the model. This procedure does not increase the core in the program, but increases the time of computation by about 30% for this specific case.



VALUES OF Z ALONG THE MODEL (1) FOR DIFFERENT CONSTANTS IN THE CONTINUATION OF THE FREE BOUNDARY AFTER 1 HOUR OF REAL TIME.

FIGURE 6



VALUES OF VELOCITY AT M= 3 AND N= 45 to 53 IN THE FREE OPEN BOUNDARY FOR DIFFERENT CONSTANTS IN THE CONTINUATION AFTER 1 HOUR OF REAL TIME.

FIGURE 7

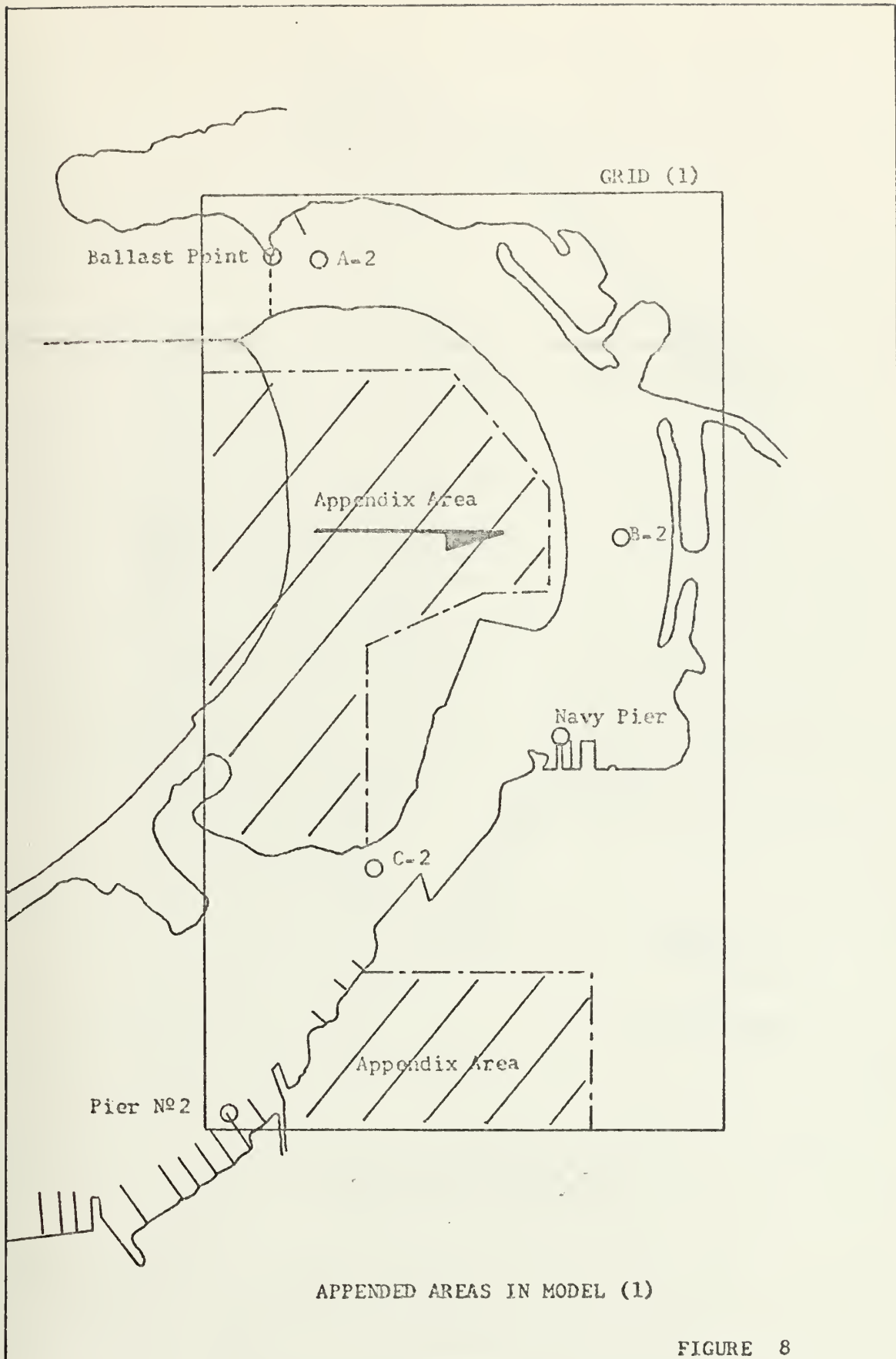


FIGURE 8

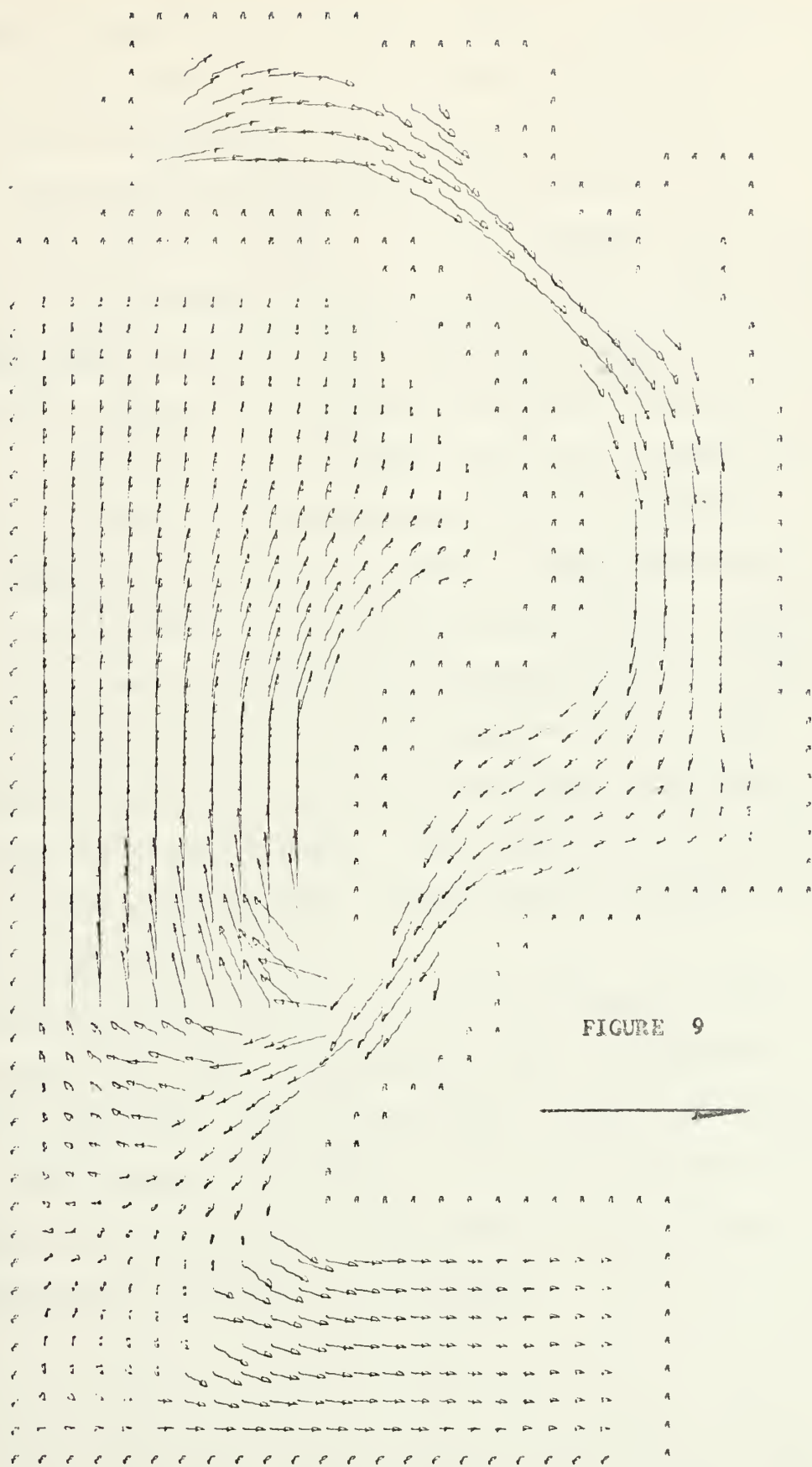


FIGURE 9

CIRCULATION IN MODEL (1) WITH APPENDED AREAS

Areas corresponding to 82% and 100% of the remaining area of the bay were tried. The results, Figures 10, 11, and 12 show an increase of water transport and current values with no appreciable modifications to the values of the water surface. The increase in volume transport and currents were proportional to the increased areas. The values of height remain stable for the different cases.

Different values of R (0.003, 0.0028 and 0.002) were applied to the model. The results show that the model is not very sensitive to the variations of this parameter. After comparing the results obtained at the points A-2, B-2 and C-2 for each of the values of R, 0.003 was adopted because it seemed to better fit the measurements at these points in the prototype. The discrepancies at A-2 were attributed to the inaccuracies of the Hansen numerical model near the open boundaries. The results of the model (1) in current, water height and net volume transport are shown in figs. 13, 14, 15.

A pictorial description of the flow throughout the entire model (1), with the appended areas, is shown in Figure 9. The real part of this model and the times of 0., 3., and 9 hours are shown in Figures 16, 17 and 18. The direction of the flow is indicated by the arrows, and its magnitude is scaled by the length.

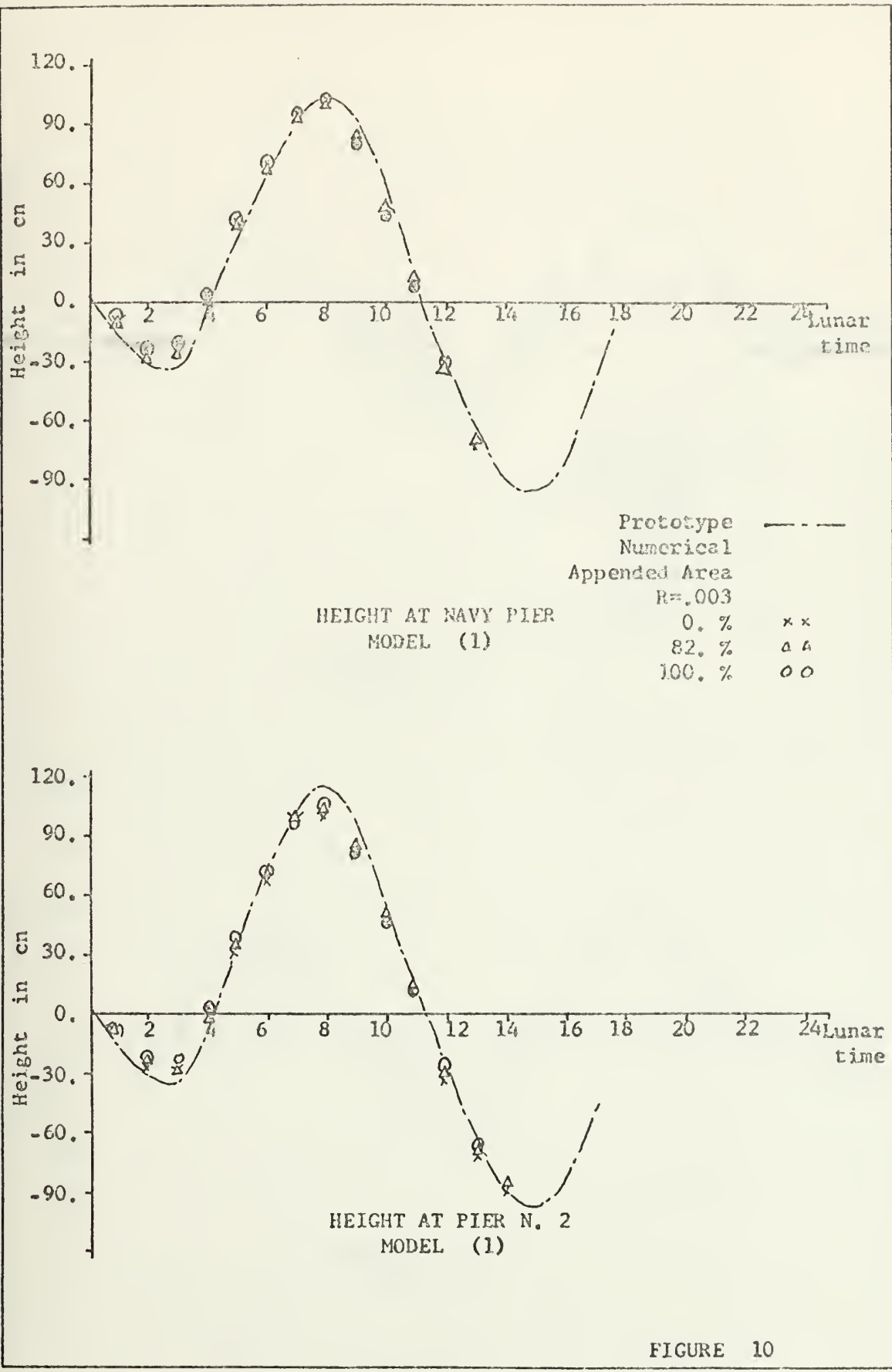


FIGURE 10

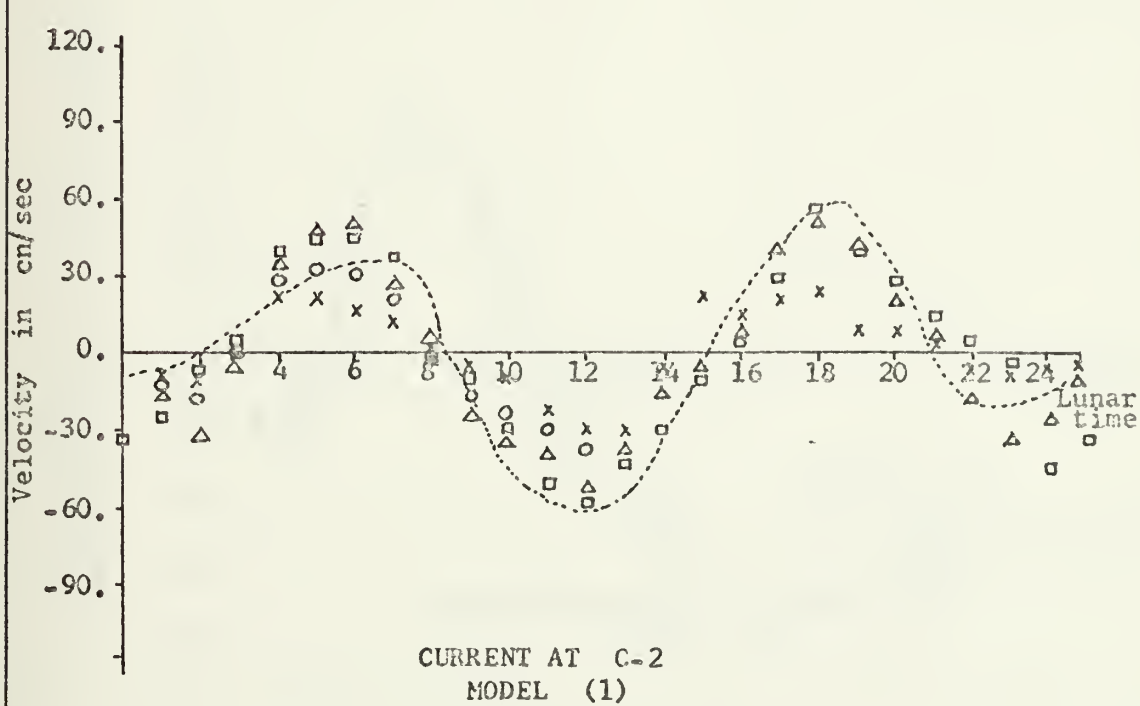
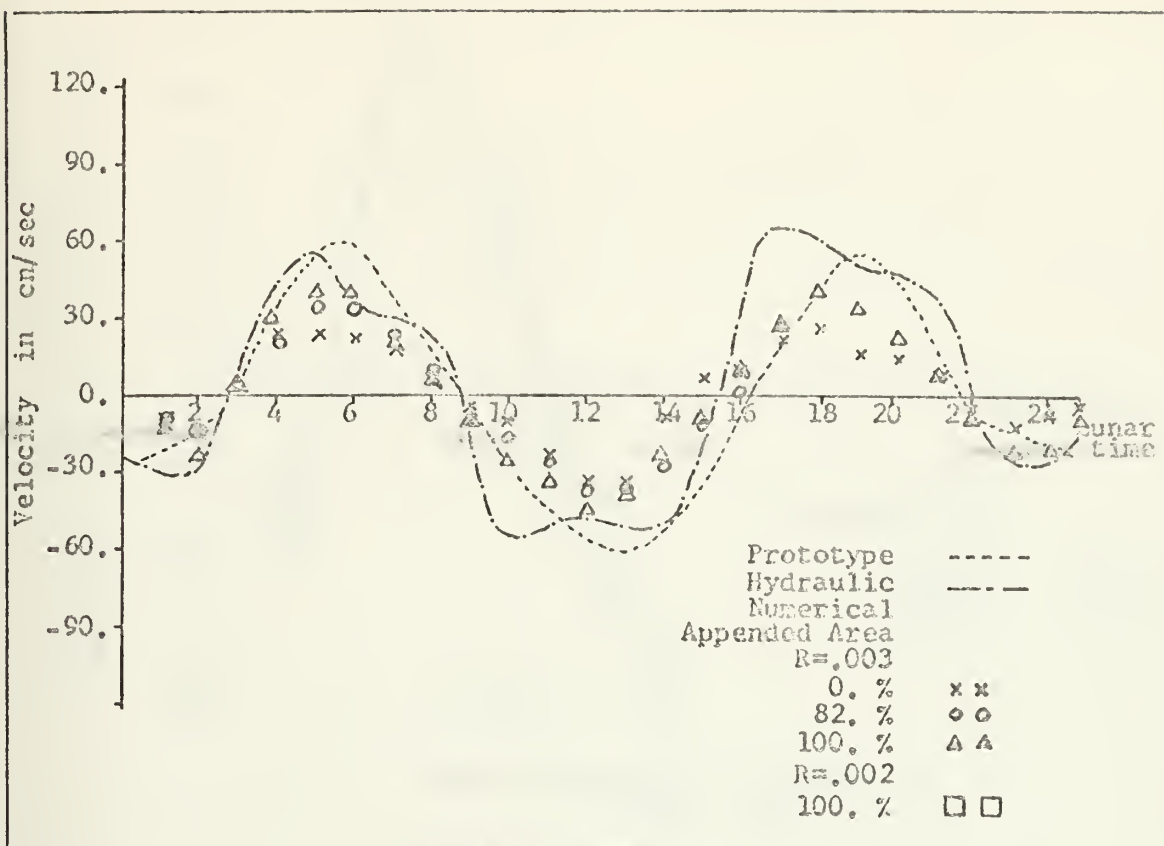


FIGURE 11

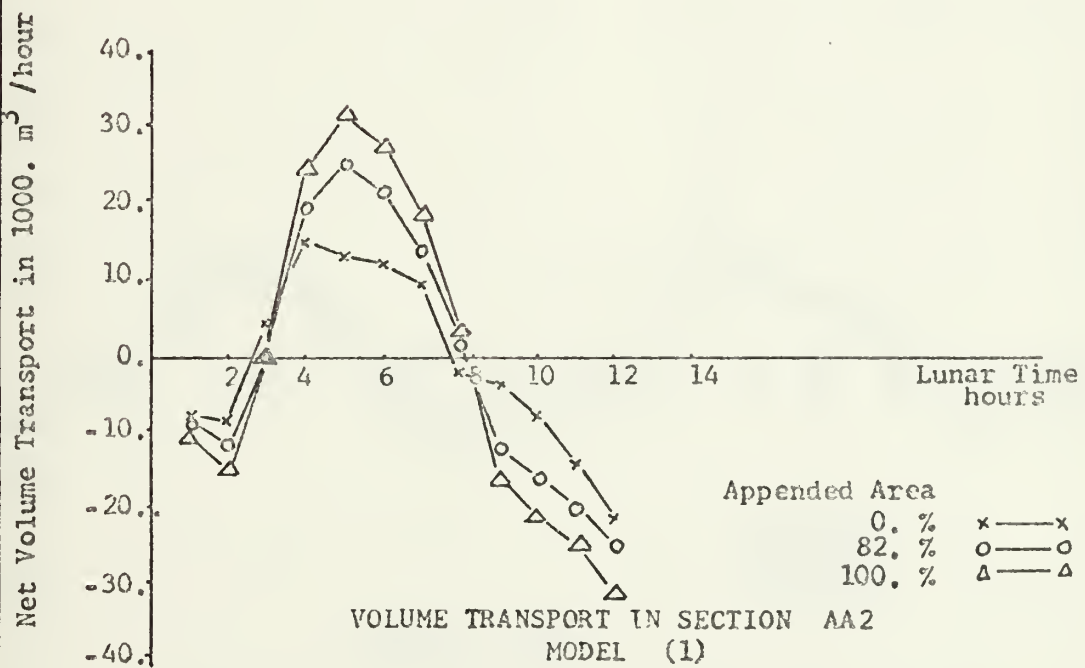
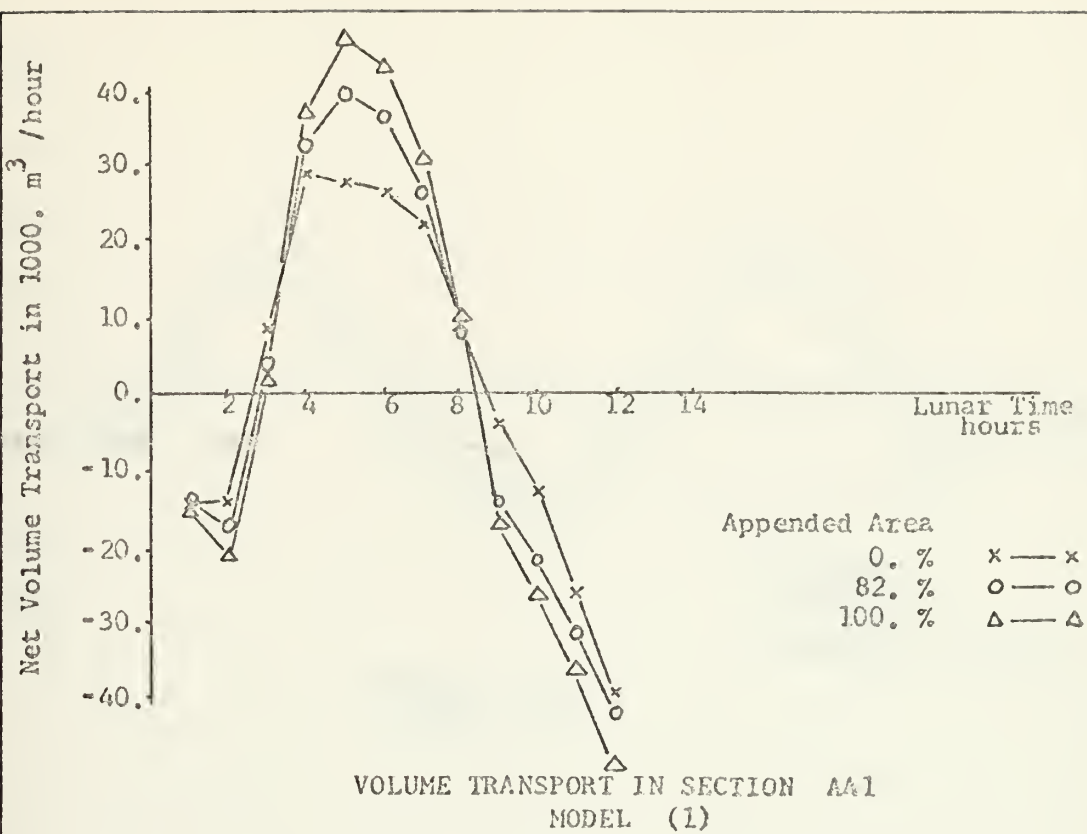


FIGURE 12

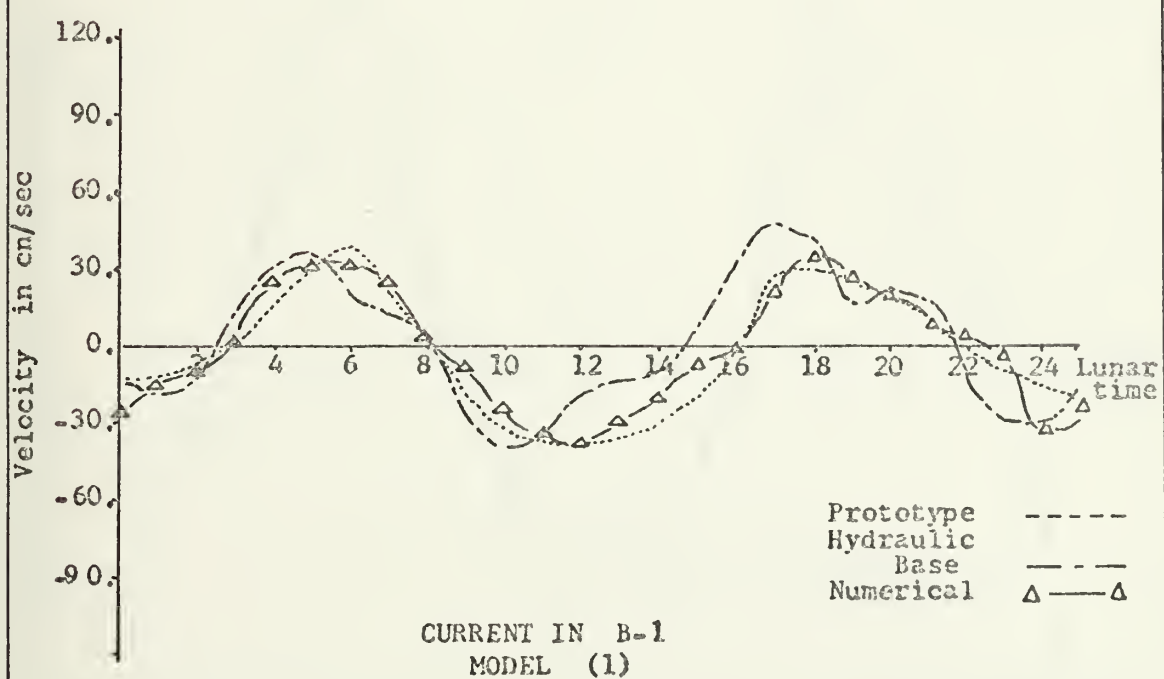
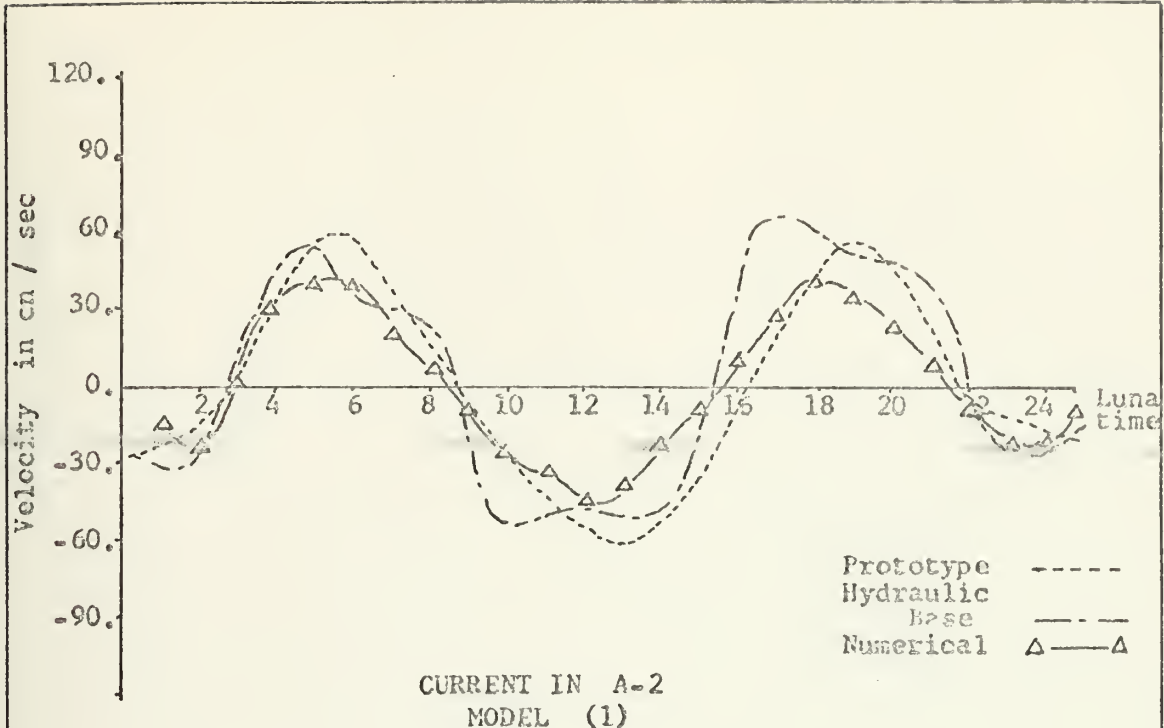


FIGURE 13

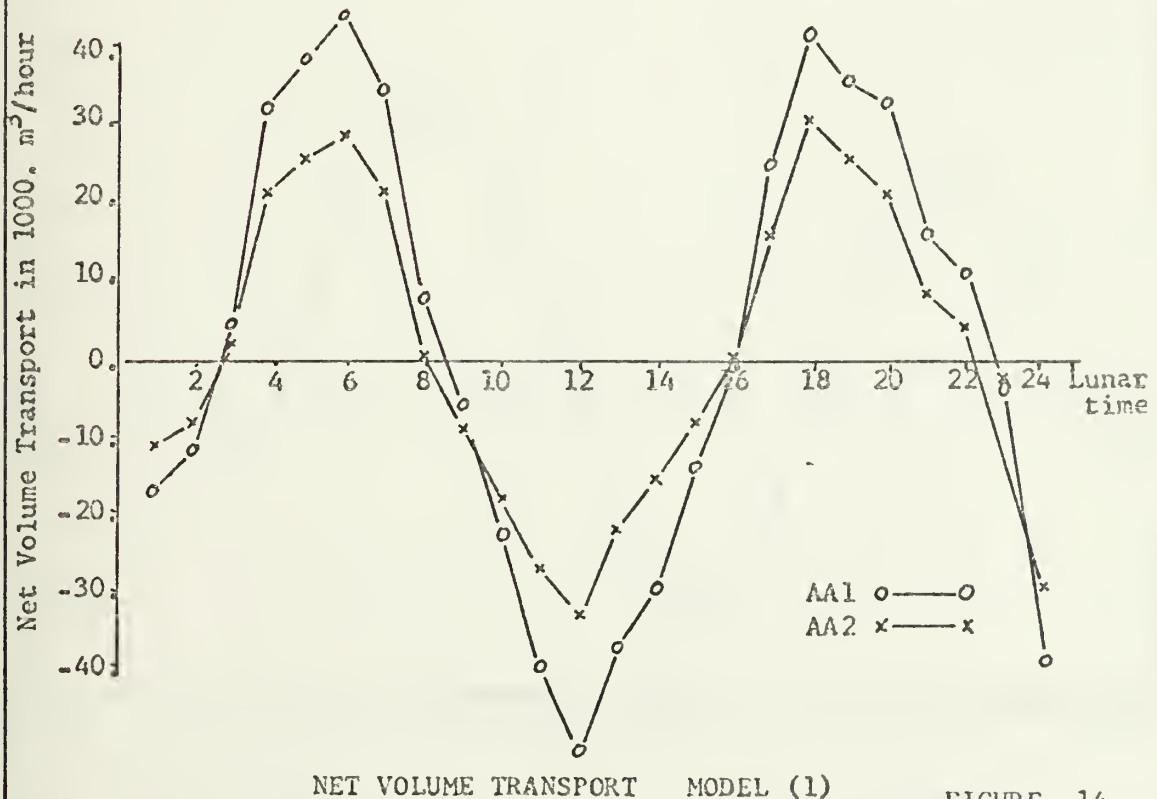
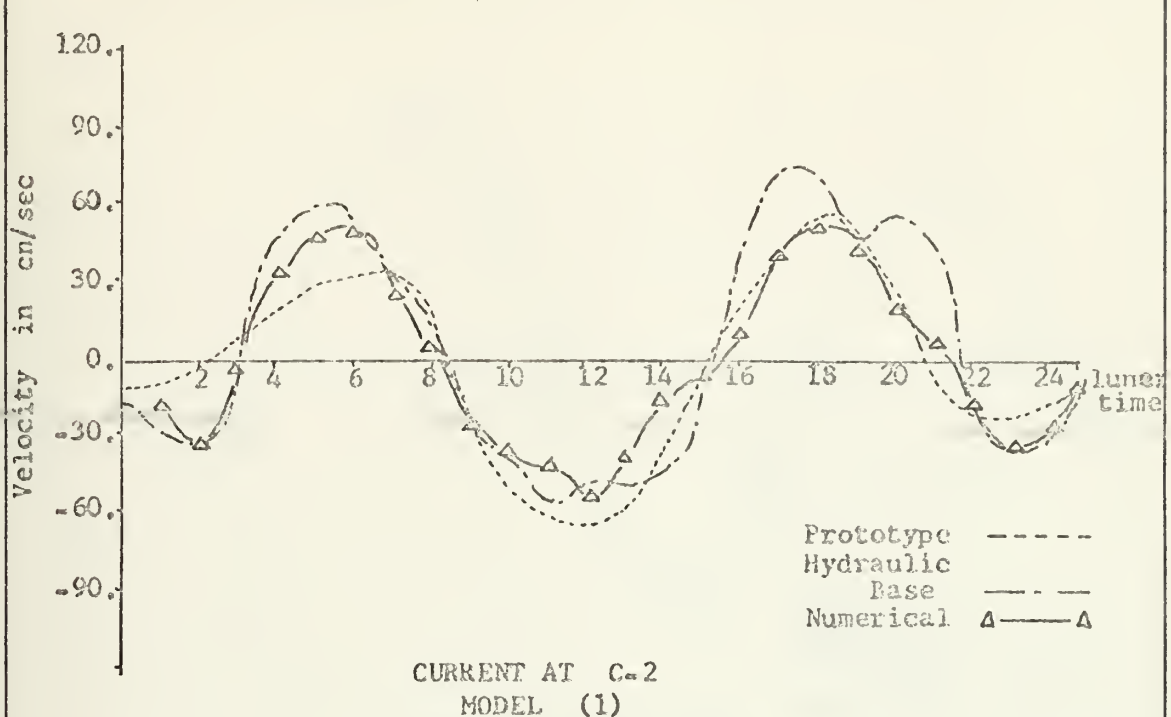


FIGURE 14

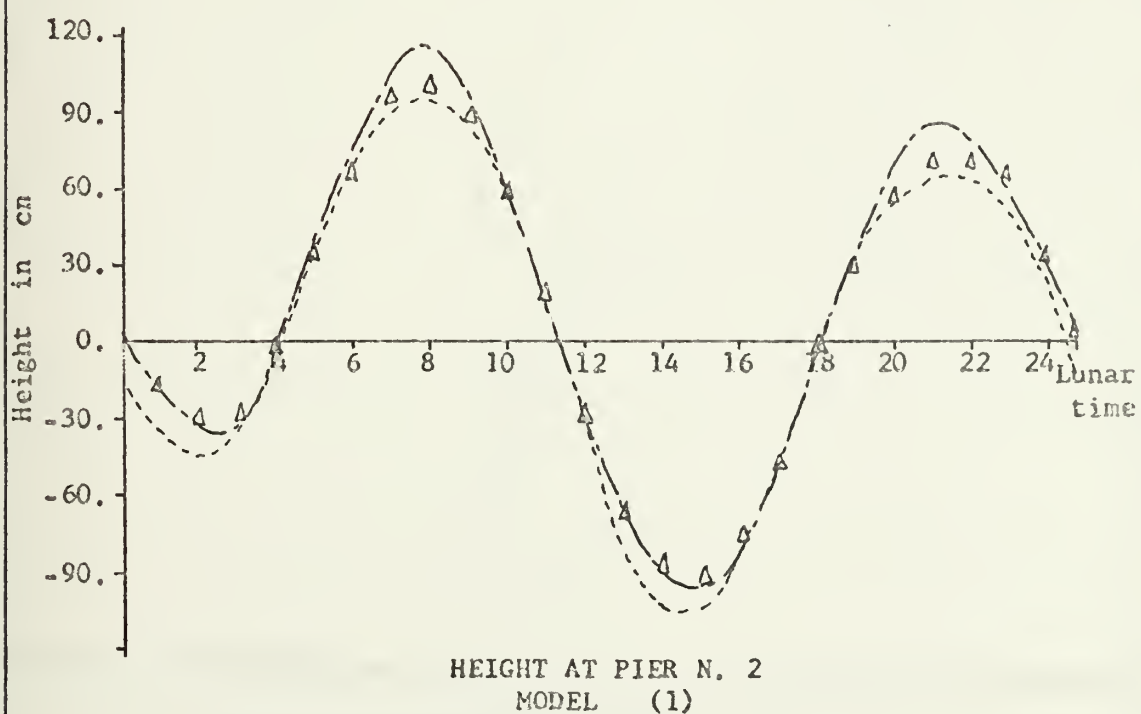
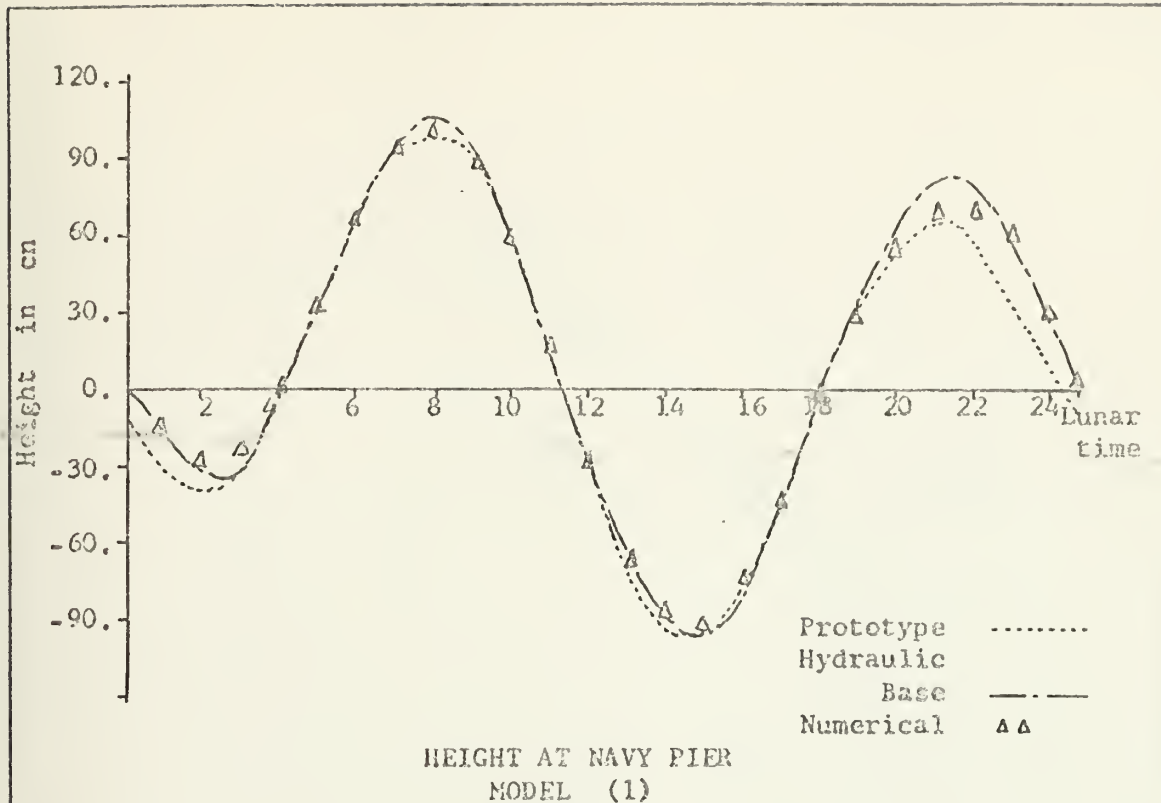
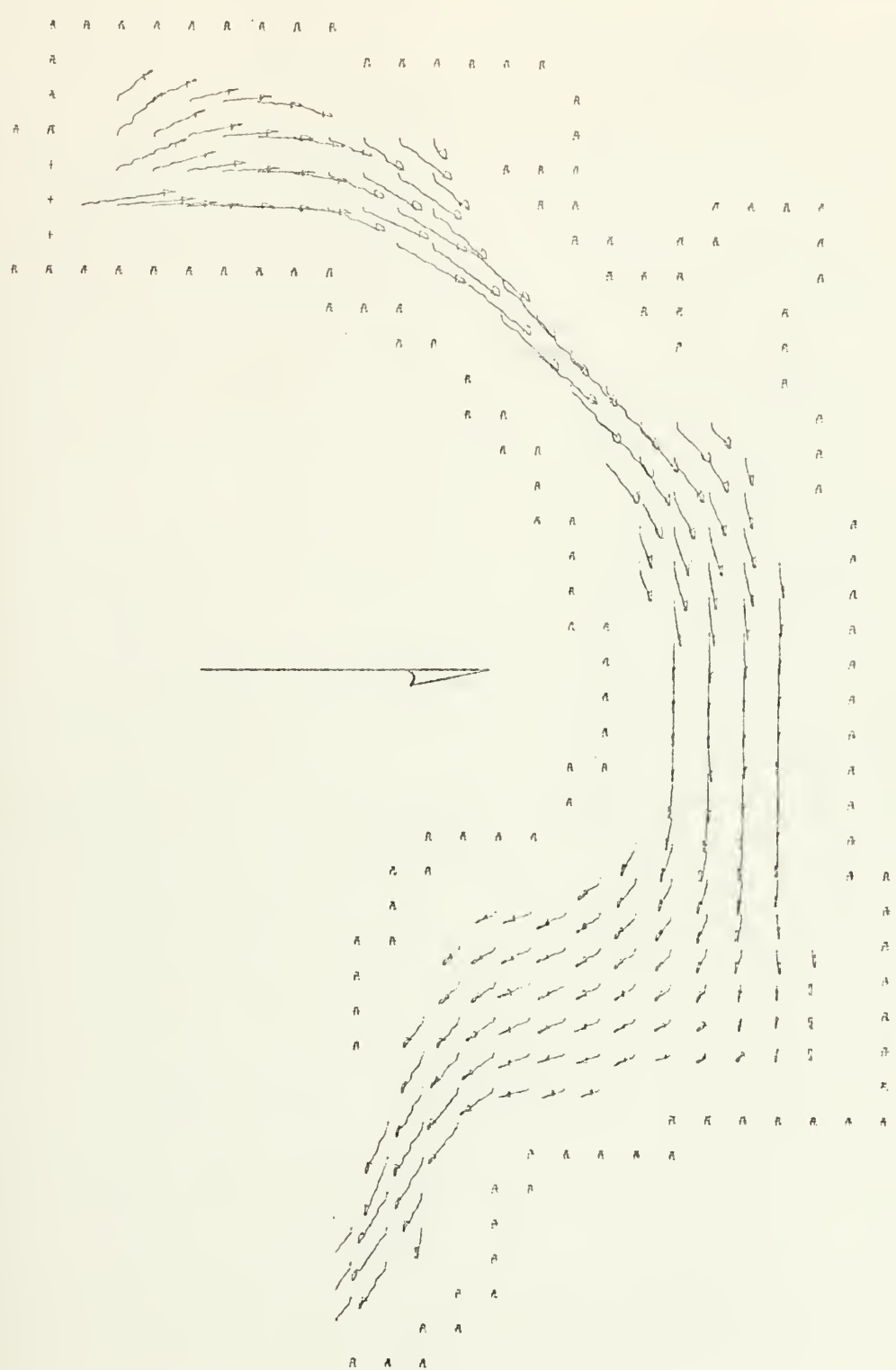


FIGURE 15

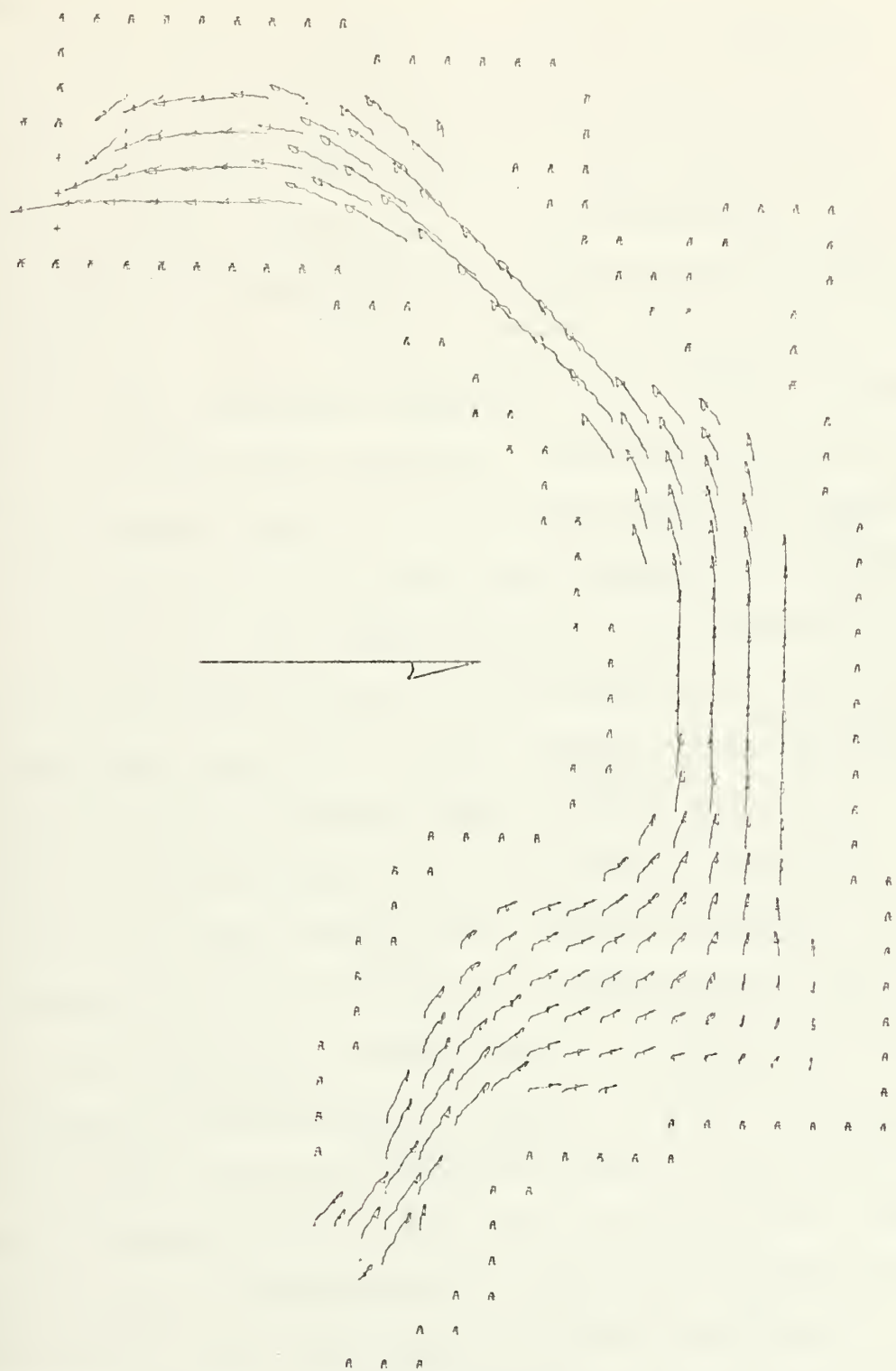
CURRENT DISTRIBUTION IN MODEL (1)
TIME = 0. hr.

FIGURE 16



CURRENT DISTRIBUTION IN MODEL (1)
TIME = 3 hr.

FIGURE 17



CURRENT DISTRIBUTION IN MODEL (1)
TIME = 9 hr.

FIGURE 18

D. MODEL (2)

From the results of model (1), tidal values were obtained for a point at the middle of the channel in the vicinity of Navy Pier Tidal Station. These values were introduced as input to model (2). The computations were attempted with the same values of R (0.003) and α (0.992) as in model (1).

Using these prescribed conditions, oscillations in the current and tidal values developed (see Figures 19 and 20). These oscillations appear to be in phase and their magnitudes increase from zero at the open boundary to a maximum value of about 30 cm/sec. and 15 cm/sec. respectively at the end of the deeper channel at the near end of the bay, and from there, the values of the current reduce proceeding to the shallower and southern part of the bay.

The oscillations seem to be activated as the tide approaches the LLW, increase their values throughout the next HW and die out by the next LW, repeating the cycle 12 hours later when LLW is reached again. The period of the oscillations is greater than 2 hours.

The causes of the oscillations could be some kind of seiching manifestations in the model, shallow water tide or oscillations characteristic of the model produced by attempting to work in extremely shallow water without introducing special prescribed conditions for these small values [8].

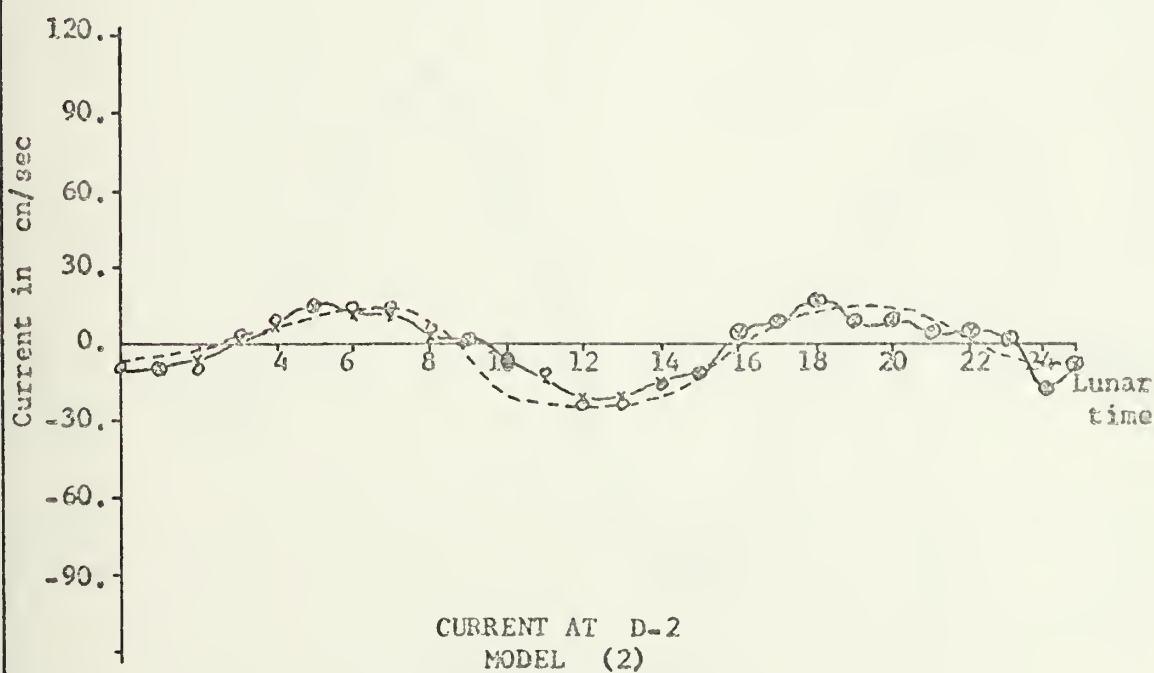
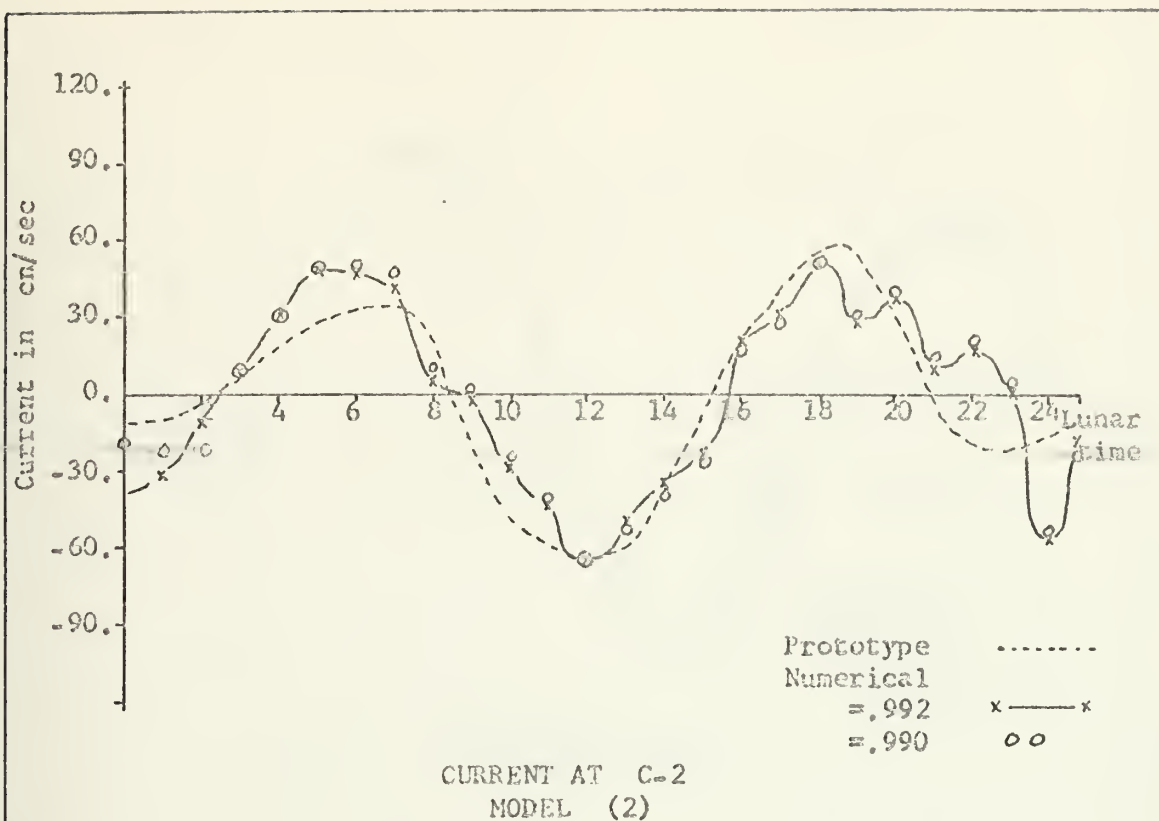


FIGURE 19

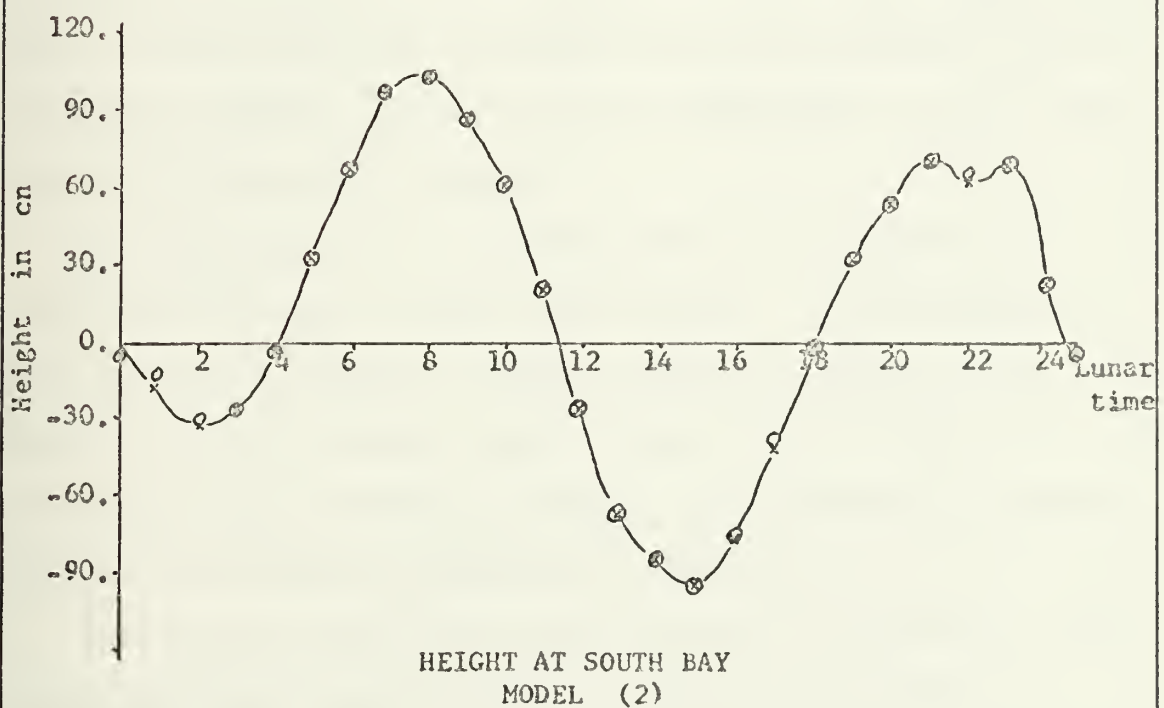
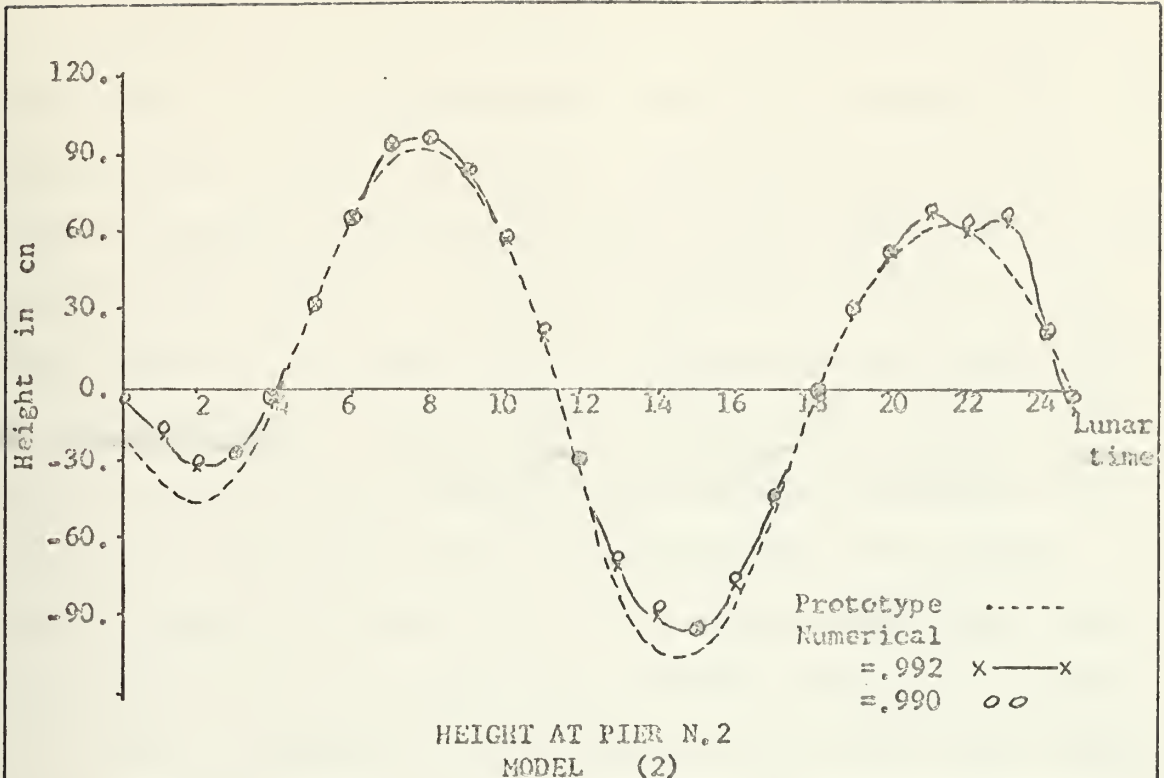


FIGURE 20

A possible mode of seiching can be calculated assuming that model (2) is an independent bay with a length of 14. km and a medium depth of 4. meters. This bay will oscillate with a fundamental period of about 2.3 hr. which agrees with the resulting values. A Fourier analysis was made of the tidal input of the model (2) and the calculated water height at South Bay Gage. Calculation of the Energy Density Spectrum was performed to compare both and see if energy from some of the harmonics from the tidal input have excited the oscillations in the bay. The spectrum shows (see Fig. 23-1) that the oscillations have periods between 2.06 and 3.55 (with a maximum at 2.3) hours and that the tidal input has negligible energy in these periods. This seiching may be activated at the LLW and damped out by the smoothing parameter α . The existence of such anomalies are not shown in the published records of the observations and its appearance depends, in case of its existence, on the time spacing of the data obtained.

The possibility of a shallow water tide seems to be reasonable because in each tidal cycle, the oscillations seem to be activated by the tide when the depth of the water is at its minimum value. This shallow water tide produces a high frequency harmonic [3] which can be amplified by the model and damped out later by α .

Because the model has linear terms only (except in the bottom and wind friction terms), it is not possible to transfer energy from one harmonic to another; then, the

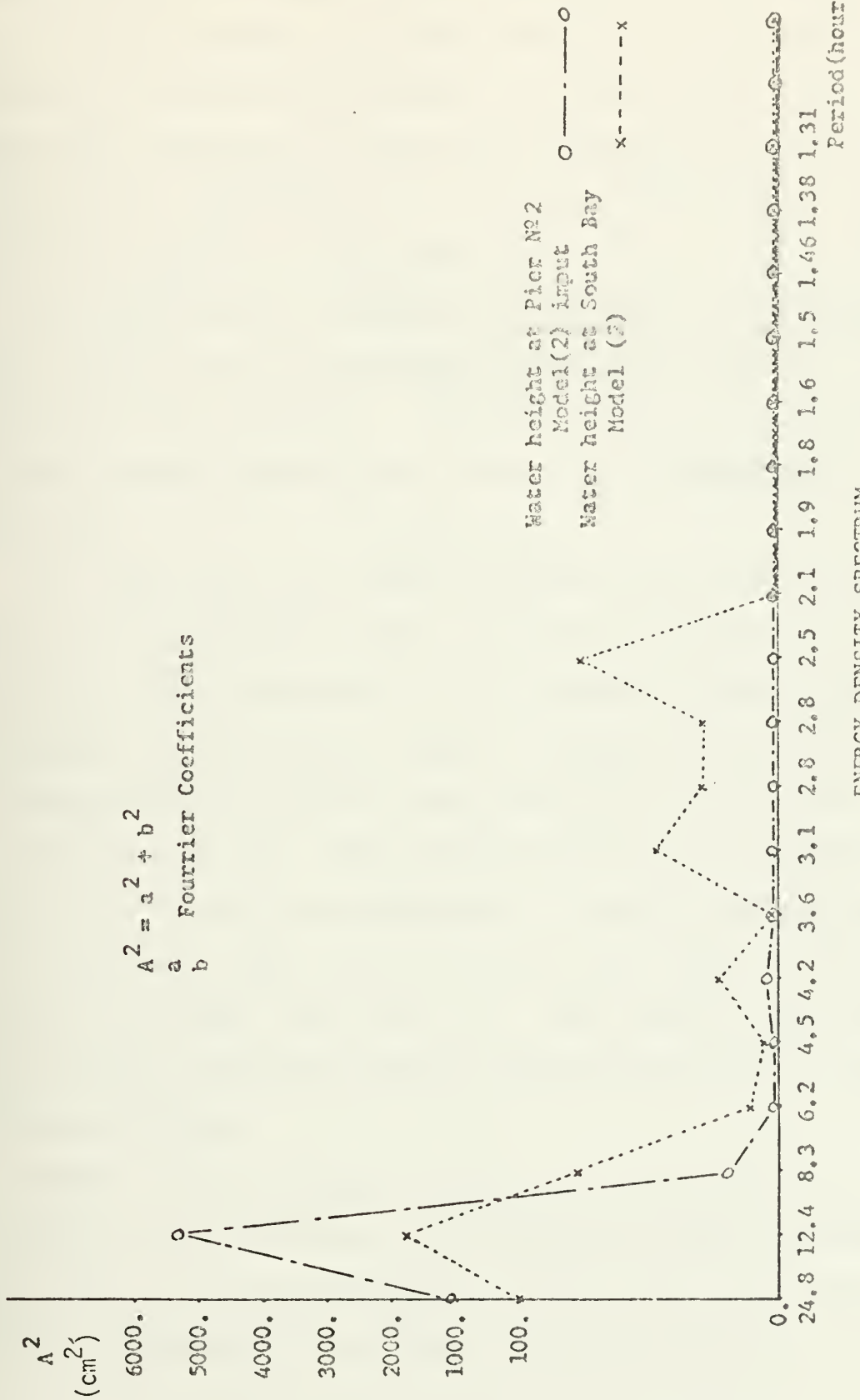


FIGURE 20-1

amplification of a high harmonic from the shallow water tide is questionable. One last possibility can be a deficiency of the difference scheme. As the tide is a continuous wave type propagation, errors are introduced in the time differential computation that could produce a harmonic that could be amplified by the same model.

An α of 0.99 was introduced in an attempt to eliminate the oscillations by increasing the smoothing, but no improvement was obtained. Lower values were not introduced because larger smoothing may affect other parameters in the model.

The need for a low value of Alpha in the model to damp out these oscillations makes the previous estimation of 0.999 of α not applicable for the southern portion of San Diego Bay. In the model 2 and 3, a minimum depth of 4. ft is established to prevent that portion of the bay from becoming dry at LLW. This minimum depth was increased up to 12. ft. to test the probability of shallow water tide with the result that similar oscillations appeared but with larger amplitudes, (see fig. 21). This new test made the possibility of seiching the most feasible mechanism causing the oscillations.

Model (3) was finally run with an α of 0.992 and an R of 0.003 and the results of current and height of water are shown in Figures 22 and 23. A pictorial description of the circulation of the Model (2) at the hours 3 and 9

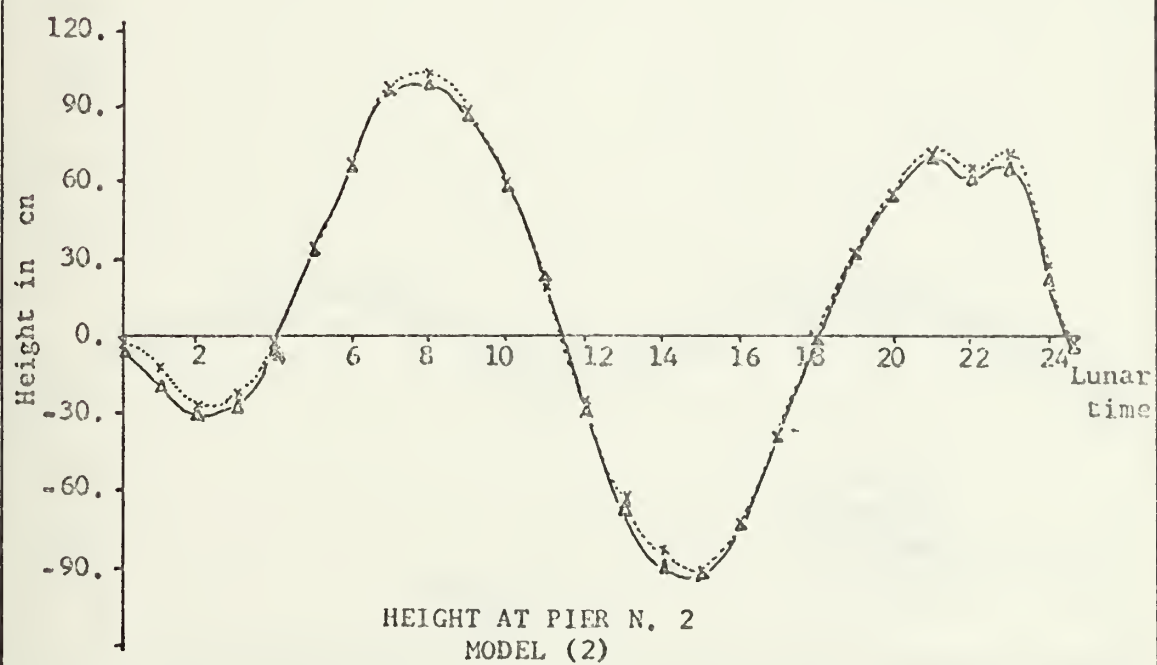
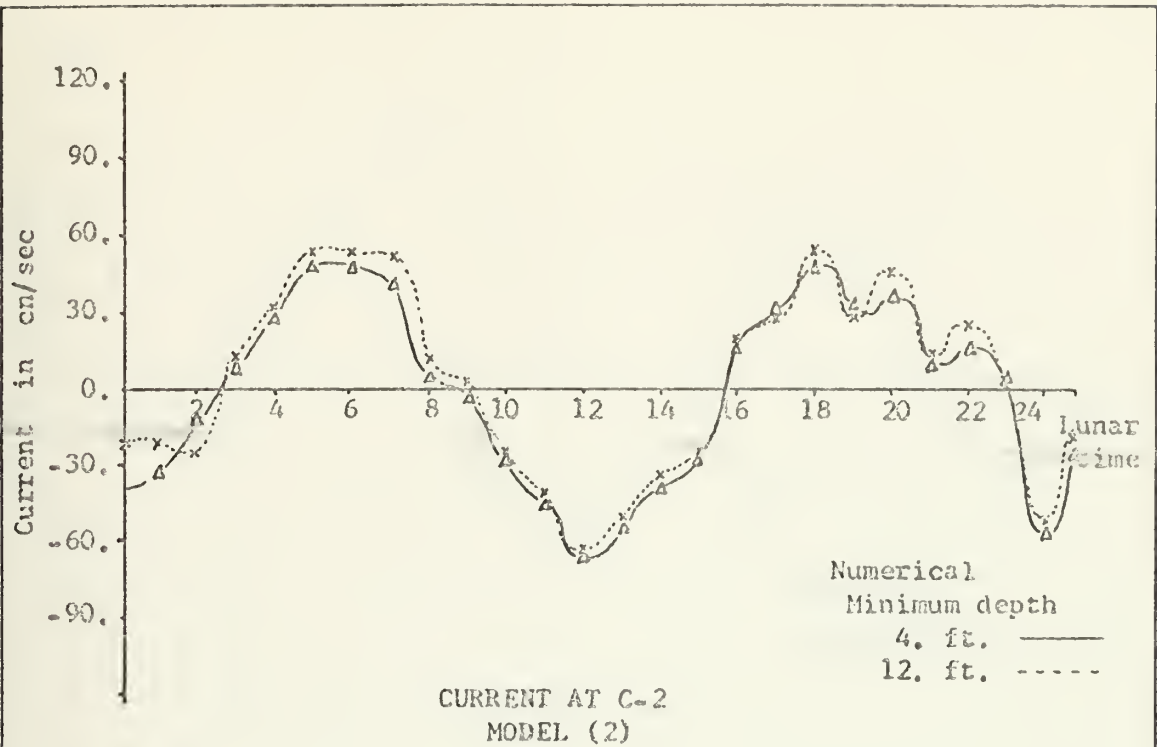


FIGURE 21

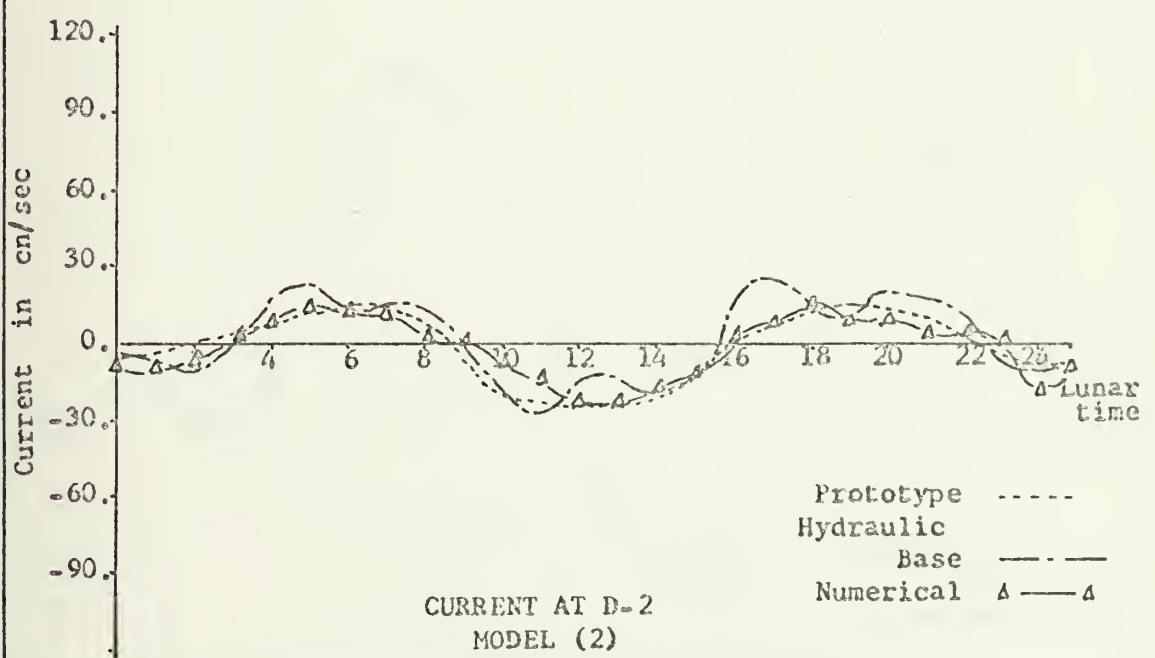
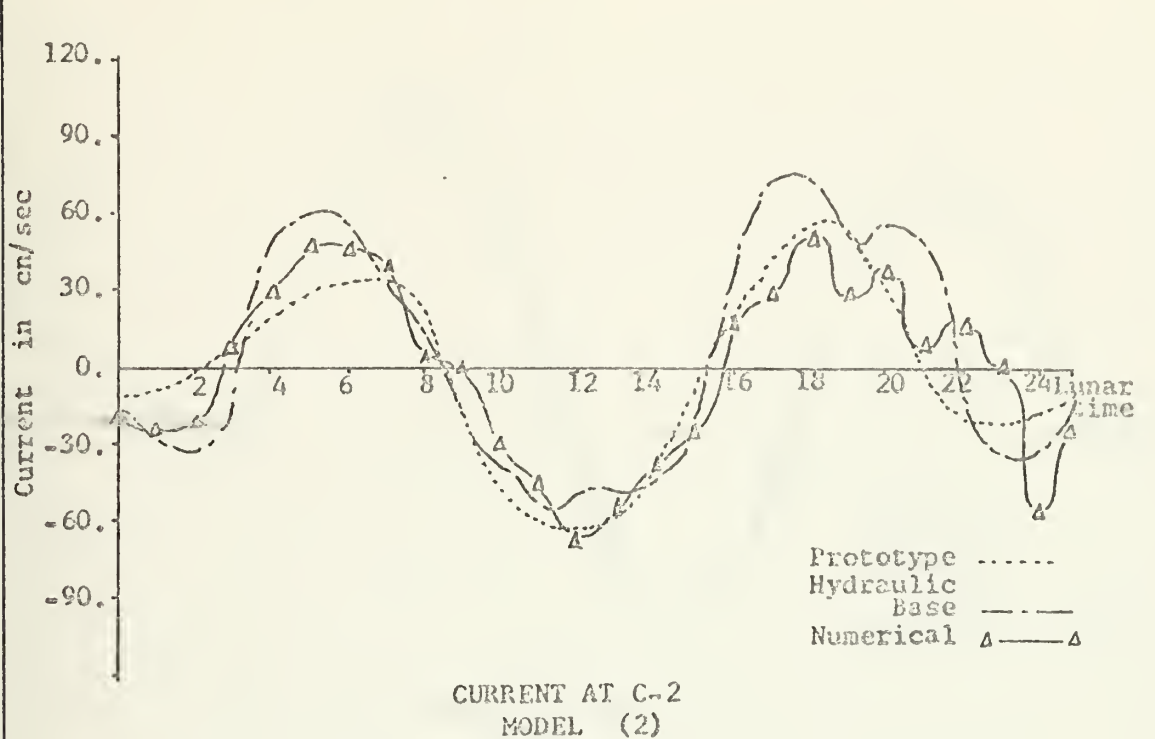


FIGURE 22

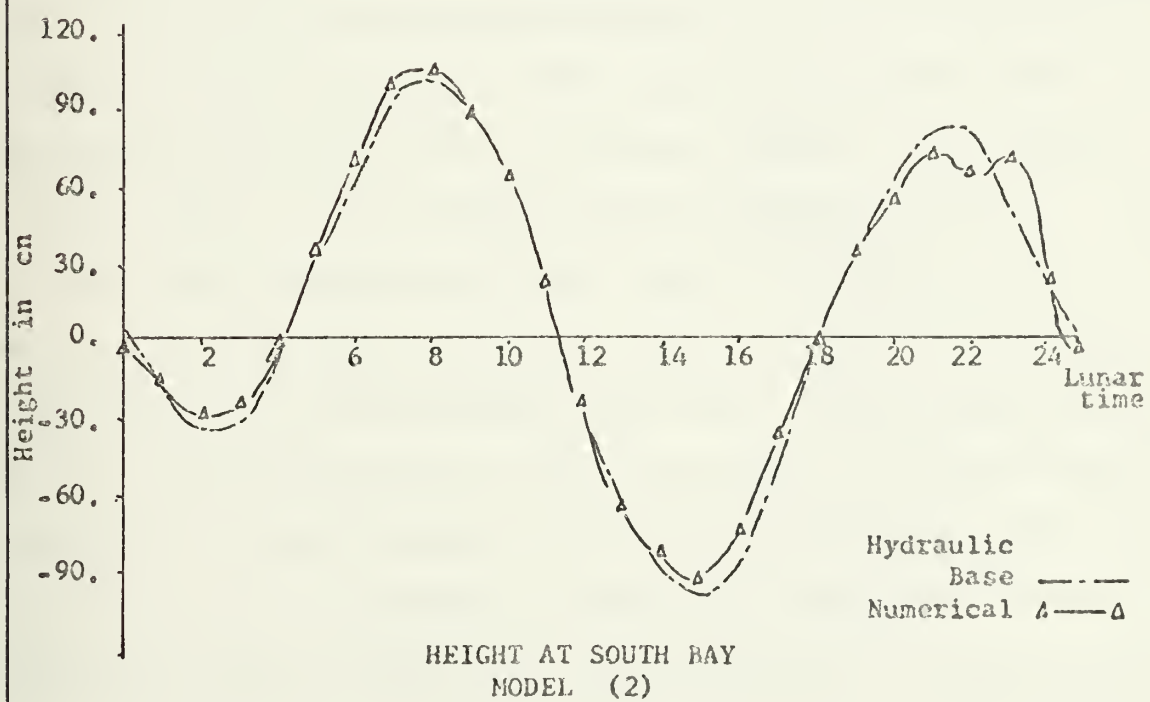
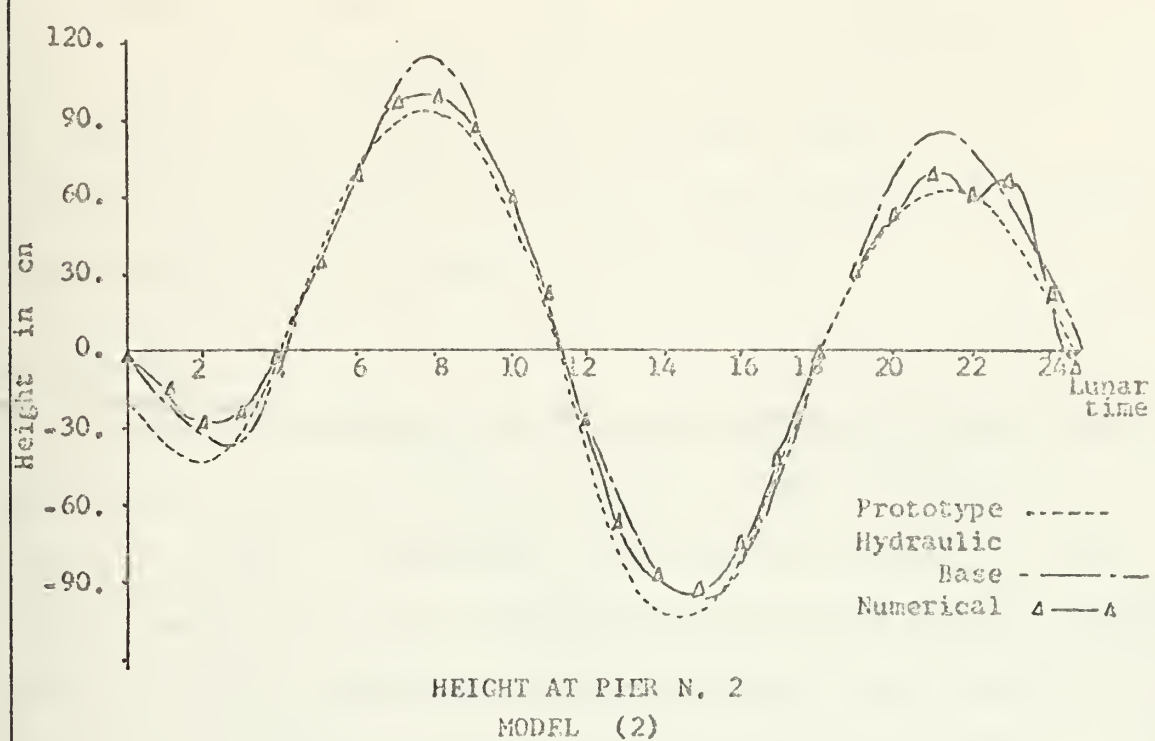


FIGURE 23

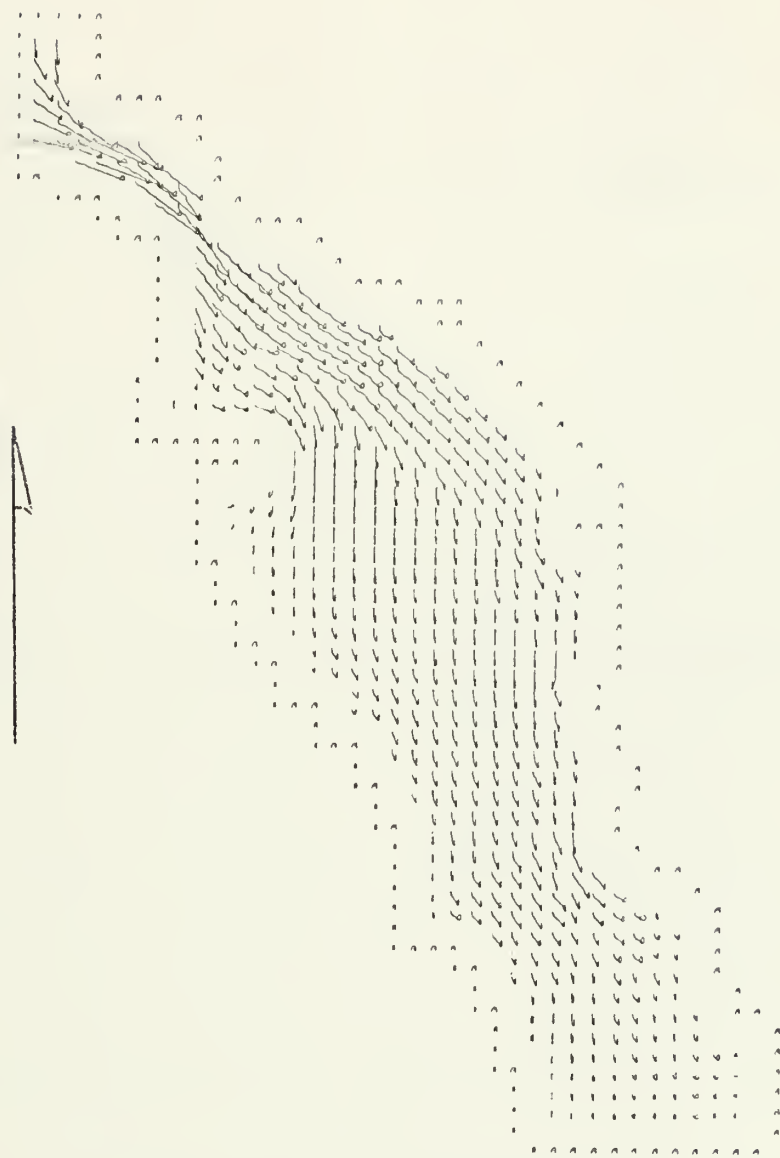
are shown in figures 24 and 25, and of the entire bay in which model (1) and model (2) have been matched is shown in Figures 26, 27, 28. In all of these figures, the direction and magnitude of the flow are represented by the direction and scaled length of the arrows.

E. MODEL (3)

Several alternatives of a second entrance and diffusion were tested by means of the hydraulic model conducted by the U. S. Corps of Engineers. Because the purpose of this work is mainly to make a comparison between different models, only one of the alternate second entrances was examined in the numerical model, and no diffusion study was made.

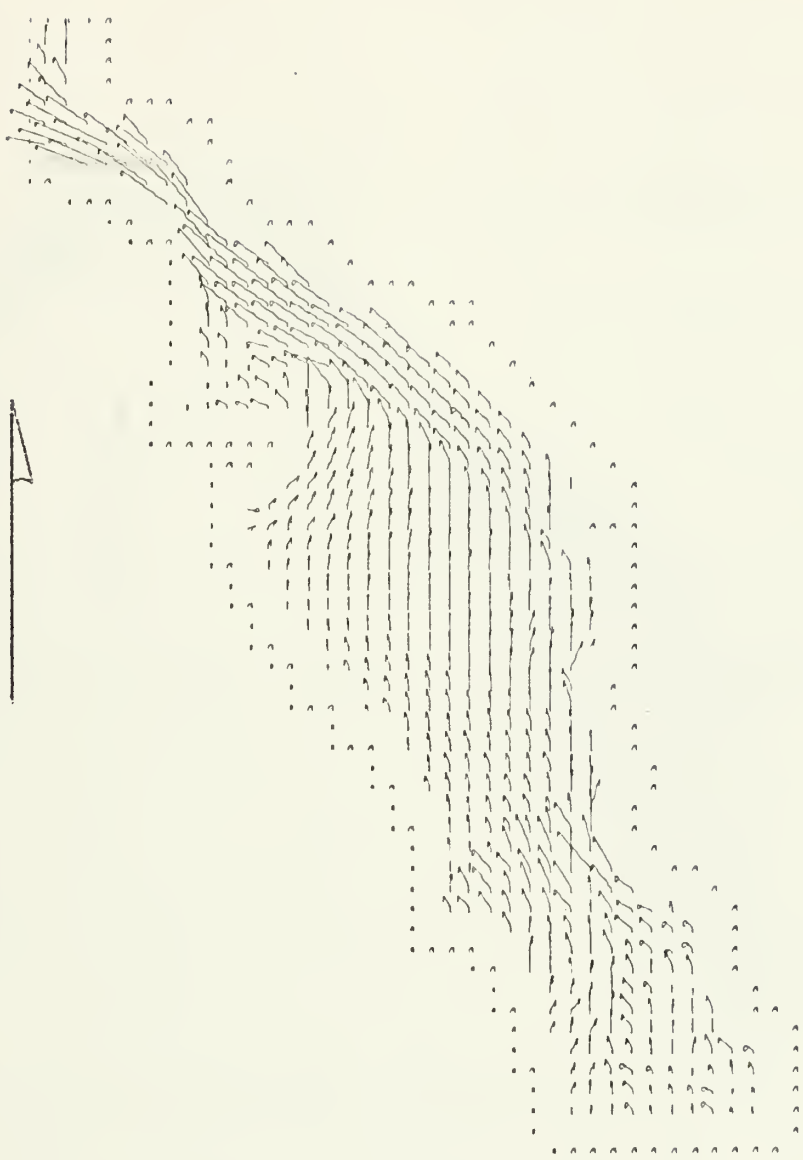
Model (3), with the proposed second open boundary at Crown Cove, was run in a similar manner to model (2). The input for the northern open boundary was obtained from the results of the model (1). The same oceanic tidal values measured at Ballast Point, in Zuniga channel, were chosen for the input at the proposed second channel entrance.

The same currents and tidal values developed in the model (2) using the prescribed conditions with α and R of 0.992 and 0.003 respectively were used. Their characteristics and interpretations were discussed in the previous section. No other values of the tuning parameters were tested because the purpose of this last model is to test model (2) with an additional open entrance.



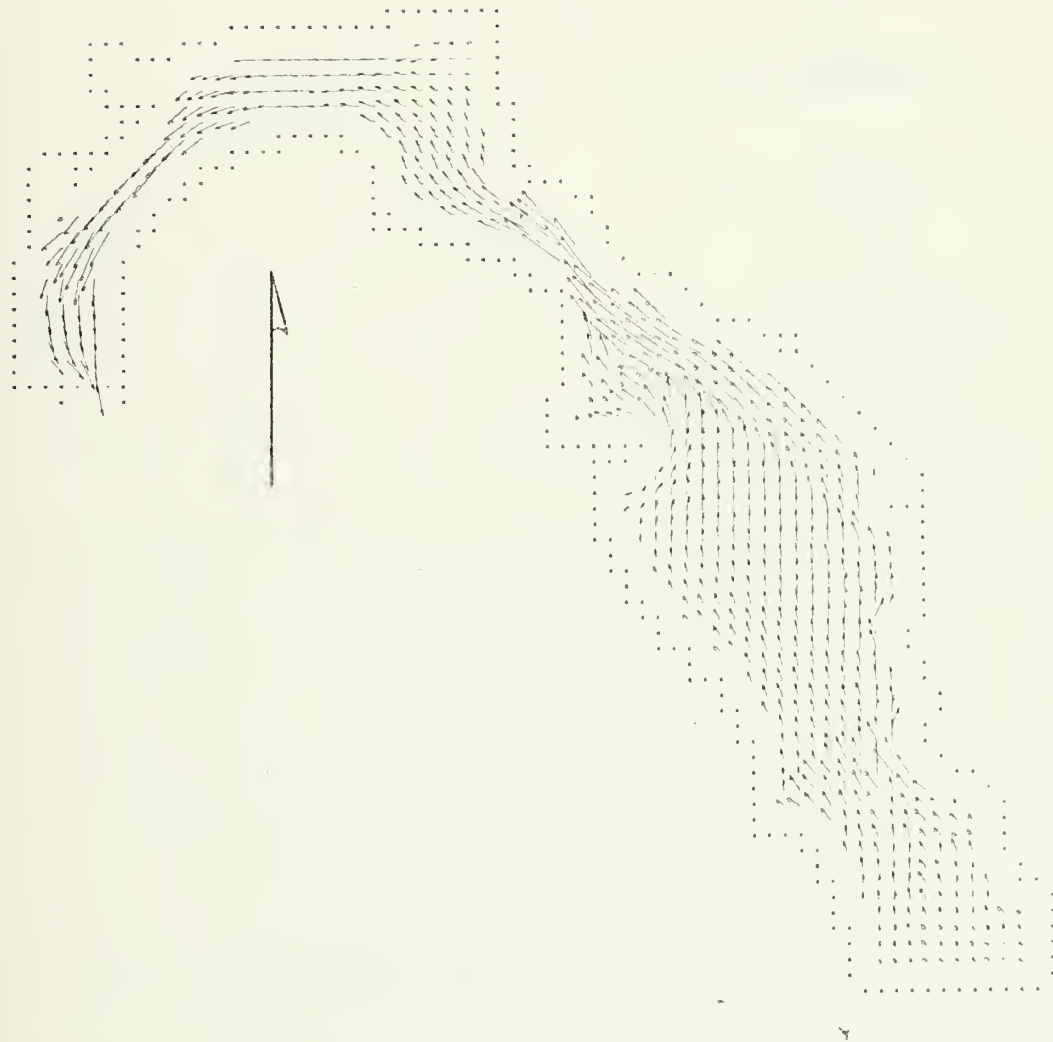
CURRENT DISTRIBUTION IN MODEL (2)
TIME = 3 hr.

FIGURE 24



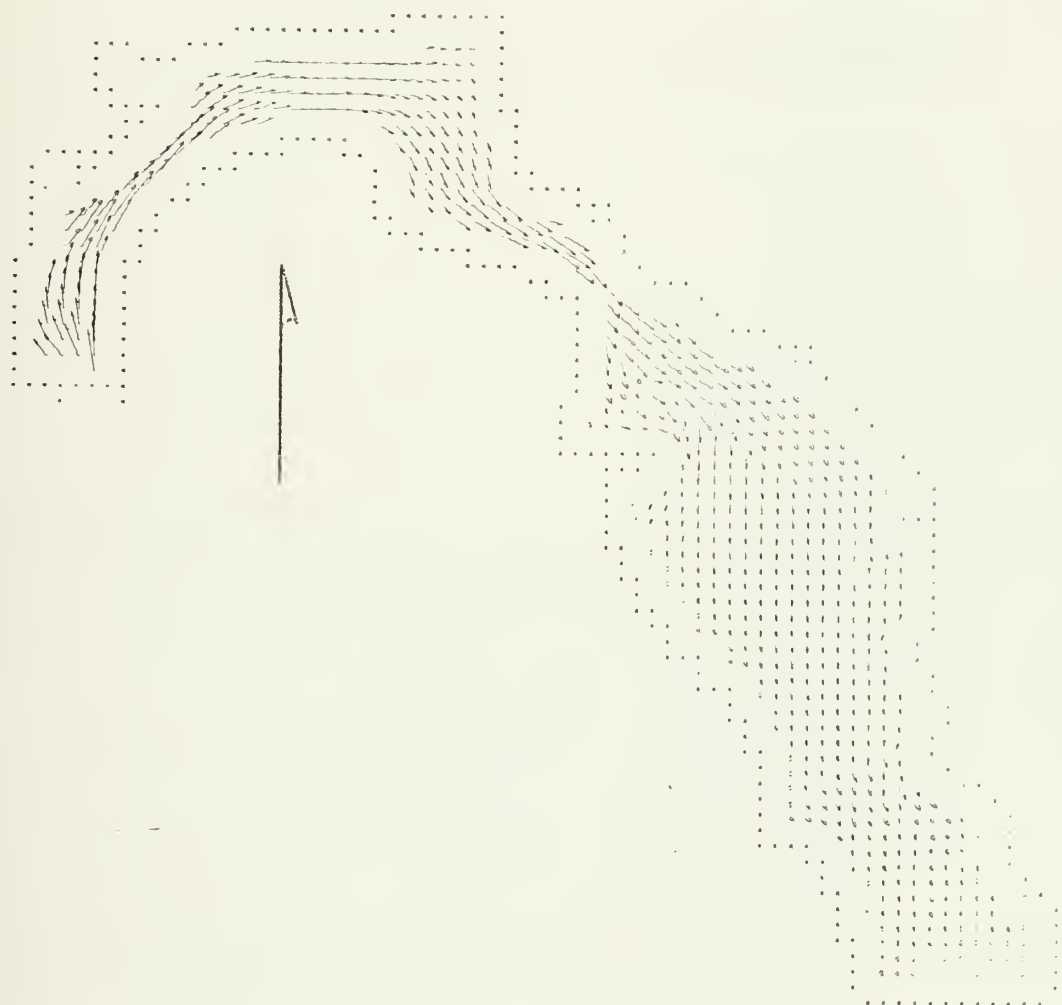
CURRENT DISTRIBUTION IN MODEL (2)
TIME = 9 hr.

FIGURE 25



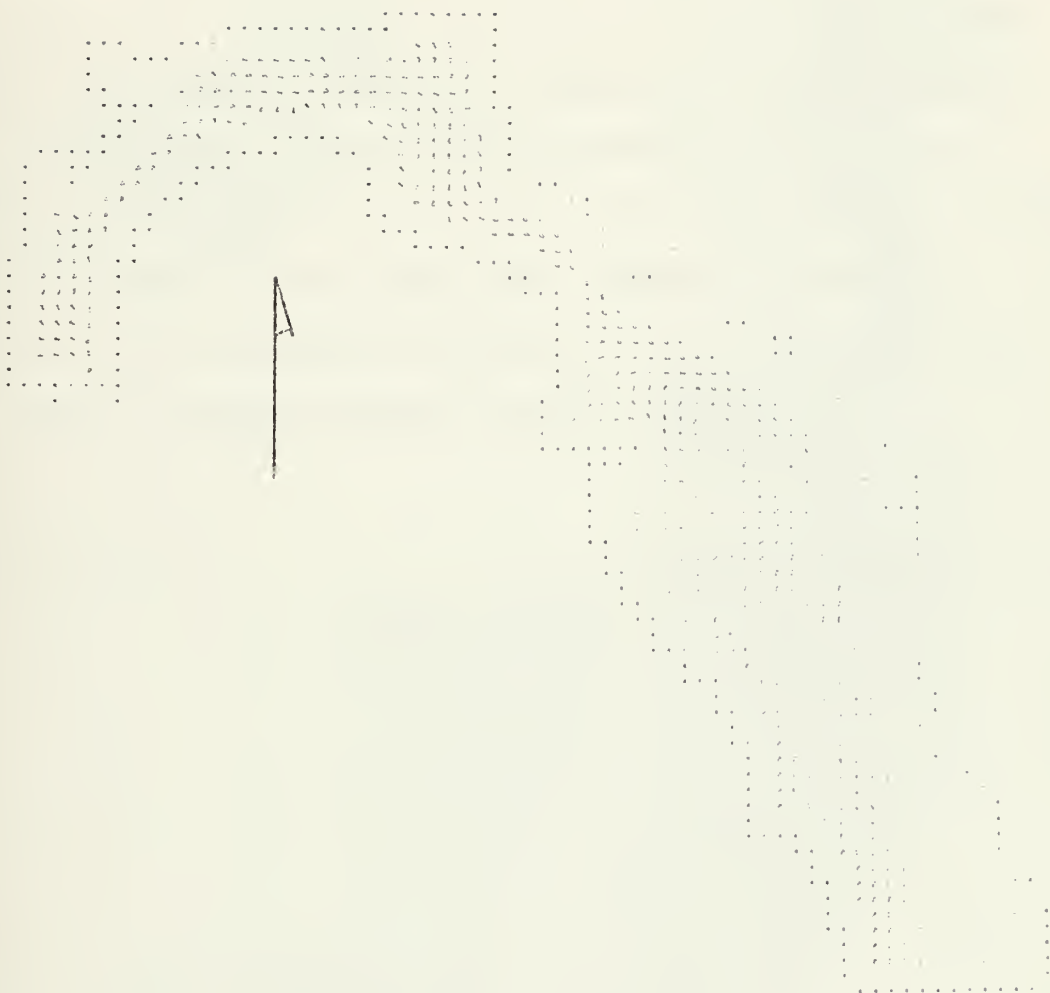
CURRENT DISTRIBUTION IN MODELS (1) and (2)
TIME = 9 hr.

FIGURE 26



CURRENT DISTRIBUTION IN MODELS (1) and (2)
TIME = 3 hr.

FIGURE 27



CURRENT DISTRIBUTION IN MODELS (1) and (2)
TIME = 15 hr.

FIGURE 28

The results obtained by the U. S. Corps of Engineers shown in Figures 29 and 30 are compared to the results in currents and height of water for this model shown in Figures 31, 32 and 33. Pictorial representations of the current distributions are shown in Figures 34 and 35. The same representation obtained from the U. S. Corps of Engineers Hydraulic model for the complete Bay with the second open boundary are shown in Figures 36 and 37. In both groups, the flow of water throughout the proposed open entrance seems to be the dominating factor of the circulation in the southern portion of the bay. The northern portion is domained by the northern circulation and a very definite rest area is located between the two systems.

FIGURE 29)

CURRENT DISTRIBUTION HYDRAULIC MODEL (BASE TEST)
TIME = 12 hr.

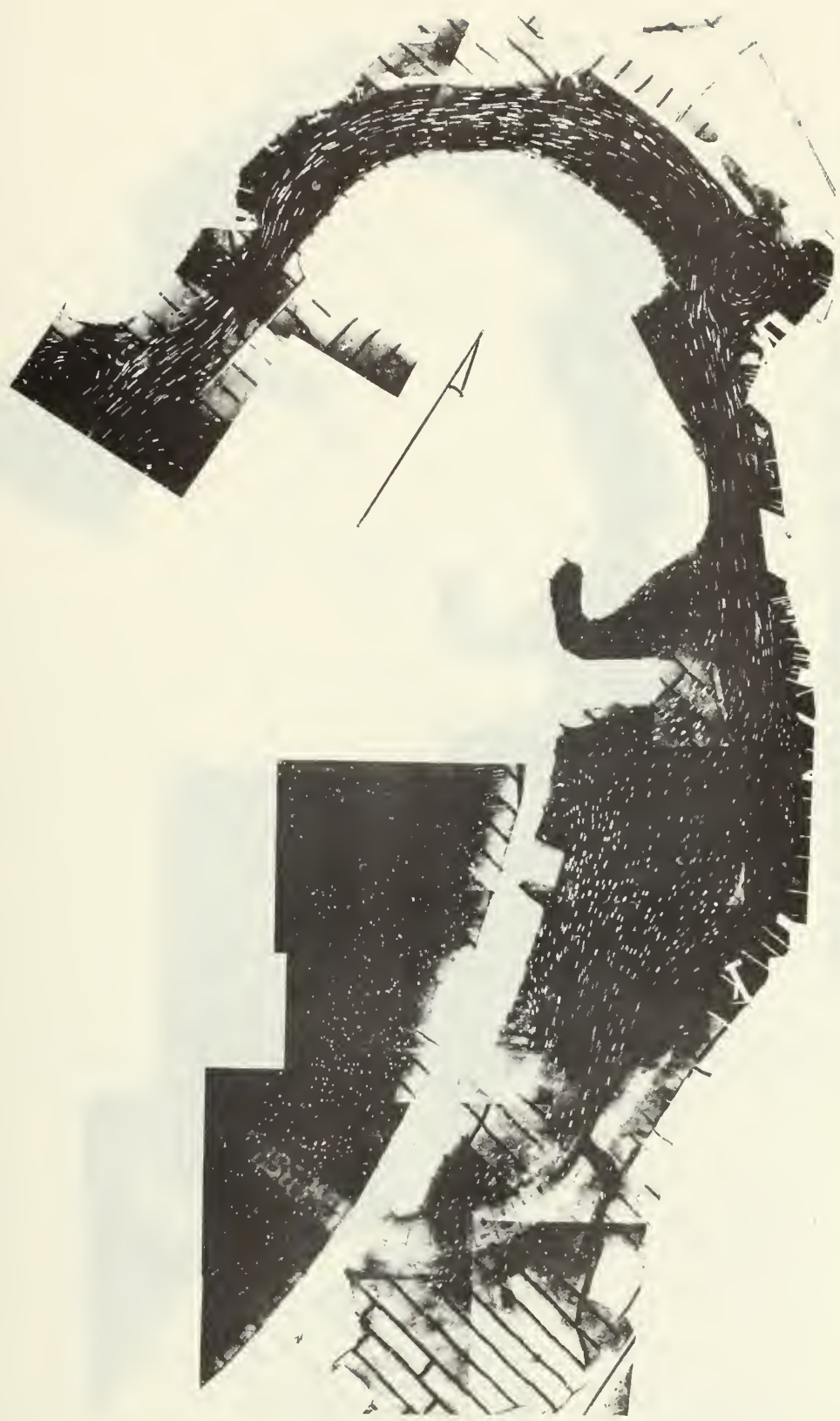
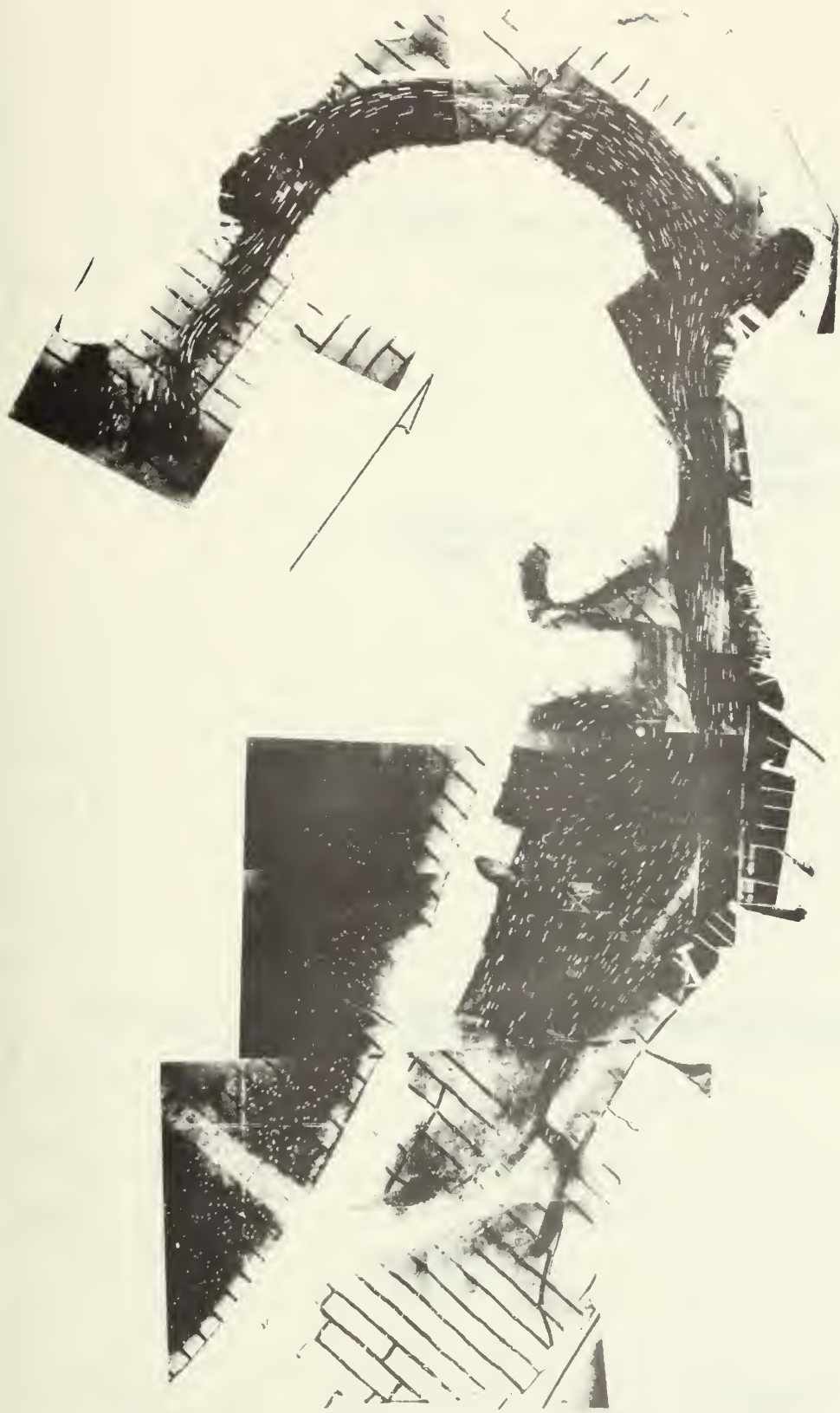


FIGURE 30

CURRENT DISTRIBUTION HYDRAULIC MODEL (BASE TEST)
TIME = 18 hr.



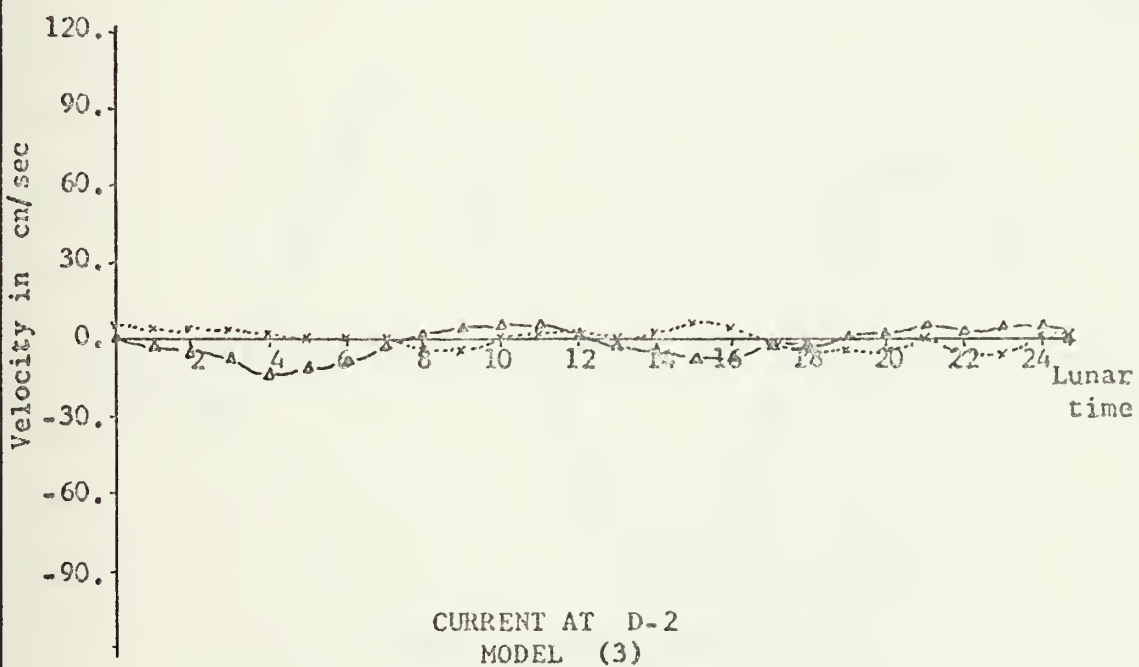
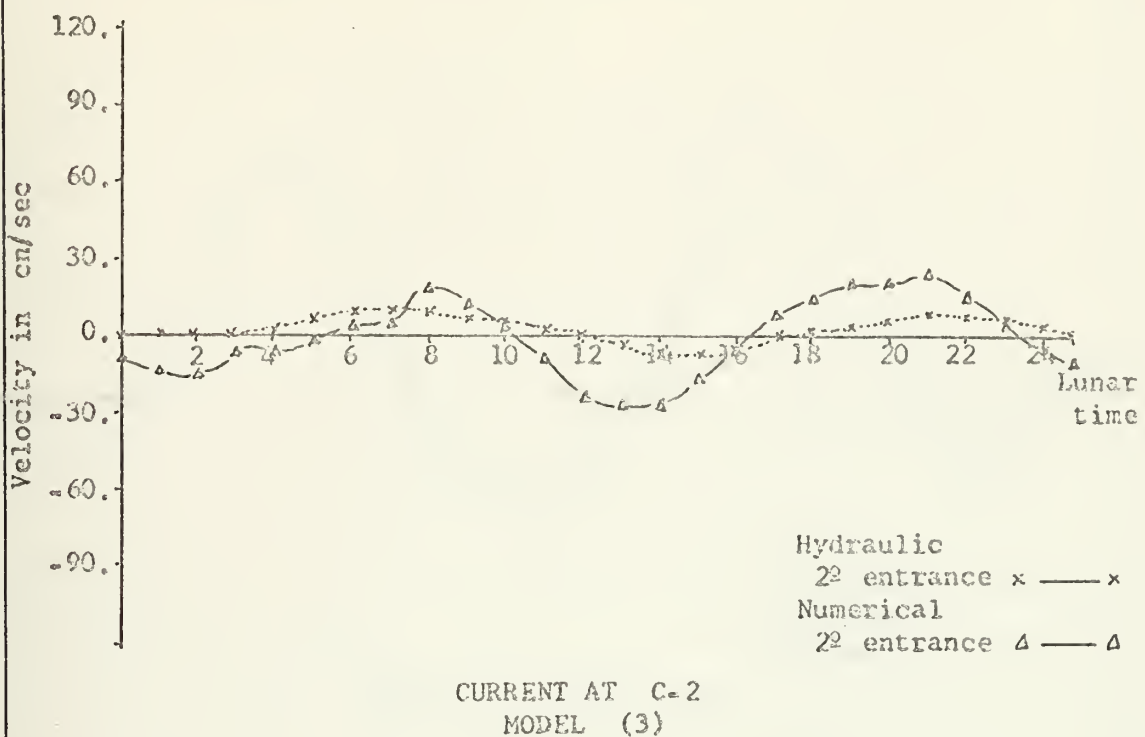


FIGURE 31

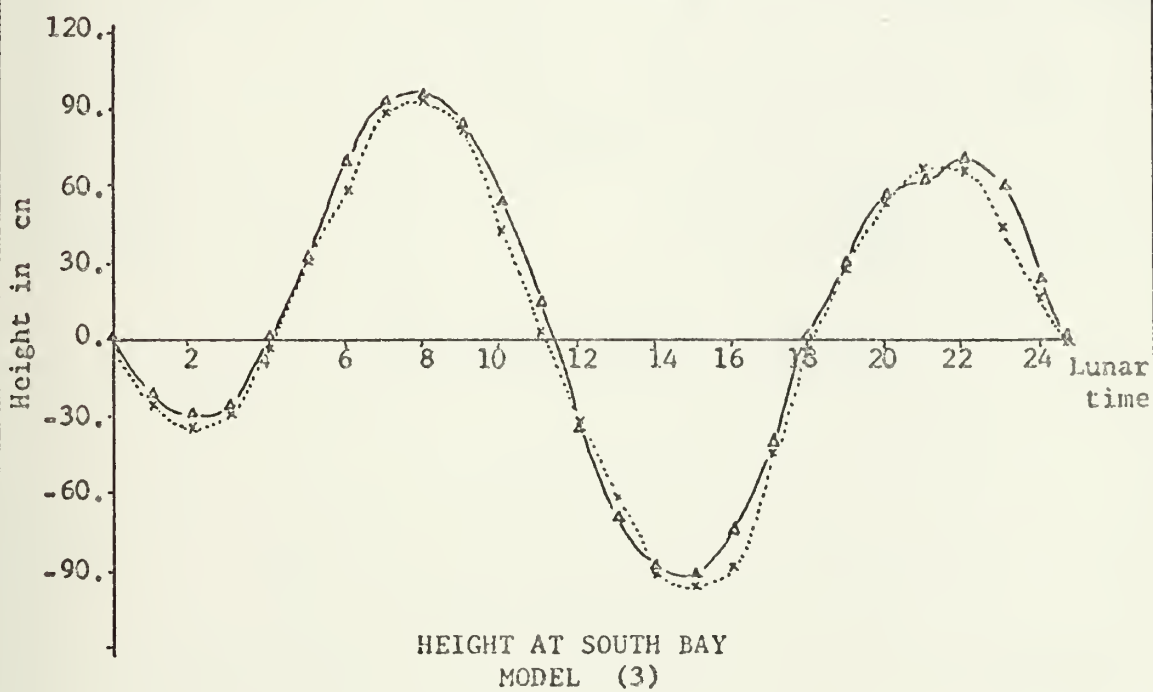
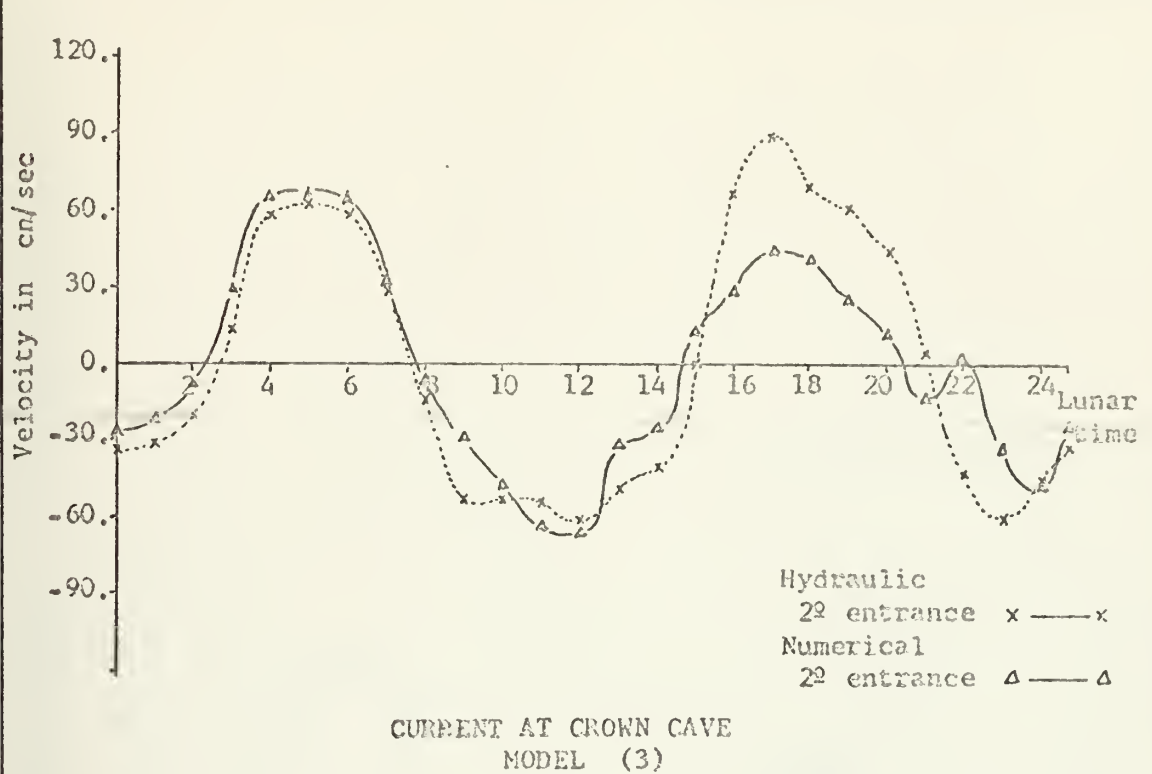
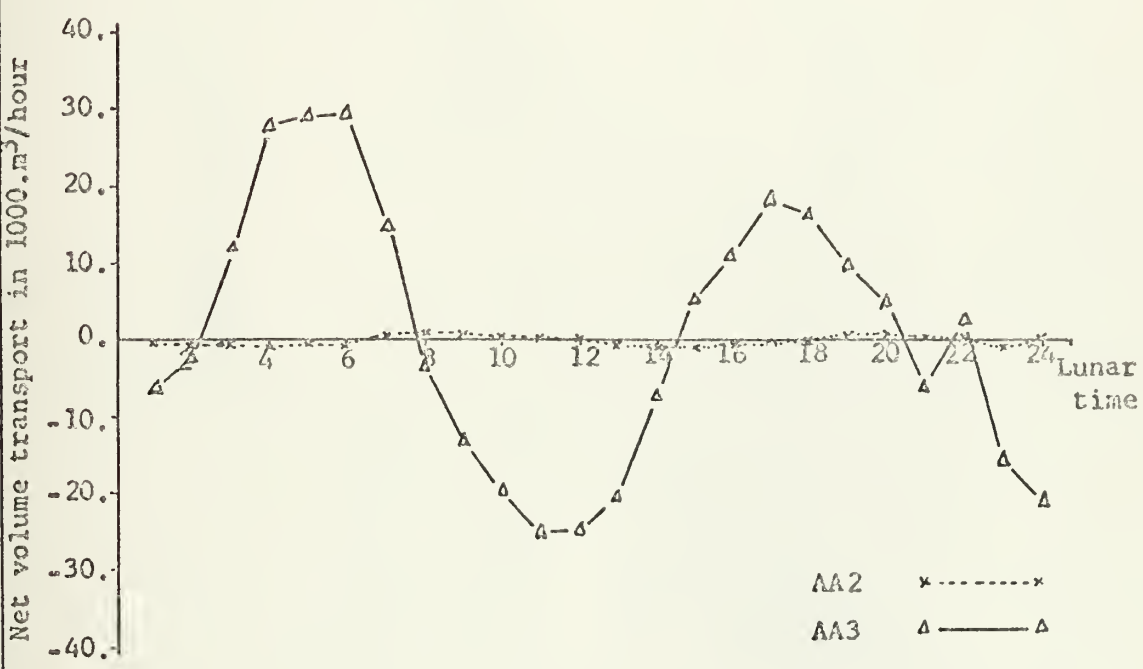


FIGURE 32



NET VOLUME TRANSPORT MODEL (3)

FIGURE 33



CURRENT DISTRIBUTION MODEL (3)
TIME = 3 hr

FIGURE 34

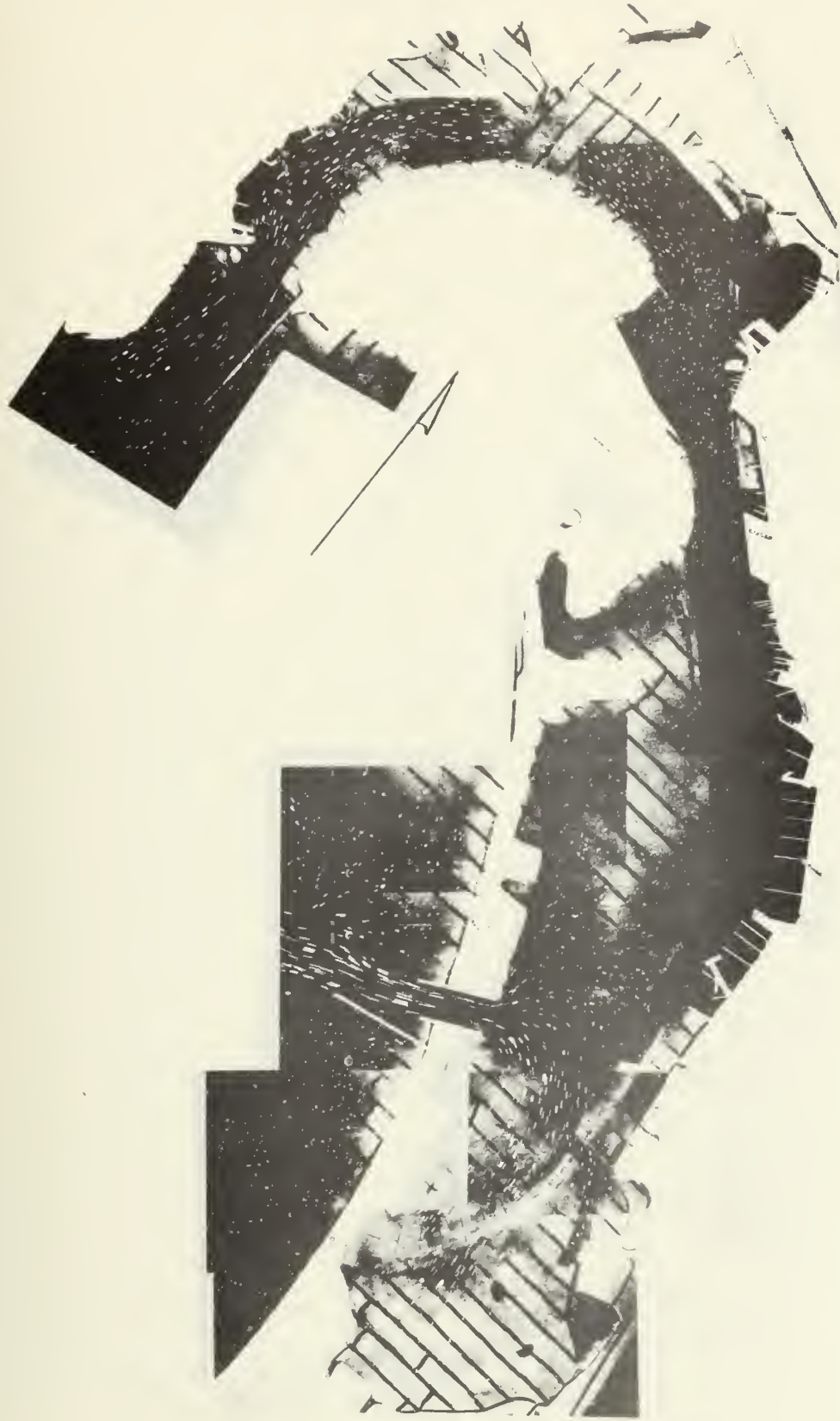


CURRENT DISTRIBUTION MODEL (3)
TIME = 9 hr

FIGURE 35

FIGURE 36

CURRENT DISTRIBUTION HYDRAULIC MODEL (PROPOSED SECOND ENTRANCE)
TIME = 12 hr





CURRENT DISTRIBUTION HYDRAULIC MODEL (PROPOSED SECOND ENTRANCE)

TIME = 18 hr

FIGURE 37

IV. MERITS OF BOTH THE HYDRAULIC AND NUMERICAL MODELS

A comparison between both models cannot be made without the results of a proper test of the models under the same conditions and on an area where accurate measurements of actual conditions have been made to compare with their results. The merits of each have previously been enumerated and the goal of this work is to evaluate them.

Before ordering the merits of the numerical and hydraulic models, it is good to recall that for this specific case, the numerical model in discussion (Hansen Model), by definition, is a barotropic ($\rho = \text{constant}$) single-layer model, and the hydraulic model used a constant density fluid. The hydraulic model was based on the Froude similarity concept (inertial and gravitational forces predominate). Although the discussion is restricted by these conditions and are not applicable to general numerical and hydraulic models, these are the most commonly applied types of models.

The spatial resolution of the hydraulic model depends on the length scale and the measuring capability. In the numerical model, topographic features are represented in terms of grid points. To obtain a good representation of bathymetry, small grid size is needed that results in an extremely large array. A compromise between spatial resolution and core size must be reached.

The time resolution in the hydraulic model depends on the similitude criteria and can be scaled to obtain a reliable result. In the numerical model, it is governed by the availability of computer time, i.e., the smaller the time step, the more computer time required.

The scaling in the hydraulic model is given by the similitude criteria. As was pointed out in the section dealing with the hydraulic model, these criteria compromise scales causing distortions in the model and oblige the use of some specific dimensionless number for each specific case. The introduction of distortions in the model limits its uses because some other terms ignored in the selection of the dimensionless number may become important.

In the numerical models, the flow is described by the solution of the equations of motion which includes terms of different orders and degrees. Each term describes some specific characteristic of the flow. The characteristics of the flow will depend on the shape, location, external forces applied, bathymetry, and properties of the fluid. In describing these flows by the equations of motion, some of the terms become dominant and some others can be considered negligible or included in some coefficients. In the case of the Hansen Model, this was accomplished by neglecting the non-linear momentum flux terms. The choosing of the proper terms becomes invalid if improper considerations are done. Then, an improper scaling can invalidate these selected portions of the equation.

Furthermore, the finite solution of this equation does not permit the continuous computation of the flow. The computation is done by time and spatial steps that may cause large errors in the model if proper precautions are not taken. For example, the coefficient of Eddy Diffusion is defined in the finite solution in terms of spatial and time steps. Then, its value becomes affected by the grid size and time step.

Obtaining data from a hydraulic model is difficult and limited by the instruments and the distortion in the scale of the model. Sizes and numbers of the measurement instruments are limited, and the region where these instruments can perform a measurement in the model is restricted by their sizes. In the numerical models, the characteristics of the flow is computed at each grid point; thus, it is available at each point and at each time step. Deficiencies in the differential solutions introduce errors in these grid points in the vicinities of the coast lines and input boundaries. In the hydraulic model, equivalent errors exist in the input boundaries; good resolutions have been claimed for near shore regions that can be questionable because difficulties in the measurements of quantities, such as current speed, in these regions makes it a not always tested assumption. Besides, surface tension becomes important in these regions that compromises the model.

The cost and time are some of the larger limitations in programs and research. Hydraulic models are expensive

and take months and sometimes years to achieve a satisfactory calibration. The use of the numerical models generally decreases considerably these limiting factors. A limitation of numerical models is that they require large computers that are not always available.

Simulated diffusion or dispersion of pollutants has been accomplished in both types of models with comparable results [1 and 5]. In the hydraulic models, this is achieved by direct measurements of dye materials introduced into the model. The conservation of mass equation is used for this computation in the numerical model. All the previous measurement and computation problems are taken into consideration for a proper evaluation of these factors.

V. CONCLUSIONS

The comparisons between the hydraulic and numerical models dealing with the modeling of San Diego Bay and its proposed modifications, are considered separately for general cases and for each of the different tests involved in this study. The Hansen Hydro-numerical Model was applied to the Bay to compare its solution against the U. S. Army Corps of Engineers hydraulic model. The description of both models and the manner of how these numerical and hydraulic models were applied to San Diego Bay has been discussed in detail.

In general, the numerical model is more easily handled for topographic changes than the hydraulic. The latter cannot be stored for future uses after being run as is done with the numerical model because of space limitation. A comparison of time and cost is not possible because no data are available for the model of the U. S. Corps of Engineers. The three numerical models consumed for final runs a total of 7 hours 15 minutes CPU time in the IBM 360/67. Adding an average of three times this amount for calibration, the cost becomes approximately \$21,000 (U.S. dollars). It would take about three weeks for a trained programmer to obtain the complete answer for this specific case.

The added easier possibility of including the input of wind gives to the numerical model better ability to represent

the prevailing conditions. The same numerical model can include the wind. Usually completely different hydraulic models must be built to simulate wind because of similitude considerations.

The hydraulic model has better space resolution than the numerical model. A method was tested for transferring boundary values from one numerical model to another to give the model the ability to divide long estuaries into smaller areas improving in this way the resolution of the numerical model. With the use of this method, two different but dependent models were run to represent the complete bay. A constriction in the configuration of the bay was chosen for the overlapping region. A similar procedure is used in the hydraulic model to save space in long hydraulic models. To achieve it, the bay is distorted in a narrow location in a fold-like procedure. The model is calibrated at both sides of the curve. This procedure gives the possibility of dealing with a model of a smaller scale that gives more details of the area, but special care must be taken so as not to introduce errors in the time scale. A similar procedure can be done in the numerical model if the excess area is small and can be accommodated in the free space of the first grid. The possibility of running two completely different hydraulic models seems to be impracticable because of economics.

The numerical model reproduced very well the sea level and currents for the cases tested, provided boundary

treatments are correct. The boundary treatments sometimes are not easily achieved and are a matter of decision in order to represent properly the coast line and channels in the grid. Representation of sea level seems to be equally correct in both models, but the current results seem to be better in the numerical model except near boundaries and shorelines. The seich-like oscillations developed in the numerical model must be taken into consideration if the model is to be representative of the total bay. If only a part of the bay is under consideration (for example model (2)), the sieche oscillations should be smoothed out because they are not representative of the bay.

No comparison can be made of net volume transport because no evaluation in the hydraulic model is available. These computations were made in the numerical model based on the computed velocities. The computed values seem to be reliable enough.

It was pointed out in the section dealing with model (2), that the boundary conditions in the numerical model must be given special treatment when the area becomes dry during low tide. A minimum depth of 120 cm was fixed in the numerical model in order to prevent any problem, and the southern extreme of the bay was eliminated because its depth was below 50 cm. No special problem seems to appear in hydraulic models, for the case of portions of the area becoming dry, but special care must be taken if areas become shallower than 1 cm. because then surface tension is important. This

minimum depth had not been discussed in previous literature for numerical models, and no attempt to evaluate these conditions was made in this study.

In the model with the proposed second entrance, the initial assumption of increasing the flushing of the bay seems to be reasonable. The circulation of the southern portion of San Diego Bay will be almost entirely governed by the second entrance. But, from the computed net volume transport in the section AA2, it is shown that the interchange of water between the northern and southern portion of the bay at this section will be almost negligible. Comparing the pictorial representations of both models for this special case, an area of decrease of current speed can be noticed between Pier No. 2 and D-2 gages where both models indicate that the flow of the bay will be divided into two separate systems and the projected second entrance will provide the water for the southern system. This would result in decreased dispersion of pollutants introduced to the bay in this region.

HANSEN'S HYDRODYNAMICS MODEL

SAN DIEGO BAY (1)

ECONOMIC ASSESSMENT

卷之三

LIST OF PARAMETERS IN THE PROGRAM

卷之三

GRID INDEX (PARALLEL TO ENTRANCE)
GRID INDEX (PERPENDICULAR TO ENTRANCE)

Z_U^(N,M) U-COMPONENT OF WATER ELEVATION (CN) (CN/SFC)

V(N,M) V-COMPONENT OF VELOCITY (CM/SEC)
RAD(N,M) RESULTANT CURRENT SPEED (CM/SEC)
ANG(N,M) ANGLE (FROM GEODESIC NORTH) OF
 SPEED (THE CURRENT DIRECTION)

ON (N, M) FIELDS FOR SUMMATION OF U AND V COMPONENTS OF CURRENTS FOR COMPUTATION OF REST CURRENTS

REST(N,M) AVERAGE SPEED OF REST CURRENT (CM/SEC)
DIR(N,M) DIRECTION OF REST CURRENT (IN GENGRAPHIC COORDINATES)

ZM(N,M) USED IN JO5 AS INTERMEDIATE FOR SMOOTHING
 ZST(N,M) USED IN JO5 AS INTERMEDIATE FOR AVERAGING
 HTZ(N,M) SYMBOLIC WATER DEPTHS AT WATER ELEVATION (Z) POINT

$HTZ = 1$ INNER POINT (COVER WATER)
 $HTZ = 0$ OUTER POINT (COVER LAND)
 $HTZ = -1$ NORMAL BOUNDARY POINT
 $HTZ = -2$ POINT ON OPEN (ENTRANCE) BOUNDARY

HTU(N, M)
HTV(N, M)
WATER DEPTH AT POINT
INNER POINT
OUTER POINT
SECONDARY POINT
DEPTHS = 0
HTV = -1

NUMERICAL PROGRAMS

$HGU(N, M)$
 $HGV(N, M)$
 $XK(N, M)$
 $YK(N, M)$
 $Q(N, M)$
 $VAC(N, M)$

$A(1)$
 $A(1)$
 $A(2)$
 $A(3)$

$NU(I)$
 $MN(I)$

$NZ(I)$
 $MZ(I)$

$NA(I)$
 $MA(I)$

$Z1(I)$
 $Z2(I)$
 $U1(I)$
 $U2(I)$

$X(I)$
 $ARG(I)$

$Y(I)$
 $CON(I)$

$V1(I)$
 $V2(I)$
 $V3(I)$
 $V4(I)$

AFGN

ACTUAL WATER DEPTH AT U POINTS ($HGU = HTU + Z$)
 U COMPONENT OF WIND CURRENT DIVIDED BY DEPTH
 V COMPONENT OF WIND CURRENT DIVIDED BY DEPTH
 FIELDS USED FOR A SPECIAL COMPUTATION (NOT SHOWN
 IN THE PROGRAM)
 CHARACTERISTICS OF THE WIND FIELD
 TIME WHEN WIND STARTS (SEC)
 WIND SPEED (M SEC)
 WIND DIRECTION (DEGREES COUNTED COUNTERCLOCKWISE
 FROM 0 GRID COORDINATE)
 WIND FIELD DELIMITERS (N AND M COORDINATES OF THE
 UPPER AND LOWER LEFT CORNERS OF THE WIND FIELD)
 COORDINATES (N, M) OF OPEN (ENTRANCE) BOUNDARY POIN
 TS ($i=1, 11$) SELECTED POINTS ($i=12, 24$)
 COORDINATES (N, M) OF THE BOUNDARY POINTS AT THE SE
 COND OPEN BOUNDARY
 AMPLITUDES OF FOUR DIFFERENT TIDAL COMPONENTS AT
 THE OPEN BOUNDARY (CM)
 AMPLITUDES OF FOUR DIFFERENT TIDAL COMPONENTS AT
 THE SECOND OPEN BOUNDARY (CM)
 INTERMEDIATE PARAMETERS FOR TIDAL COMPUTA
 TION OF ASTRODYNAMICAL TIDES AT OPEN (ENTRANCE) BOUN
 DARY
 INTERMEDIATE PARAMETERS FOR TIDAL COMPUTATIONS AT
 THE OPEN BOUNDARY
 NAMES OF SELECTED POINTS
 WATER ELEVATION AT SELECTED SPECIAL POINTS
 SPFFEN OF CURRENT AT SPECIAL POINTS
 DIRECTION OF CURRENT AT SPECIAL POINTS
 ARBITRARY PROBLEM NUMBER

F
G SIGMA
ALPHA
R
ROL
RBETA
C
DL
DT
T1
T2
T3
NE
ME
KEY
SIZE
ING
TUE
TW

TIC
LEN
POC
TRAN

BETA
A1
A2
A3
A4
A5

C1
CE

SI
NURU
NURV
JA

CORIOLIS PARAMETER (SEC-1)
GRAVITY ACCELERATION (CM SEC²)
GANGULAR VELOCITIES OF M2 TIDE (RADIAN SEC)
USED IN COMPUTATION WHERE M2 TIDE ONLY IS ENTERED AT THE OPEN BOUNDARY
SMOOTHING PARAMETER (USUALLY 0.92 TO 0.99)
DENSITY COEFFICIENT OF THE AIR (GM CM⁻³) (1-162 (X 10⁻³)
COEFFICIENT OF GHOST ROPHIC WIND (USUALLY 0.65)
DRAG COEFFICIENT (3.2 X 10⁻⁶)
1/2 STEP IN SPACE (CM) (1/2 OF GRID SIZE)
TIME (SEC)
TIME INTERVAL BETWEEN FIELD PRINTOUTS (SEC)
FIELD OUTPUT COUNT (SEC)
INITIAL TIME COUNT FOR PLOT PROGRAM
DELIMITERS OF ENTIRE FIELD (THE GRID SIZE)

END TIME OF COMPUTATION (SEC)
NUMBER OF A(1) (NUMBER OF WIND FIELDS)
NUMBER OF OPEN (CENTRANCE) BOUNDARY POINTS
NUMBER OF POINTS AT SECOND OPEN BOUNDARY
NUMBER OF WIND FIELDS
TWICE THE NUMBER OF WIND STARTS (SEC)

COUNTERS
SUMMATION OF TRANSPORT THROUGH A SPECIFIED SECTION

(1-ALFA) /4
2(DT)
F(A1)
R(A1)
DT/DL
G(A4)

INTERMEDIATE PARAMETERS

O FILE NO WIND, ELSE ANY VALUE DIFFERENT THAN 0
C(A(2))X(10000)

NOTE
10000 IS UNIT CONVERSION FACTOR. A(2) IS READ IN AS M/SEC AND MUST BE CHANGED TO CM/SEC AFTER BEING SQUARED

TIME WHEN WIND STOP NUMBER OF SELECTED POINTS
PRINTOUT LINE LINE COUNTER USED IN SO8
INDICATOR JA DIFF. 0 READ INITIAL VALUES JA EQUAL. 0 SET Z,U,V=0

NEH
NEH
NEHH
MEHH

WERTO
WERTL
WERTR
WERTOR
WERTUL
WERTUR
WURZEL
GRZ

USED IN JO5 AS INTERMEDIATE STORAGE LOCATIONS FOR U
AND V VALUES DURING SMOOTHING AND AVERAGING OPERATIO
NS

SQRT(ZM**2+ZST**2)
A3(WURZEL)

T3, T4, STV, ETV, TINCV, STH, ETH, TINCH ARE PARAMETERS USED IN THE
PLOTTING PROGRAM

T2
T3
ETH
ETV
TINCH
TINCV
STH
STV
HT
VEC
NALL
TE1
AA1
AA2

START TIME FOR STORING SPECIAL VALUES ON CYLINDER
USUALLY SET TO ZERO WHEN JA=1, SET TO STARTING TIME
START TIME FOR PRINTING VALUE ARRAYS HORIZONTALLY
TIME OF THE LAST WATER HEIGHT PLOT
TIME OF THE LAST VECTOR PLOT
TIME INCREMENT BETWEEN WATER HEIGHT PLOTS
TIME OF THE FIRST WATER HEIGHT PLOT. MUST BE GREATER
THAN T2 AND LESS THAN (T+T1+T1/2)
TIME OF THE FIRST VECTOR PLOT. MUST BE GREATER THAN T2
AND LESS THAN (T+T1+T1/2)
PLOT FLAG FOR WATER HEIGHTS
0 = DO NOT PLOT
1 = PLOT FLAG FOR VECTOR PLOTS AND A CONTROL FLAG FOR DOI
0 = DO NOT PLOT
1 = PLOT

COUNT OF THE NUMBER OF PLOTS EXPECTED
TIME SAVED FOR START AND END OF THE PROGRAM

PROFILES FOR MASS COMPUTATIONS

THE DATA INPUT CARDS

CARD 1 FORMAT 2413
JA,NE,IZE,IUE,KKE,NURU,NG
CARD 2 FORMAT 9F8.0
AFGN,G,ALPHA,RBETA,C1
CARD 3 FORMAT 9F8.0
DT,TE,TW,T1,T2,SI,T,T3
DT 102 TIME STEP (SEC)
TE LENGTH OF THE COMPUTATION
TW TIME WHEN WIND STARTS
T1 TIME INTERVAL BETWEEN PRINTPOINTS
T2 FIELD OUTPUT COUNT, IF FIELD OUTPUT DESIRED FROM START
SI IF THE COMPUTATION, OTHERWISE EQUAL TO T1
T STARTING TIME. MOST BE GREATER THAN T1
T3 TIME WHEN WIND STOP
SI TIME (INITIALIZED 0) IF PREVIOUS COMPUTATIONS MADE
AND READ FROM TAPE, GIVE THE TIME PREVIOUS
COMPUTATION ENDED
IF PLOT DESIRED, TIME WHEN FIELD ARF REQUIRED FOR
PLOTTING
CARD 4 FORMAT 6E12.4
DL,F,SIGMA,R,ROL,C
CARD 5 FORMAT 2413
NZ,MZ (FIRST BOUNDARY)
CARD 6 FORMAT 2413
NZ,MZ (SECOND BOUNDARY)
CARD 7 FORMAT 2413

NU, MU

CARD 8

FORMAT 2613

NA, MA

CARD 9

FORMAT 10A4

V1(I)

CARD 10

FORMAT 9F8.2

A(I)

CARD 11

FORMAT 12F6.0

HTZ

CARD 12

FORMAT 12F6.0

HTU

CARD 13

FORMAT 12F6.0

CARD 14

FORMAT 9F8.3

Z1,Z2,U1,U2

CARD 15

FORMAT 9F8.3

Z3,Z4,U3,U4

CARD 16

FORMAT (A8,2X,3F10.0)

HEAD,STV,ETV,TINCV

CARD 17

FORMAT (A8,2X,3F10.0)

HEAD1,STH,ETH,TINCH

Z3() Z4() TIDE COEFF.

Z5() Z6() TIDE COEFF.

Z7() Z8() TIDE COEFF.

Z9() Z10() TIDE COEFF.

BALAST POINT
PIER N²
NAVY PIER
SOUTH BAY

SAN DIEGO BAY AREA PROGRAM 1

```

COMMON/A/Z(53,30),U(53,30),V(53,30),ZM(53,30),HTV(53,30),HTZ(53,30),XK(53,30),
1HGV(53,30),HGU(53,30),HTU(53,30),HTV(53,30),ANG(53,30),Q(53,30),
2YK(53,30),RAD(53,30),ANG(53,30),NU(60),MU(60),ZI(60),Z2(60),V1(60),
1V2(60),U1(60),U2(60),V3(60),V4(60),X(4),ARG(4),NA(60),MA(60),V1(60),
1V2(60),U1(60),U2(60),V3(60),V4(60),X(4),ARG(4),NA(60),MA(60),V1(60),
2Z3(12),Z4(12),Z5(8),Z6(8),Z7(8),Z8(8),Z9(8),Z10(8)
COMMON/C/AFGN,F,A1,AA2
COMMON/C/ALPHA,R,ROL,RBETA,CIDL,DT,T,T1,T2,NE,ME,TE,KKE,IZE,IUE,TW
3,GSIGMA,A1,A2,A3,A4,A5,C1,C2,S1,NURJ,NUBY,JA,NEHH,MEHH,NG
5,GETA,TA,ETV,TINCV,STH,ETH,TINC,H,HT,VEC,NALL,TEL
5,REALN,*,8,V1
REMIND1
REMIND2
REMIND3
REMIND8
NALL=0
CALL J02
CALL J03
CALL DB1
IF(JA)2,21,2
CALL CONTINUE
21 CALL DB2
T2=T2+T1
CALL J05
2 IF(T-TE)3,5,5
T=T+A1
3 GO TO 2
IF(ABS(T-T2)-A1/2.)1,1,4
4 GO TO 2
5 CONTINUE
CALL DB2
CALL S08
CALL J06
STOP
END

```


SUBROUTINE J02

READING THE CONSTANTS AND DEPTHS


```

11H(12(1H,12(1H),2X),2X)//
130 FORMAT(//,7X,18I7,0)
131 FORMAT(17,12F7.0)
132 FORMAT(17,12F7.0)
133 FORMAT(17,17F7.0)
134 FORMAT(8F10.6)
135 FORMAT(14,S(F5.0,2X,F7.0))
136 COEFFICIENTS',//,30X,6F12.5,/)
137
138 READ 102,JA,NE,IZE,IUE,KKE,NURU,NG
139 READ 103,AFGN2,G2AL,PHA,RBET,A,C1
140 READ 104,DT,T2,W,T1,T2,SI,T3
141 READ 105,DL,T2,SGMA,R,ROL,C
142 READ 102,(NZ(I),MZ(I),I=1,IZE)
143 READ 102,(NZ(I),MZ(I),I=IN,INN)
144 READ 102,(NU(I),MU(I),I=1,IUE)
145 READ 101,(NA(I),MA(I),I=1,NG)
146 READ 101,(VI(I),I=1,NUPU)
147 READ 100,(AI(I),I=1,KKE)
148 READ 134,(Z3(N),Z4(N),N=1,4)
149 READ 134,(Z3(N),Z4(N),N=5,8)
150 READ 134,(Z3(N),Z4(N),N=9,11),Z3(12)
151 READ 134,(Z5(N),Z6(N),N=1,3),Z5(4)
152 READ 134,(Z7(N),Z8(N),N=1,3),Z7(4)
153 PRINT 135,(Z3(N),Z4(N),N=1,11),Z3(12)
154 PRINT 135,(Z5(N),Z6(N),N=1,3),Z5(4)
155 PRINT 135,(Z7(N),Z8(N),N=1,3),Z7(4)
156 NEH=NE-1
157 NEHH=NE-2
158 DO 713 N=1,NE
159 READ (5,701)(HTZ(N,M),M=1,12)
160 READ (5,701)(HTZ(N,M),M=13,24)
161 READ (5,702)(HTZ(N,M),M=25,ME)
162 READ (5,701)(INUE,N=1,NE)
163 READ (5,701)(HTU(N,M),M=1,12)
164 READ (5,702)(HTU(N,M),M=13,24)
165 CONTINUE
166 READ (5,701)(HTV(N,M),M=1,12)
713
714

```


READ(5,701) (HTV(N,M),M=13,24)
 READ(5,702) (HTV(N,M),M=25,ME)
 CONTINUE
 715

SET THE MINIMUM DEPTH
 DO 50 N=1,NE
 DO 50 M=1,ME
 IF (HTU(N,M).LT.4..AND.HTU(N,M).GT.0.) HTU(N,M)=4.
 IF (HTV(N,M).LT.4..AND.HTV(N,M).GT.0.) HTV(N,M)=4.
 50 CONTINUE

PRINT CONTROL DATA
 PRINT 110, AFGN
 PRINT 112, DT, DL
 PRINT 113, ALPHA, R
 PRINT 114, F, SIGMA
 IF(C1)211,215
 PRINT 215
 GO TO 5
 PRINT 116, TW, ROL
 PRINT 117, PRETA, C
 PRINT 3, (A(I), I=1, KKE)
 1 2 IF(TZE)6,6,7
 6 PRINT 119
 GO TO 8
 7 PRINT 120, (NZ(I), MZ(I), I=1, NZE)
 PRINT 125, (NA(I), MA(I), I=1, NG)
 8 PRINT 121, (N,N=1,18)

PRINT THE FIELDS
 PRINT 130, (N, (HTZ(N,M), M=1,18), N=1, NE)
 PRINT 131, (N, (HTZ(N,M), M=19,30), N=1, NE)
 PRINT 132, (N, (HTZ(N,M), M=1,18), N=1, NE)
 PRINT 123, (N, (HTU(N,M), M=1,18), N=1, NE)
 PRINT 120, (N, (HTU(N,M), M=1,18), N=1, NE)
 PRINT 131, (N, (HTU(N,M), M=19,30), N=1, NE)
 PRINT 132, (N, (HTU(N,M), M=19,30), N=1, NE)
 PRINT 124, (N, (HTU(N,M), M=1,18), N=1, NE)
 PRINT 120, (N, (HTV(N,M), M=1,18), N=1, NE)
 PRINT 131, (N, (HTV(N,M), M=19,30), N=1, NE)
 PRINT 132, (N, (HTV(N,M), M=19,30), N=1, NE)

WRITING OUT DEPTH GRID AT U,V POINTS SIMULTANEOUSLY
 PRINT 142, (N,M= 1, 9)


```

DO 21 N=1,NE
PRINT 140,CN,(HTZ(N,M),HTU(N,M),M=1,9)
PRINT 141,CN,(HTV(N,M),M=1,9)
21 PRINT NUE
      DO 22 N=1,NE
      PRINT 142,(M,M=10,18)
      PRINT 140,CN,(HTZ(N,M),HTU(N,M),M=10,18))
      PRINT 141,CN,(HTV(N,M),M=10,18)) M=10,18)
22 CONTINUE
      DO 23 N=1,NE
      PRINT 142,(M,M=19,27)
      PRINT 140,CN,(HTZ(N,M),HTU(N,M),M=19,27))
      PRINT 141,CN,(HTV(N,M),M=19,27)) M=19,27)
23 CONTINUE
      DO 24 N=1,NE
      PRINT 142,(M,M=28,30)
      PRINT 140,CN,(HTZ(N,M),HTU(N,M),M=28,30))
      PRINT 141,CN,(HTV(N,M),M=28,30)) M=28,30)
24 CONTINUE
      C)NTINUE
      BETA=(1.-ALPHA)/4.
22      A1=2.*DT
      A2=F*A1
      A3=R*A1
      A4=DT/DL
      A5=G*A4
      C3=C*A1*10000.
      AA1=0.
      AA2=0.
      REWIND 4
      WRITE(4) HTZ,V1,NURU,ME,NE
      ENDFILE 4
      RETURN
      END

```


SUBROUTINE J03

READING THE BEGINNING VALUES

```

COMMON/A/Z(53,30),U(53,30),V(53,30),ZM(53,30),ZST(53,30),
1HSV(53,30),HGU(53,30),HTU(53,30),HTV(53,30),HZ(53,30),
2YK(53,30),RAD(53,30),ANG(53,30),O(53,30),
COMMON/B/A(60),NZ(90),WZ(90),NJ(60),VJ(60),V1(60),
1Y2(60),U1(60),U2(60),V3(60),V4(60),X(4),ARG(4),NA(60),
2Z3(12),Z4(12),Z5(8),Z6(8),Z7(8),Z8(8),Z9(8),Z10(8),
COMMON/C/AFGN,F,A1,A2,CIDL,DT,T,T1,T2,NE,ME,TE,KK,E,IZE,IJE,TW
3,SIGMA,ALPHA,R,ROL,RBETA,C1,C3,SIN,VPU,NURV,JAE,NEHH,MEHH,NG
4,BETAI,A1,A2,A3,A4,A5,C1,C3,SIN,HT,INC,H,HT,V,VEC,NALL,TEI
5,T3,ST,V,V1
REALFORMAT(9F8.3)
100 FORMAT(18F4.1)
113 FORMAT(18F4.1)
2000 F0RML=,F10.0,
1           ,//,/

```

CONVERT THE DEPTH'S CHART IN FEET TO CENTIMETERS

```

DO 3 N=1,NE
 3 M=1,ME
  IF(HTU(N,M)=HTU(N,M)) GO TO 21
  HTU(N,M)=HTU(N,M)*30.48
21  CONTINUE
  IF(HTV(N,M)=HTV(N,M)) GO TO 22
22  HTV(N,M)=HTV(N,M)*30.48
23  CONTINUE

```

READ CONTINUATION VALUES WHEN PREVIOUS COMPUTATION EXIST

```

IF(JA)2,7,2
2 READ(8) Z(N,M),M=1,ME),N=1,NE),
1   U(N,M),M=1,ME),N=1,NE),
2   V(N,M),M=1,ME),N=1,NE),
3   HSU(N,M),M=1,ME),N=1,NE),
4   HGV(N,M),M=1,ME),N=1,NE),
5   TFI
5 WRITE(6,2000)TEI
GO TO 14

```

CLEAN THE ARRAYS


```

SET INITIAL WATER ELEVATIONS
7      DO 12 N=1,NE
       DO 12 M=1,ME
       Z(N,M)=0.
       U(N,M)=0.
       V(N,M)=0.
12     CONTINUE

SET SMALL VALUES TO PREVENT UNDERFLOW
30     DO 30 N=1,NE
       DO 30 M=1,ME
       IF(HTZ(N,M))30,30,31.
31     CONTINUE
30     DO 32 N=1,NE
       DO 32 M=1,ME
       IF(HTU(N,M))34,34,33
33     U(N,M)=0.2
34     IF(HTV(N,M))32,32,35
35     V(N,M)=0.2
32     CONTINUE

INITIALIZATION OF ACTUAL DEPTH.
15     DO 14 N=1,NE
       DO 14 M=1,ME
       IF(HTU(N,M))5,5,4
       HGU(N,M)=(Z(N,M)+Z(N,M+1))/2.
4      HGU(N,M)=HTU(N,M)
       GO TO 13
5      HGV(N,M)=0.
13     IF(HTV(N,M))8,8,6
       HGV(N,M)=HTV(N,M)+(Z(N,M)+Z(N,M+1))/2.
16     HGV(N,M)=0.
       GO TO 14
8      HGV(N,M)=0.
14     CONTINUE

INITIALIZATION OF VARIOUS PARAMETERS
10     DO 10 N=1,NE
       DO 10 M=1,ME
       Q(N,M)=0.
       XX(N,M)=0.
       ZST(N,M)=0.
       ZW(N,M)=0.
       YK(N,M)=0.
10     RETURN
      END

```


SUBROUTINE J04

WRITING OF THE VALUE FIELDS 104

```

COMMON/A/Z/(53,30),U/(53,30),V/(53,30),Z/(53,30),HT/(53,30),X/(53,30),
1HGV/(53,30),HGU/(53,30),HTU/(53,30),HTV/(53,30),HZ/(53,30),
2YK/(53,30),RAD/(53,30),ANG/(53,30),Q/(53,30),MJ/(60),Z1/(60),Z2/(60),V1/(60),
COMMON/B/A/(60),NZ/(90),NU/(60),V3/(60),V4/(60),ARG/(4),NA/(60),HA/(60),
1V2/(60),U1/(60),U2/(60),Z5/(8),Z6/(8),Z7/(8),Z8/(8),Z9/(8),Z10/(8),
2Z3/(12),Z4/(12),C1/A1,A2,R/ROL,RBETA,C/DL/DT,T/T1,T2,NE/METE,KKE/IZE,IUE,TW
COMMON/C/AFGN,ALPHA,R3,SIGMA,ALPHAI,A2,A3,A4,A5,C1,C3,SI,NURV,JIA,NEHH,NEHH,NG
3,G,BETAV,ETV,TINC,V,STH,ETH,TINCH,HT,VEC,NALL,TEI
4,T3,REAL,*8,V1
5,FORMAT(1H1,14X,2I4)WATER HEIGHT AFTER T = ,F10.0,T,V2,V3,V4,/,/
50,FORMAT(1H1,14X,2I4)WATER HEIGHT AFTER T = ,F9.0,SH SEC (CM)/7X,17,181
224,17/
228,FORMAT(17,18F7.0/)
229,FORMAT(18,3F8.0,/,)
230,FORMAT(12,2X,F4.0,1X,F4.0,/,)
231,FORMAT(5,2X,F4.0,0,1X,F4.0,/,)
232,FORMAT(5,2X,F4.0,0,1X,F4.0,/,)
233,FORMAT(5,2X,F4.0,0,1X,F4.0,/,)
234,FORMAT(1I9)CURRENT SPECIMEN POINT = ,F10.0,/,10(3X,A8,10X,F8.2,8X,F8.2
235,FORMAT(1I9)CURRENT DEGREES) AFTER T = ,F9.0,SECONDS,/,)
236,FORMAT(1I9)CURRENT MAGNITUDE(CM/SEC)
237,FORMAT(1I9)CURRENT DIRECTION(DEGREES)
238,FORMAT(17,17F7.0/)
328,FORMAT(17,17X,17,1817/)
404,FORMAT(17,17X,17,218)
405,FORMAT(17,17X,17,5X,1)
406,FORMAT(17,12F7.0/)
1228,FORMAT(17,12F7.0/)

PRINT OF Z VALUES
PRINT 224,T,(N,N=1,18)
PRINT 223,(N,(Z(N,M),M=1,18),N=1,NE)
PRINT 404,(N,(Z(N,M),M=19,30),N=1,NE)
PRINT 1223,(N,(Z(N,M),M=19,30),N=1,NE)
PRINT 180./3,1415926

COMPUTATION OF CURRENT DIRECTION
DO 432 N=1,NE
DO 432 M=1,ME
IF(V(N,M)**2+U(N,M)**2.EQ.0.)GO TO 101

```



```

100 PAD(N,M)=SQR(T(V(N,M)**2+U(N,M)**2))
101 RAD(N,M)=0.0.
102 GO TO 432
    ABC=ABC*(V(N,M))/RAD(N,M)
    ABC1=ABC*(10**10)
    IF(ABC1.LT.0)GO TO 1
    ANG(N,M)=ARSIN(ABC)
    ANG(N,M)=ANG(N,M)*PIR
    GO TO 2
1  ANG(N,M)=0.0
    IF(V(N,M).GE.0..AND.U(N,M).GE.0..)GO TO 433
    IF(V(N,M).GE.0..AND.U(N,M).LT.0..)GO TO 500
    IF(V(N,M).LT.0..AND.U(N,M).LE.0..)GO TO 501
    GO TO 502
500 ANG(N,M)=180.-ANG(N,M)
501 ANG(N,M)=180.+ANG(N,M)
502 ANG(N,M)=360.-ANG(N,M)
433 ANG(N,M)=90.-ANG(N,M)
    IF(ANG(N,M).LT.0.)ANG(N,M)=360.+ANG(N,M)
432 CONTINUE
    DO 10 N=1,NF
    DO 10 M=1,ME
    IF(V(N,M).EQ.0..)GO TO 10
    RAD(N,M)=1.
    ANG(N,M)=666.
    Q(N,M)=0.
10 CONTINUE

```

WRITING THE SPETIAL POINTS

```

IF(NURU.EQ.0)GO TO 12
DO 9 I=1,NURU
    MZ=MZ(I+IZE)
    N=NZ(I+IZE)
    V2(I)=Z(N,M)
    V3(I)=PAD(N,M)
    V4(I)=ANG(N,M)
    NALL=NALL+1
    WRITE(1)T,(V2(I),I=1,NURU),
    1          (V3(I),I=1,NURU),
    2          (V4(I),I=1,NURU)
9 CONTINUE
12 PRINT 59,T

```


PRINTING OF CURRENTS AND DIRECTION

```
WRITE(6,298)T
WRITE(6,406){N,N=1,12}
PRINT 230,{{RAD(N,M),ANG(N,M),M=1,12),N=1,NE}
WRITE(6,406){N,N=1,3;24}
PRINT 230,{{RAD(N,M),ANG(N,M),M=13,24),N=1,NE}
WRITE(6,406){N,N=2,5;ME}
PRINT 232,{{RAD(N,M),ANG(N,M),M=25,ME),N=1,NE}
PRINT 233,T,(V1(I),V2(I),V3(I),V4(I)),I=1,NURU)
RETURN
END
```


SUBROUTINE J05

COMPUTATION AND MANIPULATION

```

COMMON/A/Z(53,30),U(53,30),V(53,30),Z4(53,30),ZST(53,30),
1H3V(53,30),HGU(53,30),HTU(53,30),HTZ(53,30),XX(53,30),
2YK(53,30),ANG(53,30),Q(53,30),NU(53,30),
COMMON/B/A(60),NZ(90),NU(60),V(60),Z1(60),Z2(60),NA(60),
1V2(60),U1(60),U2(60),V4(60),X(4),ARG(4),NA(60),MA(60),
2Z3(12),U1(60),U2(60),Z5(8),Z6(8),Z7(8),Z8(8),Z9(8),Z10(8)
COMMON/C/AFGN,F,A1,A2,RDL,RBETA,CIDL,DT,T1,T2,NE,ME,TE,KKE,IZE,IUE,TH
3,G,SIGMA,ALPHA,R,RL,CLC3,S,NUPU,NURV,JA,NEH,MEH,NEHH,NG
4,BETA,A1,A2,A3,A4,A5,CLTH,STH,TINCV,STH,TINCH,HT,VEC,NALL,FI
5,REAL*8,VI

```

SET TIDE VALUES AT OPEN BOUNDARIES

```

IF(IZE.EQ.0)GO TO 709
PER=24.*633333*3600.
PI=3.1415927
TT=T+0.

```

```

DO 77 I = 1, IZE
N = NZ(I)
M = MZ(I)
SUM=0.

```

```

D1 L=1,1
ZTIDE=SUM+COS((L)*2.*PI*TT/PER)+Z4(L)*SIN((L)*2.*PI*TT/PER)

```

```
10
```

```

SUM=SUM+ZTIDE
Z(N+M)=SUM+Z3(12)
CONTINUE

```

```

77 TEF(NG*FO,O)GO TO 709

```

```
172
```

```

DO 78 I = 1, NG
N=NA(I)
M=MA(I)
SUM=0.

```

```
20
```

```

DO 20 L=1,3
ZTIDE=Z7(L)*COS((L)*2.*PI*TT/PER)+Z8(L)*SIN((L)*2.*PI*TT/PER)
SUM=SUM+ZTIDE
Z(N+M)=SUM+Z7(4)
CONTINUE

```

```
78
```

```

CONTINUATION OF Z IN THE OPEN BOUNDARIES
709 DO 30 N=6,8
Z(N,4)=Z(N,5)

```


30 CONTINUE

SMOOTHING OF Z VALUES

```
DO 470 N=2,NEH  
DO 470 M=2,MEH  
IF(HTZ(N,M))710,470,75  
710 IF(HTZ(N,M)+2)470,75,470  
75 IF(1-N)28,6,28  
28 IF(HTZ(N-1,M))57,6,57  
57 WERT0=Z(N-1,M)  
GO TO 7  
7 WERT0=Z(N,M)  
IF(NE-N)18,9,18  
18 IF(HTZ(N+1,M))58,9,58  
58 WERTU=Z(N+1,M)  
9 WERTU=Z(N,M)  
5 IF(1-M)29,12,29  
29 IF(HTZ(N,M-1))59,12,59  
59 WERTL=Z(N,M-1)  
GO TO 13  
12 WERTL=Z(N,M)  
13 IF(ME-M)17,15,17  
17 IF(HTZ(N,M+1))60,15,60  
160 WERTR=Z(N,M+1)  
15 WERT0=Z(N,M)  
22 ZM(N,M)=ALPHA*Z(N,M)+BETA*(WERT0+WERTU+WERTL+WERTR)  
470 CONTINUE
```

```
DO 70 N=2,NEH  
DO 70 M=2,MEH  
IF((HGV(N,M))GT.900000.)*OP.(HGU(N,M)*GT.900000.)1GO TO 91  
IF((IV(N,M))GT.100000.)*OR.(U(N,M)*GT.100000.)1GO TO 92  
IF(HTZ(N,M))70,70,3355  
70 CONTINUE
```

CONTINUITY EQUATION FOR COMPUTATION OF Z

```
3355 DHV = HGV(N-1,M)*V(N-1,M)-HG(V(N,M))*V(N,M)  
355 DHU = HGU(N,M)*U(N,M)-HGU(N,M-1)*U(N,M-1)  
361 Z(N,M) = ZM(N,M)-A4*(DHU+DHV)  
70 CONTINUE
```

CONTINUATION OF THE OPEN BOUNDARIES

```
DO 71 M=2,23  
71 Z(52,M)=Z(52,M)  
71 CONTINUE
```



```

DO 171 N=1,53
Z(N,1)=Z(N,2)
171 CONTINUE
DO 271 N=6,8
Z(N,4)=Z(N,5)-(Z(N,6)-Z(N,5))
271 CONTINUE

ACTUAL DEPTH COMPUTATION

72 DO 82 N=1,NEH
    DO 82 M=2,MEH
        IF(HTU(N,M)=HTU(N,M))76,76,81
        81 HGU(N,M)=HTU(N,M)+(Z(N,M)+Z(N,M+1))/2.
        76 IF(HTV(N,M)=HTV(N,M))82,82,87
        87 HGV(N,M)=HTV(N,M)+(Z(N,M)+Z(N+1,M))/2.
        82 CONTINUE
    DO 1901 M=2,6
        HGU(53,M)=HGU(52,M)
        HGV(53,M)=HGV(52,M)
1901 DO 1002 N=43,53
        HGU(N,1)=HGU(N,2)
        HGV(N,1)=HGV(N,2)
1002 IF(C1.EQ.0)GO TO 103
        IF(T.LT.TW)GO TO 103

CALL WIND SUBROUTINE
CALL S01

SMOOTHING OF U

103 DO 512 N=2,NEH
    DO 512 M=2,MEH
        IF(HTU(N,M))512,512,128
        128 IF(HTU(N-1,M))157,157,157
        157 WERTO=U(N-1,M)
        GO TO 118
106 WERTO=U(N,M)
118 IF(HTU(N+1,M))158,109,158
1158 WERTU=U(N+1,M)
        GO TO 129
109 WERTU=U(N,M)
129 IF(HTU(N,M-1))159,112,159
1159 WERTL=U(N,M-1)
        GO TO 117
112 WERTL=U(N,M)
113 IF(ME-N)117,115,117
117 WERTR=U(N,ME)
1160 WERTR=U(N,ME+1)

```



```

GO TO 23
115 WERTR=U(N,M)
223 ZM(N,M)=ALPHA*U(N,M)+BETA*(WERTO+WERTU+WERTL+WERTR)

```

AVERAGING OF U

```

IF(HTV(N-1,M))61,32,61
61 WERTUL=V(N-1,M)
62 IF(HTV(N-1,M+1))62,35,62
62 WERTOR=V(N-1,M+1)
60 TO 36
32 WERTOL=V(N-1,M+1)
35 IF(HTV(N,M))63,38,63
36 IF(HTV(N,M+1))63,38,63
63 WERTUL=V(N,M+1)
64 IF(WERTUR=V(N,M+1))64,41,64
64 WERTUR=V(N,M+1)
60 TO 42
38 WERTUL=V(N,M+1)
41 WERTUR=WERTUL
42 ZST(N,M)=(WERTOL+WERTOR+WERTUL+WERTUR)/4.
512 CONTINUE

```

COMPUTATION OF U

```

DO 412 N=2,NEH
DO 412 M=2,MEH
412 IF(HTU(N,M))412,412,513
513 IF(ZM(N,M)*EQ.0.AND.ZST(N,M)*EQ.0)GO TO 514
      WURZEL=SQR(ZM(N,M)**2+ZST(N,M)**2)
      GRZ=A3*WURZEL
      GO TN 515
514 WURZEL=0.0
515 GRZ=CHGU(N,M)-GRZ)94,94,702
702 IF(HTU(N,M)-99999)14,790,700
700 ZM(N,M)=ZM(N,M)+A2*ZST(N,M)-A5*(Z(N,M+1)-Z(N,M))+XXK(N,M)
14 ZM(N,M)=(1.-CRZ/HGU(N,M))*A2*ZST(N,M)+ZM(N,M)-A5*(Z(N,M+1)-Z(N,M))
14 XXK(N,M)
14 GO TO 412
94 Q(N,M)=1.
412 CONTINUE

```

AVERAGING OF U

```

DO 528 N=1,NEH
DO 528 M=2,MEH
528 IF(HTV(N,M))528,528,429

```



```

429 IF(HTU(N,M-1))65,44,65
65 WERTCL=U(N,M-1)
   WERTUL=U(N+1,M-1)66,46,66
66 WERTUL=U(N+1,M-1)
44 WERTOL=U(N+1,M-1)
46 WERTOL=WERTOL
47 IF(HTU(N,M))67,49,67
67 WERTOR=U(N,M)
   IF(HTU(N+1,M))68,52,68
68 WERTUP=U(N+1,M)
   GOTO 53
49 WERTUP=U(N+1,M)
52 WERTUP=WERTOR
53 ZST(N,M)=(WERTOL+WERTUL+WERTOR+WERTUP)/4.
528 CONTINUE

```

SMOOTHING OF V

```

DO 4100 N=2,NEH
DO 4100 M=2,MFH
   IF(HTU(N,M))4100,4100,4101
4101 U(N,M)=ZM(N,M)
CONTINUE
DO 431 N=1,NEH
DO 431 M=2,MEH
   IF(HTV(N,M))431,431,432
432 IF((1-N)/228;206;228
228 IF(HTV(N-1,M))257,206,257
257 WERTC=V(N-1,M)
   DO TCO=213
206 WERTC=V(N,M)
   IF(HTV(N+1,M))258,209,258
218 WERTU=V(N+1,M)
258 WERTU=V(N,M)
   GOTO 229
229 IF(HTV(N,M-1))259,212,259
259 WERTL=V(N,M-1)
   GOTO 217
212 WERTL=V(N,M)
217 IF(HTV(N,M+1))260,215,260
260 WERTR=V(N,M+1)
   GOTO 25
215 WERTR=V(N,M)
25 ZM(N,M)=ALPHA*V(N,M)+BETA*(WERTO+WERTU+WERTL+WERTR)
431 CONTINUE

```

COMPUTATION OF V


```

DO 428 N=2,NEH
DO 428 M=2,MEFH
   IF(HTV(N,M))428,428,529
   IF(ZM(N,M).EQ.0.AND.ZST(N,M).EQ.0)GO TO 530
529 WURZEL=SQR(T(ZM(N,M)**2+ZSF(N,M)**2))
   CRZ=A2*WURZEL
   GO TO 521
530 WURZEL=0.0
   CRZ=0.0
531 IF(HGV(N,M)-GRZ)300,300,703
300 IF(HTV(N,M)-9999.0)415,701,701
701 IF(HTV(N,M)=ZM(N,M)-A2*ZST(N,M)-A5*(Z(N,M)-Z(N+1,M))+  

    701 V(N,M)=(1.-GRZ/HGV(N,M))*ZM(N,M)-A2*ZST(N,M)-A5*(Z(N,M)-Z(N+1,M))+  

    415 YK(N,M)
1 GO TO 428
300 Q(N,M)=1.
428 CONTINUE

```

COMPUTATION OF MASS TRANSPORT

```

11 IF(T-T2)400,5250,5250
5250 IF(T-ETH)5251,5251,400
5251 AA1=AA1+(U(3,10)*HTU(3,10)*A1*2*DL+  

1 U(4,10)*HTU(4,10)*A1*2*DL+  

1 U(5,10)*HTU(5,10)*A1*2*DL+  

1 U(6,10)*HTU(6,10)*A1*2*DL+  

1 U(7,10)*HTU(7,10)*A1*2*DL+  

1 U(8,10)*HTU(8,10)*A1*2*DL+  

1 AA2=AA2-(V(34,14)**HTV(34,14)+A1*2.*DL+  

1 V(34,15)**HTV(34,15)+A1*2.*DL+  

1 V(34,16)**HTV(34,16)+A1*2.*DL+  

1 V(34,17)**HTV(34,17)+A1*2.*DL+  

1 V(34,18)**HTV(34,18)+A1*2.*DL)/1000000.
400 RETURN
91 PRINT 1
92 PRINT 2,T,N,M
1 FORMAT(1X,7HEPR0R,V)
2 FORMAT(F11.0,5X,1H(,I2,I2,I2,2H))
3 END

```


SUBROUTINE S01

S01 VARIABLE WIND IN SUBAREAS, INTERMITANTLY

```

COMMON/A/Z(53,30),U(53,30),V(53,30),ZM(53,30),ZST(53,30),
1 HGV(53,30),HTU(53,30),HTV(53,30),HZ(53,30),XK(53,30),
2 YK(53,30),AD(53,30),ANG(53,30),C(53,30),
3 COMKON,ZN(60),NZ(60),VYU(60),MU(60),Z1(60),V1(60),
4 VY2(60),U2(60),V3(60),V4(60),Z2(60),VA(60),MA(60),
5 Z23(COMMON/C/CGESTA,AA1,AA2,AA3,AA4,AA5,C1,C3,S1,NURU,
6 ,TINCV,HTV,TINCV,STH,EIH,TINCH,HT,VEC,NALL,TE1
7 REAL*8 V1
8 IF(SI-T)12,10,2
9 KF=IUE/2
10 IF(T-A(1))9,4,9
11 D9 N1=NU(2*I-1)
12 N2=NNU(2*I-1)
13 M1=MU(2*I-1)
14 M2=MU(2*I-1)
15 DO 8 M=M1,M2
16 DO 8 N=N1,N2
17 IF(T-A(1))9,4,4
18 DO 8 M=1,ME
19 DO 8 N=1,ME
20 IF(HTU(N,M))1,1,3
21 IF(HGU(N,M))1,2,5
22 3 )**2*COS(A(3)*0.017453)/2000.
23 XKF(HTV(N,M))=C3*A(1,2)**2*COS(A(
24 1 )**2*SIN(A(3)*0.017453)/2000.
25 XKF(HTV(N,M))=C3*A(1,2)**2*SIN(A(
26 YK(N,M))=C3*A(1,2)**2*SIN(A(
27 CONTINUE
28 GO TO 12
29 DO 11 N=1,ME
30 10 N=1,ME
31 XKF(HCV(N,M))=0.
32 YK(N,M)=0.
33 RETURN
34 END

```

for fields

SUBROUTINE S08

S08 OUTPUT FOR SPECIAL POINTS

```

COMMON/A/Z(53,30),U(53,30),V(53,30),ZW(53,30),TZST(53,30),
1 HGV(53,30),HGU(53,30),HTV(53,30),HTZ(53,30),XK(53,30),
2 YK(53,30),RAD(53,30),ANG(53,30),Q(53,30)
CJMM40,V/A(60),NZ(90),MZ(90),NU(60),MJ(60),Z1(60),Z2(60),V1(60),
1 V2(60),U1(60),U2(60),V3(60),V4(60),ARG(4),NA(60),MA(60),
2 Z3(12),Z4(12),Z5(8),Z6(8),Z7(8),Z8(8),Z9(8),Z10(8)

COMMON/C/AFCN,F,A1,A2
COMMON/SIV,STH,ETH,TINCH,HT,VEC,NALL,TE1
3,CIESTA,V1
4,REAL,*8
5,T3,SIV,A2,A3,A4,A5,A6
FORMAT(//,7X,4HNAME,4X,15(2X,A6)/15X,14(2X,A6)/)
1130 FORMAT(1H1,5X,114HWATER ELEVATION(CM) AND CURRENT VELOCITY RESULTS
1131 FORMAT(MAGNITUDE IN CM/SEC AND DIRECTION IN DEGREES) AT SPECIAL POINTS
1132 FORMAT(6X,5HCOND,4X,15(2X,A6)/15X,14(2X,A6)/)
1133 FORMAT(* TIME OF COMPUTATION = *,F10.0,*SECONDS*,*,6X,*HEIGHT
1134 FORMAT(5X,14HEND OF PROGRAM,/,/,/,/,/
1135 FORMAT(* VELOC,DIP*,2X,F7.0,1H,,F4.0,14(F4.0,1H,,F4.0)/
1136 14X,14(F4.0,1H,,F4.0)/
1137 TFL=T
NURV=0
PRINT 131,(V1(I),I=1,NURV)
PRINT 132,(MZ(I+IZE),I=1,NURV),
1 FNDFL(F
1 REWIND 1
1 READ(1)T,(V2(I),I=1,NURV),
2 (V3(I),I=1,NURV),
2 (V4(I),I=1,NURV),
2 NURV=NUP V+
1 IF(NURV<50)3,3,4
4 PRINT 130,(V1(I),I=1,NURV)
1 1
3 PRINT 133,T,(V2(I),V4(I),I=1,NURV),
3 PRINT 135,(V3(I),V4(I),I=1,NURV),
4 WRITE(?,(V3(I),V4(I),I=1,NURV)
1 2
2 IF((T-T)2,2,1
2 ENDIF E2
PRINT 134
RETURN

```


END

SUBROUTINE DB1

```
COMMON/A/Z(53,30),U(53,30),V(53,30),ZM(53,30),HTZ(53,30),XK(53,30),
1HGCV(53,30),HGU(53,30),HTU(53,30),HTV(53,30),HT(53,30),
2YYK(53,30),RAD(53,30),ANG(53,30),Q(53,30),
COMMON/B/A(60),NZ(90),NU(60),V(60),W(60),X(60),Y(60),V1(60),
1V2(60),U(60),V2(60),V4(60),Z1(60),Z2(60),NA(60),MA(60),
2Z2(60),Z5(8),Z6(8),Z7(8),Z8(8),Z9(8),Z10(8),
COMMON/C/AA1,AA2,RBETA,C,DL,DT,T,T1,T2,NE,METE,KKE,IUE,IUF,TW,
3,SESTICNA,ALPHA,R,ROL,QBETA,C1,C3,S1,NURJ,NURV,JA,NEH,MEH,NG,
4,BETA,A1,A2,A3,A4,A5,C1,E1,TH,TINC,V,TE1
5,T2,STV,FTV,TINCV,STH,E1H,TINC,H1,V,TE1
DEAL*8 V1
```

```
REAL*8 HEAD,HEAD1
111 FOPENAT('CHECKPARAMETERS',DB1,'STH = ',F7.0)
111 ! T = ! F7.0,T1 = ! F7.0,STV = ! F7.0
400 FOPENAT('31',DB2,'T = ! F10.0,O,T,VEC,HT,RAD,ANG,Z
1,/')
401 FORMAT(' MASS TRANSPORT AT T = ! F10.0, DURING THE LAST HOUR PE
1P,1/1
1000 FORMAT(A8,2X,3F10.0)
1001 FORMAT(//,20X,A8,2X,3F10.0)
```

ENTRY TO READ VECTOP + HEIGHT CARDS

```
READ 1000,HEAD,STV,ETV,TINCV
READ 1000,HEAD1,STH,ETH,TINCCH
PRINT 1001,HEAD,STV,ETV,TINCV
PRINT 1001,HEAD1,STH,ETH,TINCCH
RETURN
```

ENTRY TO WRITE DATA IN DISK FILE 3 FOR VECTOR AND WATER HEIGHT PLOTS

```
HT=0.
VEC=0.
WRITE(6,111)T,T1,STV,STH
111 IF(ABS(T-STV).GT.T1/2.)GO TO 100
STV=STV+TINCV
VEC=1.
100 IF(ABS(T-STH).GT.T1/2.)GO TO 200
STH=STH+TINCCH
HT=1.
```



```

200 IF(HT+VEC.EQ.0.)GO TO 300
      WRITE(3) T,VEC,HT,RAD,ANG,Z
      PRINT 401,T,AA1,AA2
      AA1=0.
      AA2=0.
      RETURN
      END

```

SUBROUTINE J06

SUBROUTINE FOR WRITING IN TAPES FOR FUTURE USES OF COMPUTATIONS

```

COMMON/A/2(53,30),U(53,30),V(53,30),ZM(53,30),ZT(53,30),
      HGU(53,30),HTU(53,30),HTZ(53,30),XK(53,30),
      1HG(53,30),RAD(53,30),ANG(53,30),G(53,30),
      2YK(53,30),NU(60),MJ(60),Z1(60),Z2(60),V1(60),
      COMMON/B/ A(60),NZ(90),MZ(90),V2(60),V3(60),
      COMMON/C/ V4(60),U(60),V5(60),Z6(8),Z7(8),Z8(8),Z9(8),Z10(8)
      1Y2(60),Z4(12),Z5(8),Z6(8),Z7(8),Z8(8),Z9(8),Z10(8)
      2Z3(12),Z4(12),Z5(8),Z6(8),Z7(8),Z8(8),Z9(8),Z10(8)
      COMMON/D/ AFGN,F,AAL,A42,RAETA,C,DL,DT,T,T1,T2,NE,ME,TE,KKE,IZE,IUE,TW
      3,G,STIGMA,ALPHA,R,RCOL,RC3,SIN,NURJ,NURV,JA,NEH,NEHH,MEHH,NG
      4,BETAST,V,ETV,THIC,V,STH,ETH,TINCH,HT,VEC,NALL,TE1
      5,T3,STV,ETV,THIC,V,STH,ETH,TINCH,HT,VEC,NALL,TE1
      REAL*8 V1
      ENDFILE F3
      REWIND 2
      REWIND 3
      REWIND 4
      REWIND 8
      REWIND 9
      READ(4) HTZ,V1,NURU,ME,NE
      WRITE(9) HTZ,V1,NURU,ME,NE,NALL

```



```

11 PRINT 11
11 FORMAT(2 T, (V2(I), I=1,NURU), (V3(I), I=1,NURU), (V4(I), I=1,NURU))
12 READ(2 T, (V2(I), I=1,NURU), (V3(I), I=1,NURU), (V4(I), I=1,NURU))
12 WRITE(9) T, (V2(I), I=1,NURU), (V3(I), I=1,NURU), (V4(I), I=1,NURU)
13 PRINT 10, T
10 FORMAT(1 F(TE-T) 4, 4, 2
11 READ(3 T, VFC, HT, RAD, ANG, Z
11 WRITE(3 T, VFC, HT, RAD, ANG, Z
11 PRINT 12, T
12 FORMAT(12, T, AROTE(9) SUBROUTINE JO6 T =', F10.0, 'T, VEC, HT, RAD, ANG, Z
12 1 F(TE-T) 5, 5, 4
12 5 WRITE(8) ((Z(N, M), M=1, ME), N=1, NE);
12 1 ((U(N, M), M=1, ME), N=1, NE);
12 2 ((V(N, M), M=1, MF), N=1, NE);
12 3 ((HG(U(N, M), M=1, ME), N=1, NE),
12 4 ((HG(V(N, M), M=1, ME), N=1, NE));
12 5 TEL
12 5 PRINT 11 TEL
12 5 //, ! PARTIAL RESULTS HAD BEEN WRITTEN IN TAPE 8 AT TIME
12 5 //, ! SECOND, //,
12 5 PRINT 6, NALL - NALL - NUMBER OF PLOT ORDERED = ', I3, //, /
12 6 FORMAT(6 ENDFILE 8
12 6 REWIND 8
12 6 ENDFILE 9
12 6 RETURN
12 6 END

```


HANSEN PROGRAM PLOTS

PLOTS OF TIDE AND VELOCITY CURVES

CARD 1

THMIN MINIMUM VALUE OF WATER HEIGHT ON Y AXIS SCALE
THMAX MAXIMUM VALUE OF WATER HEIGHT ON Y AXIS SCALE
YPN SCALE OF Y AXIS IN UNITS/INCH
XPN SCALE OF TIME AXIS IN UNITS/INCH
SKIP NO. OF TIME STEPS IN BF SKIPPED OVER BETWEEN PLOTED PO

CARD 2

START START TIME OF FIRST WATER HEIGHT VECTOR PLOT
TMAX START TIME OF LAST WATER HEIGHT VECTOR PLOT
TINC TIME INTERVAL BETWEEN STARTED TIMES
TLEN TIME INTERVAL BE PLOTTED
YPN TIME SCALE IN UNITS/INCH (MIN. & MAX VALUES ARE
WATER HEIGHT SCALE UNITS/INCH)
ZPN THOSE ON THE TIDE CARD
VECTOR SCALE IN UNITS/INCH

MAIN PROGRAM

```

COMMON/A/, V1(60), V2(60), V3(60), V4(60), HTZ(53,30), RAD(53,30),
1  ANG(53,30), Z(53,30), X(3), Y(3), NURU, ME, T, VEC, HT
REALIND 2
REWIND 3
REWIND 4
REWIND 9 READ(9,*,NALL)
PPINAT(11,*,READED(9,*) HTZ, V1, NURU, ME, NE, NALL,
      NALL = *, T3, *)
11 1 NURU = ? I3 ? / PRINT(1, *(HTZ(N,M), M=1,20), N=1,NE)
      PRINT(1, *(HTZ(N,M), M=21,ME), N=1,NE)
      PRINT(2, *(V1(I), I=1,NURU))
      PRINT(3, *NE, ME)
      PRINT(4, *NURU)
      FORMAT(10A10) HTZ(*,I2,*;*,I2,*;*,I2,*;*,I2,*)
      FORMAT(10F6.1) V1(*,I2,*;*,I2,*;*,I2,*;*,I2,*)
      FORMAT(10F6.1) V2(*,I2,*;*,I2,*;*,I2,*;*,I2,*)
      DO 5 K=1,NALL
      READ(9,*,T) (V2(I), I=1,NURU), (V3(I), I=1,NURU), (V4(I), I=1,NURU)
      WRITE(2,*,T) (V2(I), I=1,NURU), (V3(I), I=1,NURU), (V4(I), I=1,NURU)
      WRITE(3,*,T) (V2(I), I=1,NURU), (V3(I), I=1,NURU), (V4(I), I=1,NURU)
      PRINT(20,*,T) READED(9,*) T, V2(I), V3(I), V4(I), NURU, AT T = *, F10.0, /
      PRINT(21,*(V2(I), V3(I), V4(I), I=1,NURU))
      PRINT(22,*(V2(I), I0X, V3(I), I0X, V4(I), I, 5X, 3F10.0, /)
      CONTINUE
      DO 6 I=1,NALL
      READ(9,*,T) VFC, HT, RAD, ANG, Z,
      WRITE(4,*,T) VEC, HT, RAD, ANG, Z,
      PRINT(12,*,T) READED(9,*) T, VEC, HT, PAD, ANG, Z, AT T = *, F10.0, /
      PRINT(17,*,T) (RAD(N,M), M=1,20), N=1,NE)
      PRINT(17,*,T) (ANG(N,M), M=21,20), N=1,NE)
      PRINT(17,*,T) (Z(N,M), M=21,20), N=1,NE)
      PRINT(17,*,T) (Z(N,M), M=21,ME), N=1,NE)
      CONTINUE
      CONDFILE 2
      ENDFILE 3
      ENDFILE 4
12

```



```
REWIND 2
REWIND 3
REWIND 4
REWIND 9
PRINT 101,NURU,ME2,NE2,VEC,HT,BEEFORE PASSED TO SUBROUTINE T01',/
101 FORMAT(1X,I5,I5,I5,F10.0,F10.0,F10.0,/)
CALL T01
CALL TEST(NALL,NURU)
STOP
END
```



```

SUBROUTINE T01
COMMON/V1/V1(60),V2(60),V3(60),V4(60),HTZ(53,30),RAD(53,30),
1ANG(53,30),Z(53,30),X(3),Y(3),NUPU,ME,NE,T,VEC,HT
DIMENSION V1(10000),V2(10000),V3(10000),V4(10000),TT(1500)
REAL*8 V1,V2,V3,V4
DIMENSION VV2(10000),VV3(10000),VV4(10000),TT(1500)
COMPUTE UPPER BOUNDS OF STORAGE AREA. DATA WILL BE STORED IN
THE FOLLOWING ORDER, AREA(TIME,NURU)
KK = 10000/NURU
CALL PLOTS(NRUP,ME,NE,T,VEC,HT
PRINT 2000,NRUP,ME,NE,T,VEC,HT
KK = 10000/NURU
READ TIDE CYCLE CARD
READ 1000, THMIN,THMAX,YPN,XPN,SKIP
PRINT 1001, THMIN,THMAX,YPN,XPN,SKIP
M=SKIP
DO 110 I = 1, KK
KKK = (NRUP-1)*KK+I
READ(2,END=200) TT(I) (VV2(J), J=1, KK), (VV3(J), J=1, KK), (VV4(J), J=1, KK),
1 (VV4(J), J=1, KK)
1 PRINT 3000, I, TT(I)
150 IF(M.EQ.0) GO TO 110
DO 100 J=1,M
READ(2,END=210)
100 CONTINUE
110 KKK=KK
GC TO 250
200 KKK=I-1
GO TO 250
210 READ TIDEVECTOR CARD
250 READ 1000, TMIN,THMIN,TLEN,XPY,YPN,ZPN
PRINT 1000, TMIN,THMIN,TLEN,XPY,YPN,ZPN
PLCT WATER HEIGHTS FOR ENTIRE RUN FOR EACH SPECIAL POINT
DO 300 I = 1,NURU
K = K*(I-1)+1
300 CALL TINPL(TT,VV3(K),VV4(K),KKK,V1(I),10,XPY,YPN,ZPN,
1 THMAX,O,ZPN,I,TT,TT(KKK),.07,7200.)
350 DC 400 M=1,KKK
IF (TT(M).GE. TMIN) GO TO 500
400 CONTINUE
M=KKK
GO TO 900
500 TIMEEND = THMIN+TLEN
DO 600 J = M,KKK
IF (TIMEEND .LT. TT(J)) GO TO 700
600 CONTINUE

```



```

J=KKK+1
PRINT 9999,J,M,KKK,TMIN,TIMEND,TT(M),TT(J)
J = J-M
DO 800 I = 1,NURU
K = KK*(I-1)+M
800 CALL TEMPL (TT(M),VV3(K),VV4(K),VV2(K),J,V1(I),8,XPN,THMIN,YPN,
1 THMAX,ZPN,O,TT(M),TT(M)+TLEN,07,7200.)
1 TMIN=TMIN+TINC
IF(TMIN.LT.TMAX) GO TO 350
350 CALL PLOT
900 RETURN
FJPMAT(10X TIDECYCLE,7F10.0)
1000 FORMAT(10X TIDECYCLE,7F10.0)
1001 FORMAT(10X TWHVECTOR,7F10.0)
1002 FORMAT(10X READ2TT(,I2,)=,F10.0)
8000 FORMAT(10X NURUME,NEUT,VFC,HT PASSED TO THE SUBROUTINE T01:,/
9000 FORMAT(15I5,F10.0,F10.0,F10.0,/)
9999 FORMAT(3I10,4F10.0)
END

```



```

SUBROUTINE TIMPL (TIME, VELOC, DIREC, HEIGHT, MAXDIM, PLNAM , N, XPN,
1 THMIN, YPN, THMAX, SKIP, ZPN, NAROW, TEND, TST, MAXDIM, PLNAM , N, XPN,
1 INTEGR, SKIP
REAL*8 VI
DIMENSION TIME(MAXDIM), VELOC(MAXDIM), DIREC(MAXDIM), HEIGHT(MAXDIM),
1 PLNAM(4), NAM2(3), NAM3(3)
1 DATA NAM1//TIME,,IN,,SEC0,,INDS,,/
1 DATA NAM2//HEIGHT,,HT1,,N CM,,/
1 DATA NAM3//LAS,,L SA,,HA,,INSEN,, MOD,,EL,, SAN,,DIEG,,/
1 C(1) /X = (TEND-TST)/XPN
1 CALL PLT(0,0,3)
1 PX = X/2.-6./7.*H*FLNAT(N)
1 CALL SYMBOL(PX,-1.,H*2.*NA M3,0,0,37)
1 CALL SYMBOL(PX,-5.H*2.*NA M3,0,0,N)
1 CALL CXIS2 (TST,25,NA M1,15,TST,XPN,0.,1.,0.,TST,
1 XPN,XPN,6.*TEND,6,-1.,07)
1 ZERLIN = THM IN/YPN
1 CALL PLOT (X,ZERLIN,3)
1 CALL PLT(0,0,2)
1 CALL CXIS2 (TST,THMIN,NA M2,2)
1 270.= (TIME(C1)-TMIN,50.*THMAX,4,-1.,07) ,12,TST,XPN,THMIN,YPN,
1 DUM1=(HEIGHT(C1)-THMIN)/YPN
1 DUM2=(HEIGHT(C1)-THMIN)/YPN
1 CALL PLT(DUM1,DUM2,3)
1 DF 300.=1/MAXDIM
1 Y = (HEIGHT(C1)-THMIN)/XPN
1 X = (TIME(C1)-TST)/XPN
1 IF(SKIP.EQ.0) GO TO 210
200 CALL PLT(X,Y,2)
200 GO TO 215
210 CALL PLT(X,Y,2)
1 IF(ZPN.EQ.0) GO TO 200
215 DIST = VELOC(I)/ZPN
1 IF( DIFEC(I).GT.360.) GO TO 300 ,360.)*.0174532925
SI = DMOD(I)
CC = COS(SI)
SI = SIN(SI)
VX = DIST*S1+X
VY = DIST*S1+Y
CALL PLT(VX,VY,2)
CALL ARWP(I,(VX,VY,CO,S1))
1 IF(SKIP.EQ.0) GO TO 300
250 CALL PLT(X,Y,3)
250 CONTINUE
250 CALL PLT(0.,Y+6.,-3)
END

```



```

SUBROUTINE CXIS2 (X,Y,XNAME,ZINT,ZNUM,ZMAX,NC,NS,H)
      INTEGER Y1,XNAME
      REAL DIMENSION XNAME(2)
      DIMENSION THETA(2).0174532925
      SI = -SIN(XX)
      C0NT = COS(XX)
      CXINT = SI*ZINT/ZPN
      YTIC = SI*.05
      CO* .05
      YY = H*1.5
      XX = H*3.7 *H*FLOAT(NC)
      XLFT = -SI*YY-C0*XX
      YLFT = -C0*YY+SI*XX
      XLI = ZNUM*XINT
      YLI = ZNUM*YINT
      XY = H*5.7 *H*FLOAT(NLET)
      XTIT = -SI*YY-C0*XX
      YTTT = -C0*YY+SI*XX
      XX = (X-XMIN)/XPN
      YY = (Y-YMIN)/YPN
      CENT = ZVAL+(ZMAX-ZVAL)/2.
      XTIT = XX+XTIT+(CENT-ZVAL)/ZPN*CO
      YTIT = YY+YTIT+(CENT-ZVAL)/ZPN*SI
      Z=ZVAL
      ZZ=Z
      CALL PLOT (XX,YY,3)
      XLET = XLET+XX
      YLET = YLET+YY
      IF (NC.LE.0.CR.* ABS(ZZ-Z)*GT.*ZINT/2.) GO TO 200
      CALL NUMBER (XLET,YLET,H,ZZ,THETA,NS)
      XLET = XLET+XL
      YLET = YLET+YL
      ZZ = ZZ+ZINT
      CALL PLOT (XX,YY,3)
      XX = XX+XINT
      YY = YY+YINT
      Z = Z+ZINT
      CALL PLOT (XX,YY,2)
      IF (Z.GE.ZMAX) GO TO 500
      CALL PLOT (XX+XTIC,YY+YTIC,2)
      CALL PLOT (XX,YY,2)
      IF (Z.GT.CENT .AND. NLET.GT.0) GO TO 400

```



```
400 GO TO 100
CALL SYMBOL (XX,YY,3,YTIT,H*2.,XNAME,THETA,NLET)
CALL PLOT (XX,YY,3)
CENT =3.*ZMAX
GO TO 100
IF (INC.LE.0 .OR. ZZ.NE.Z) RETURN
500 CALL NUMBER (XLET,YLET,H,ZZ,THETA,NS)
RETUPN
END
```

```
SUBROUTINE ROT(X,Y,DEG,MM)
DIMENSION X(MM),Y(MM)
SI=DEG*0.01745329
CC=COS(SI)
SI=SIN(SI)
DO 100 I = 1,MM
```



```

X1=Y(I)
Y(I)=X1*CO + Y1*SI
Y(I)= Y1*CO - X1*SI
RETURN
END
100

```

```

SUBROUTINE ARWPT (X,Y,CO,SI)
REAL*8 V1
DATA H/.07/
YY = SI*H
XX = CO*H
XXX=YY*.25
YYY=XX*.25
XX=X-XX
YY=Y-Y
CALL PLOT (XX-XXX,YY+YYY,2)
CALL PLOT (XX+XXX,YY-YYY,2)
CALL PLOT (X,Y,2)
CALL PLOT (X,Y,3)
RETURN
END

```

```

SUBROUTINE TEST(NALL,NURU)
DIMENSION VA2(50,50),VA3(50,50),VD2(50),VD3(50),V2(50),V3(50),V4(5
10),VE2(50),VE3(50),TA(50)
REAL*8 NAME
REAL*8 VI
COMMON /C/ VB3(8),VB2(8),VC3(16),VC2,VF3,TB

```



```

REAL*8 ITATLE(12),*VALUES 0.,*F WATER,*,*HEIGHT *,*EASURE *,*DAN
1DCA,*,*LCULATED*,*CUTBAY(1,2),*VALUES 0.,*F CURREN*,*T
2DIEL*8 ITETL(12),*VALUES 0.,*F CURREN*,*T
1DCA,*,*LCULATED*,*CUTBAY(1,2),*VALUES 0.,*F EASURE *,*DAN
2DIEG*,*LCULATED*,*CUTBAY(1,2),*VALUES 0.,*F EASURE *,*DAN
READ(3) T,(V2(K),K=1,NURU),(V3(K),K=1,NURU),(V4(K),K=1,NURU)
DO 1 I=1,NALL
READ(3) T,PPRINT(600,T)
TA(I)=T,K=1,NURU
D2(I,K)=V2(K)
VA2(I,K)=V3(K)
VA3(I,K)=V4(K).GT.180.)VA3(I,K)=-VA3(I,K)
CONTINUE
21 DN 3 K=1,NURU
CALL REC1NAME
READ(21,I,NALL
TB=TA(I)
CALL REC2
VDC2(I)=VDC2
VD3(I)=VDC3
VE2(I)=VA2(I,K)
VE3(I)=VA3(I,K)
4 CONTINUE
PRINT 900,NAME
CALL DRAW(NALL,TA,VD2,1,0,LABEL,ITATLE,0.0,0.0,4,2,2,8,8,1,LAST)
PRINT 900,NAME
CALL PLOT(0.0,0.5,0.14,NAME,0.0,8)
CALL PLOT(0.0,-3)
CALL DRAW(NALL,TA,VE2,3,1,LEBEL,ITATLE,0.0,0.0,4,2,2,2,8,8,1,LAST)
PRINT 750,NAME
PRINT 900,NAME
CALL DRAW(NALL,TA,VD3,1,0,LABEL,ITETL,0.0,0.0,4,2,2,2,8,8,1,LAST)
PRINT 750,NAME
PRINT 900,NAME
CALL PLOT(0.0,0.0,3)
CALL SYMBOL(2.0,0.5,0.14,NAME,0.0,8)
CALL PLOT(0.0,-3)
CALL DRAW(NALL,TA,VE3,3,1,LEREL,ITETL,0.0,0.0,4,2,2,2,8,8,1,LAST)
PRINT 750,NAME
PRINT 900,NAME
3 CONTINUE

```



```

21 RETURN(A8) READED IN TEST DISC(3) T = *,F10.0, //)
690 FORMAT(*,NAME = *,A8,/)
750 FORMAT(*,LAST = *,I1,I)
900 END

```

```

SUBROUTINE PEC
COMMON/C/,VB2(8),VB3(16),VC2,VC3,TB
CENTRY REC1
READ 20,((VB2(I),I=1,6),VB2(7)
READ 20,((VB3(I),I=1,3),VB3(7)
READ 20,((VB3(I),I=4,6),VB3(7)
DO 10 I=1,10
ENTER PY DEC2
PER=24.*2600.
PI=3.1415927
TB=TB+39800.
SUM=0.
DO 1 L=1,3
ZTIDE=VB2(L)*COS((L)*2.*PI*TB/PER)+VB2(L+3)*SIN((L)*2.*PI*TB/PER)
1 SUM=SUM+ZTIDE
VC2=SUM
SUM=0.
DO 2 L=1,3
ZCUPR=VB3(L)*COS((L)*2.*PI*TB/PER)+VB3(L+3)*SIN((L)*2.*PI*TB/PER)
2 SUM=SUM+ZCUPR
VC3=SUM
10 RETURN
20 FORMAT( 8F10.5)
END

```



```

***** HANSEN PROGRAM PLOTS *****

GPP1 GRID POINTS PER INCH ON VECTOR AND HEIGHT PLOTS
VVS  VELOCITY VECTOR SCALE UNITS/INCH
WHS  WATER HEIGHT SCALE
ROTDEG RIGHT ANGLE FROM NORTH TO Y AXIS OF HANSE PROG GRID
NS   NO. OF STRIPES
X{1}, I=1,3 STRIP ORIGIN IN TENS OF GRID POINTS
NTHPT DISTANCE BETWEEN PLOTED POINTS
LAND DISTANCE FROM LAND

CARD 2 TITLE OF THE PROGRAM

CARD 3 MINIMUM VALUE OF WATER HEIGHT ON Y AXIS SCALE
      MAXIMUM VALUE OF WATER HEIGHT ON Y AXIS SCALE
      SCALE OF Y AXIS IN UNITS/INCH
      SCALE OF TIME AXIS IN UNITS/INCH
      NU.OF TIME STEPS TO BE SKIPPED OVER BETWEEN PLOTED PO

CARD 4 START TIME OF FIRST WATER HEIGHT VECTOR PLOT
      START TIME OF LAST WATER HEIGHT VECTOR PLOT
      TIME INTERVAL BETWEEN START TIMES
      TIME INTERVAL TO BE PLOTED
      TIME AXIS SCALE IN UNITS/INCH
      WATER HEIGHT SCALE UNIT/INCH (MIN. QMAX VALUES ARE
      THOSE ON THE SIDE CARD CYCLE)
      VECTOR SCALE IN UNITS/INCH

COMMON /A/ V1(60), V2(60), V3(60), V4(60), HTZ(53,30), RAD(53,30),
1ANG(53,30), Z(53,30), X(3), Y(3), NURU, ME, NE, NALL
REAL*8 V1
REWIND 2
REWIND 3
REWIND 4
REWIND 9
READ(9) HTZ, V1, NURU, ME, NE, NALL
PRINT 11, NALL, NURU

```



```

111 FORMAT (' READED( 9 ) HTZ,V1,NURU,ME,NE,NALL,      NALL = ',I3,',')
112 PRINT 1, { (HTZ(N,M),M=1,20),N=1,NE)
113 PRINT 7, { (HTZ(N,M),M=21,ME),N=1,NE)
114 PRINT 2, { V1(I),I=1,NURU)
115 PRINT 3, NE,ME
116 PRINT 4, NURU)
117 FORMAT (20F0.1)
118 FORMAT (10A10)
119 PRINT 1, HTZ('12;'), '12;, //)
120 FORMAT (10F6.1)
121 DO 5 K=1,1,NALL
122 READ (9) T,V2(I),I=1,NURU,V3(I),I=1,NURU,(V4(I),I=1,NURU)
123 WRITE (20,T,V2(I),I=1,NURU),(V3(I),I=1,NURU),(V4(I),I=1,NURU)
124 PRINT 20,T READED (9) T,V2,I=1,NURU,V3,I=1,AT,T=,V4,I,O,/ )
125 CONTINUE
126 DO 6 I=1,NALL
127 READ (9) T,VEC,HT,RAD,ANG,Z
128 WRITE (3) T,VEC,HT,RAD,ANG,Z
129 PRINT 12,T READED (9) T,VEC,HT,RAD,ANG,Z,      AT T = ,F10.0,/
130 PRINT 1, { (RAD(N,M),M=1,20),N=1,NE)
131 PRINT 7, { (RAD(N,M),M=21,ME),N=1,NE)
132 PRINT 1, { (ANG(N,M),M=1,20),N=1,NE)
133 PRINT 7, { (ANG(N,M),M=21,ME),N=1,NE)
134 PRINT 1, { (Z(N,M),M=1,20),N=1,NE)
135 PRINT 7, { (Z(N,M),M=21,ME),N=1,NE)
136 CONTINUE
137 ENDFILE 2
138 ENDFILE 3
139 REWIND 2
140 REWIND 4
141 REWIND 9
142 PRINT 190,NURU,ME,NE,HT,VEC,HT,BEFORE PASSED TO SUBROUTINE PO
143 PRINT 15,IS,F10.0,F10.0,/,/
144 CALL P01
145 CALL WATLV(NALL)
146 STOP
147 END

```



```

SUBROUTINE P01
COMMON/V1/V1(60),V2(60),V3(60),V4(60),HTZ(53,30),RAD(53,30),
1ANG(53,30),Z(53,30),X(3),TITLE(20),Y(3),NURU,ME,NE,HT
1DIMENSION SYMBOL(3),TITLE(20),VEC,HT
1,TITLE*8 V1
INTEGER*8 V1
REAL*8 V1
PARAMETER SYMBOL/*,*,-,/,_
DATA SYMBOL/,*,-,/,/
CALL PLOTS
READ 10001,GPPI,VVS,WHS,ROTDEG,NS,(X(I),Y(I)) I=1,3),NTHPT,LAND
PRINT 10001,GPPI,VVS,WHS,ROTDEG,NS,(X(I),Y(I)) I=1,3),NTHPT,LAND
READ 20000,(TITLE(I),I=1,20)
READ 20000,(TITLE(I),I=1,20)
READ 10002,THIN,THMAX,YPN,SKIP
READ 10002,THIN,THMIN,YPN,SKIP
READ 10002,THIN,TMAX,TINC,TLEN,YPN,YPN,ZPN
VVS=ZPN
WHS=YPN
SET UP X,Y GRID
DO 100 J=1,ME
DO 100 I=1,NE
XCOORD(I,J)=J
100 YCOORD(I,J)=I
DO 150 Y(I)=Y(I)
150 ROTATE ORIGIN POINTS
ROTATE ROT(X,Y,ROTDEG,NS)
ROTATE GRID POINTS
CALL ROT(XCOORD,YCOORD,ROTDEG,ME*NE)
READ(4,END=200)T,VEC,HT,RAD,ANG,Z
PRINT 200, T,LT,THMIN,OR,T.GT.TMAX) GO TO 270
IF(T.LT.THMIN) GO TO 270
TMIN=THMIN+TINC
GO TO 260
270 IF(T.EQ.TMAX) GO TO 260
260 PRINT 4000,((TITLE(MM),MM=1,20),T)
IF(VEC.EQ.0.) GO TO 300
CALL VECTOR(.07,SMBOL,NTHPT,GPPI,TITLE,LAND,ME,NE,HTZ,X,Y,NS,
1XCOORD,YCOORD,RAD,ANG,VVS,T)
300 IF(HT.EQ.0.) GO TO 200
PRINT 4000,((TITLE(MN),MN=1,20),T)
CALL WATIT(.07,SMBOL,NTHPT,GPPI,TITLE,LAND,ME,NE,HTZ,X,Y,NS,
1XCOORD,YCOORD,Z,WHS,T)
400 GO TO 200
900 CALL PLOTE
RETURN
1000 FORMAT(10X PARAMETER',F10.0,3F6.0,4X,I1,6F3.0,I3,4X,I1,/)
1001 FORMAT(10X PARAMETER',F10.0,3F6.0,4X,I1,6F3.0,I3,4X,I1,/)

```



```

1002 FORMAT(10X ,7F10.0)
12000 FORMAT(20A4) READED 4 T = ' ',F10.0,/)
30000 FORMAT(6H TIME F10.0,4H SEC)
30000 FORMAT(10H PLOT FOR ,20A4,F10.0)
40000 END

```

```

SUBROUTINE VECTOR( SSIZE, SYMBOL, NTHPT, GPP1, TITLE, LAND, ME, NE,
1 HTZ, YNS, XCOORD, VELOC, ANG, VVST, T)
1 DIMENSION HTZ(53,30), VELOC(53,30), ANG(53,30), XCOORD(53,30),
1 YCOORD(53,30), X(NS), Y(NS), TITLE(20), SYMBOL(3)
1 TATE(20)
1 REAL*8 V1, SYMBOL, TITLE, TATE
1 INTEGER I, J, K, NN
1 DO 400 I=1,NE
1 NN=MAX0(NE,ME)
1 CALL PLOT(0.,0.,3)
1 CALL PLOT(0.,2.,-3)
1 CALL SYMBOL(0.,0.,5,0.14,TITLE,0.0,80)
1 CALL NUMBER(8.5,-.5,0.14,T,0.0,0)
1 DO 300 J=1,NE
1 DO 300 K=1,NE
1 TOPOG=HTZ(J,K)
1 IF( TOPOG.EQ.0.) GO TO 300
1 IF( TOPOG.EQ.1.) AND. (MOD(J,NTHPT).NE.0 .OR. MOD(K,NTHPT).NE.0) )
160 TO 300
1 YJK=(YCOORD(J,K)-Y(I))/GPP1
1 IF( YJK.LT.0. OR. YJK.GT.15.) GO TO 300
1 XJK=(XCOORD(J,K)-X(I))/GPP1
1 IF( XJK.LT.-1.) GO TO 300
1 IF( XJK.LT.1.) 210,220,230

```



```

210 CONTINUE
211 CALL SYMBOL (XJK,YJK,SSIZE ,SYMBOL (2),0.,1)
212 GO TO 300
220 CONTINUE
221 CALL SYMBOL (XJK,YJK,SSIZE ,SYMBOL (1),0.,2)
230 IF (LAND.EQ.0) GO TO 260
J1=J-LAND
J2=J+LAND
K1=K-LAND
K2=K+LAND
DO 240 L=J1,J2
DO 240 M=K1,K2
1F (HTZ(L,M).EQ.-1.) GO TO 300
240 CONTINUE
DIST=VELOC(J,K)/VVS
TFT(ANG(J,K)*GT/360.) GO TO 300
SI=(450.*ANG(J,K))*.0174532925
CO=COS(SI)
SI=SIN(SI)
CALL PLOT (XJK,YJK,3)
XJK=XJK+DIST*CO
YJK=YJK+DIST*SI
CALL PLCT (XJK,YJK,2)
CALL ARWPT (XJK,YJK,CO,SI)
300 CONTINUE
400 CALL PLOT(0.,NN/GPPI+3.,-3.)
RETURN
END

```



```

SUBROUTINE WATHT (SSIZE, SYMBOL, NTHPT, GPP1, TATTLE, LAND, NE,
1 HTZ, XNS, YNS, ZNS, WHS)
1 DIMENSION SMBOL(3), TITLE(20), HTZ(20), X(NS), Y(NS), XCORD(53,30)
1, YCOORD(53,30), Z(53,30)
1 REAL*8 V1
1 INTEGER SMBOL, TITLE, TATTLE
1 DO 400 I=1,NS
1    NN=MAX0(NE,ME)
1    CALL PLOT(0.,0.,0.,3)
1    CALL PLOT(0.,2.,-3)
1    CALL SYMBOL(0.5,-.5,0.14,TATTLE,0.0,0,80)
1    CALL NUMBER(0.5,-.5,0.14,TITLE,0.0,0,80)
1    DO 300 J=1,NE
1       DO 300 K=1,ME
1          TOPOG=HTZ(J,K)
1          IF( TOPOG.EQ.0.) GO TO 300
1          IF( TOPOG.EQ.1.) AND.(MOD(J,NTHPT).NE.0 .OR. MOD(K,NTHPT).NE.0) )
1             160 TO 300
1             YJK=(YCOORD(J,K)-Y(I))/GPP1
1             IF( YJK.LT.0. OR. YJK.GT.15.) GO TO 300
1             XJK=(XCOORD(J,K)-X(I))/GPP1
1             IF( XJK.LT.-1.) GO TO 300
1             IF( XJK.GT.1.) 210, 220, 230
1             CONTINUE
1             CALL SYMBOL(XJK,YJK,SSIZE,SYMBOL(2),0,1)
1             GO TO 300
1             CONTINUE
1             CALL SYMBOL(XJK,YJK,SSIZE,SYMBOL(1),0,2)
1             GO TO 300
1             IF( LAND.EQ.0) GO TO 260
1             J1=J-LAND
1             K1=K-LAND
1             J2=J+LAND
1             K2=K+LAND
1             DO 240 N=K1,J2
1                DO 240 M=N,K2
1                   IF( HTZ(L,M).EQ.-1.) GO TO 300
1                   CONTINUE
1                   CALL SYMBOL(XJK,YJK,SSIZE,SYMBOL(3),0,2)
1                   IF( Z(J,K).EQ.0.) GO TO 300
1                   CALL PLOT(XJK,YJK,Z(J,K),WHS)
1                   YJK=YJK+Z(J,K)/WHS
1                   CALL PLOT(XJK,YJK,2)
1                   UP=1
1                   IF( Z(J,K).LT.0.) UP=-1.
1                   CALL ARWPT(XJK,YJK,0.,UP)
1                   CONTINUE
1             300

```



```
400 CALL PLOT(0.,NN/GPPI+3.,-3.)
      RETURN
      END
```

```
SUBROUTINE ROT(X,Y,DEG,MM)
DIMENSION X(MM),Y(MM)
REAL*8 V1
SI=DEC*0.01745329
CO=COS(SI)
SI=SIN(SI)
DO 100 I = 1,MM
X1=X(I)
Y1=Y(I)
X(I) = X1*CO + Y1*SI
Y(I) = Y1*CO - X1*SI
100 RETURN
      END
```

```
SUBROUTINE ARWPT (X,Y,CO,SI)
REAL*8 V1
DATA H/.06/
YY = SI*H
XX = CO*H
XXX = YY**.25
YYY = XX**.25
XXX = X-XX
YY = Y-YY
CALL PLOT (XX-XXX,YY+YYY,2)
CALL PLOT (XX+XXX,YY-YYY,2)
CALL PLOT (X,Y,2)
CALL PLOT (X,Y,3)
RETURN
      END
```



```

SUBROUTINE WATLV(NALL)
DIMENSION Z(58,40),CL(11)
LOGICAL*1 LTG(3)
REAL*8 TITLE(12),WATER,HE,CON,TCURS,L.SALAS
100 BAY()
100 TIME()
200 LTG(1) = .TRUE.
LTG(2) = .TRUE.
LTG(3) = .TRUE.
CL(1) = -125.
DC 200 KKK=211
CL(KKK)=CL(KKK-1)+25.
200 CONTINUE
DO 100 KK=1,NALL
READ(3) T,Z
CALL CCNTUR(Z,58,40,58,CL,11,TITLE,8,8,LTG)
100 CONTINUE
RETURN

```


BIBLIOGRAPHY

1. U.S. Army Engineer District, Los Angeles (Preliminary) Summary Report. San Diego Bay Model Study. Hydraulic Model Study. U. S. Army Engineer Waterways Experiment Station. Corps of Engineers, Vicksburg, Mississippi, June 1971.
2. Bowden, K. F., "The Mixing Processes in a Tidal Estuary," J. Air and Water Pollution, Pergamon Press 1963, Vol. 7, pp. 343-356.
3. Doodson, A. T., and Warburg, H. D., Admiralty Manual of Tides, Her Majesty's Stationery Office, 1941.
4. Dr. Laevastu, T., and Rabe, K., A Description of the EPRE Hydrodynamical-Numerical Model, U. S. Navy Environmental Prediction Research Facility, Technical Paper No. 3 - 72, March 1972.
5. Dr. Laevastu, T., and CDR Hamilton, G. D., Computation of Flushing and Dispersion of Pollutants in the Pearl Harbor and in San Diego Bay with Hydrodynamical-Numerical Models, U. S. Navy Environmental Prediction Research Facility, Monterey, Calif. 1972.
6. Dr. Laevastu, T., and Stevens, P., Application of Numerical-Hydrodynamical Model in Ocean Analysis/Forecast. Rrt 1; The Single-Layer Models of W. Hansen, Fleet Numerical Weather Central, Monterey, Calif., Technical Note No. 51, July 1969.
7. Dr. Laevastu, T., and CDR Hamilton, G. D., Reproduction of Current in the Strait of Florida with a Hydrodynamical-Numerical (HM) Model, U. S. Navy Environmental Prediction Research Facility, Monterey, Calif., April 1972.
8. Ramming, H. G., Investigation of Motion Processes in Shallow Water Areas and Estuaries, Institut Für Meereskunde Der Universität, Hamburg, Proceedings Symp. on Coastal Geodesy, München, July 1970, pp. 439-452.
9. Ramming, H. G., Hydrodynamical-Numerical Investigations and Horizontal Dispersion of Seston in the River Elbe, Institut Für Meereskunde Der Universität Hamburg, Report No. 18, Feb. 1971, 72 pgs. 31 figs.

10. Simmons, H. S. and Herrmann, F. A., Influences of Proposed Second Entrance on the Flushing Characteristics of San Diego Bay, Calif., FAO Technical Conference on Marine Pollution and its Effects on Living Resources and Fishing, Rome, Italy, 9-18 December 1970.
11. Sverdrup, H. Q., Johnson, M. W., and Fleming, R. H., The Oceans, Prentice-Hall, Inc. 1942.
12. Von Arx, W. S., An Introduction to Physical Oceanography, Addison Wesley Publishing Co. Inc. 1962.

INITIAL DISTRIBUTION LIST

	No. copies
1. Defense Documentation Center Cameron Station Alexandria, Virginia. 22314	2
2. Library, Code 0212 Naval Postgraduate School Monterey, California 93940	2
3. Department of Oceanography Naval Postgraduate School Monterey, California 93940	3
4. CDR Leopoldo Salas R. Dirección de Hidrografía y Navegación Apartado 6745 Caracas, Venezuela	5
5. Escuela Naval de Venezuela Escuela de Posgrado Meseta de Mamo, Catia la Mar Venezuela	1
6. Dr. Edward B. Thornton Department of Oceanography Naval Postgraduate School Monterey, California 93940	5
7. Dr. Taivo Laevastu Environmental Prediction Agency Fleet Numerical Weather Center Monterey, California 93940	2
8. Lt. Jose Saldanha Instituto Hidrografico Ministerio de Marinha Lisboa, Portugal	1
9. Mr. F. A. Herrmann Estuaries Branch U. S. Army Waterways Experiment Station Corps of Engineers, PO Box 631 Vicksburg, Mississippi 39180	2
10. Mr. Edward Koehm Engineering Division Corps of Engineers 300 N. Los Angeles Los Angeles, Calif.	1

11. Mr. George M. Fisackerly 1
Harbor Entrance Section
U.S. Army Corps of Engineers
P.O. Box 631
Vicksburg, Mississippi 39180
12. Mr. Stuart L. Kufferman 1
College of Marine Studies
University of Delaware
Newark, Delaware 19711
13. Mr. Dennis F. Polio 1
College of Marine Studies
University of Delaware
Newark, Delaware 19711
14. Mr. Sheldon M. Lazanoff 1
Fleet Numerical Weather Central
Monterey, California 93940
15. Dr. J. A. Galt 1
Department of Oceanography
Naval Postgraduate School
Monterey, California 93940
16. Dr. D. J. Baumgartner 1
Federal Water Quality Administration
Northwest Region
Pacific Northwest Water Laboratory
200 Southwest 35th street
Corvallis, Oregon 97330
17. Dr. R. G. Dean 1
Coastal and Oceanographic Engineering Department
University of Florida
Gainesville, Florida 32601
18. Environmental and Fishery Forecasting Center 1
National Marine Fisheries Service
National Oceanic and Atmospheric Administration
U. S. Department of Commerce
C/O Fleet Numerical Weather Central
Monterey, California 93940
19. Dr. John Huth 1
Special Assistant to Director of Navy Laboratory
Code 03⁴
Naval Ship System Command
Washington, D. C. 20350

20. LCDR Charles A. Farrel 1
Ocean Services
Naval Undersea Research and Development Center
San Diego, California 92132
21. CDR Richard D. Fasing 1
Pollution Control Office
11th Naval District
San Diego, California 92132
22. CDR Joseph D'Emidio 1
OP 45
Director of the Environmental Protection Div.
Pentagon Building, Room 4B516
Washington, D. C. 20350
23. Mr. R. L. Reisbig 1
Mechanical Engineering School
University of Missouri
Rolla, Mo. 65401
24. Mr. H. G. Ramming 1
Institut für Meereskunde
Universität Hamburn
Hamburg, Germany
25. Dr. W. Hansen 1
Institut für Meereskunde
Universität Hamburg
Hamburg, Germany
26. Director Instituto Nacional de Canalizaciones 1
Av. Andrés Bello
Edificio Atlantic 6^o
Los Palos Grandes
Caracas, Venezuela
27. Division de Ingeniería 1
Insituto Nacional de Canalizaciones
Av. El Milagro
Maracaibo, Venezuela
28. Departamento de Oceanografía 1
Universidad Simón Bolivar
Caracas, Venezuela
29. Departamento de Oceanografía 1
Universidad de Oriente
Cumaná, Venezuela

30. Director 1
National Oceanic and Atmospheric Administration
U.S. Department of Commerce
Washington, D.C. 20235
31. Division of Oceanography 1
Environmental Science Service Administration
Silver Springs, Maryland 20910
32. Commanding Officer 1
Office of Naval Research Branch Office
Box 39
Fleet Post Office
New York 09510
33. Chief of Naval Research 1
Ocean Science and Technology Group
Code 480
Office of Naval Research
Washington, D.C. 20360
34. Chief of Naval Research, Code 480 1
Attn: Dr. Osteno
Office of Naval Research
Washington, D.C. 20360
35. Oceanographer of the Navy 1
Office of the Oceanographer of the Navy
732 North Washington St.
Alexandria, Virginia 22314
36. Director 1
Coastal Engineering Research Center
Corps of Engineers, U.S. Army
5201 Little Falls Road, N.W.
Washington, D.C. 20315
37. Commandant 1
U.S. Coast Guard
Headquarters
Washington, D.C. 20591
38. Director, Naval Research Laboratory 1
Attn: Technical Information Officer
Washington, D.C. 20390
39. Director 1
Office of Naval Research Branch Office
1030 East Green St.
Pasadena, California 91101

40. Sr. Presidente 1
Comite de Hidrografía
Instituto Panamericano de Geografía e Historia
Ex-Arzobispado 29
Mexico 18, D.F. Mexico
41. Dirección de Hidrografía y Navegación 1
Camandancia General de la Marina
Apartado 6745
Caracas, Venezuela
42. LTjg Rafael Steer 1
Calle 70. Nº 59-15
Barranguilla, Colombia
43. Dr. Noel Boston 1
Department of Oceanography
Naval Postgraduate School
Monterey, California 93940
44. CDR Karl L. Schriner 1
Headquarters, Fifth Naval District
Norfolk, Virginia 23511

Security Classification

DOCUMENT CONTROL DATA - R & D

(Security classification of title, body of abstract and indexing annotation must be entered when the overall report is classified)

ORIGINATING ACTIVITY (Corporate author)

Naval Postgraduate School
Monterey, California 93940

2a. REPORT SECURITY CLASSIFICATION

Unclassified

2b. GROUP

REPORT TITLE

Comparison of Numerical and Hydraulic Oceanographic Prediction Models

DESCRIPTIVE NOTES (Type of report and, inclusive dates)

Master's Thesis; September 1972

AUTHOR(S) (First name, middle initial, last name)

Leopoldo Salas R.

EPORT DATE September 1972	7a. TOTAL NO. OF PAGES 141	7b. NO. OF REFS 12
CONTRACT OR GRANT NO.	9a. ORIGINATOR'S REPORT NUMBER(S)	
PROJECT NO.	9b. OTHER REPORT NO(S) (Any other numbers that may be assigned this report)	

DISTRIBUTION STATEMENT

Approved for public release; distribution unlimited.

SUPPLEMENTARY NOTES	12. SPONSORING MILITARY ACTIVITY Naval Postgraduate School Monterey, California 93940
---------------------	---

ABSTRACT

The Hydro-Numerical Prediction Model developed by Hansen is applied to San Diego Bay, and the results compared both with the hydraulic model and the real data obtained by field measurements. This allows one of the few good comparisons between numerical and hydraulic models for the prediction of actual conditions.

The bay was divided into two sections that were run separately in order to obtain the desirable spatial resolution. This division required solving the problems of proper tuning and matching techniques between both portions. The solution involved the addition of an appended pseudo-bay to the first section of the model in order to compensate for the correct tidal prism. The effects of a proposed second open entrance in the southern part of the bay were studied. This resulted in an increase of flushing in the southern portion of the bay but caused the currents in the center of the bay to be small which decreased dispersion in the central portion of the bay. In general, both models produced similar and reliable results, but there was a considerable reduction of cost and time with the numerical model.

KEY WORDS

LINK A LINK B LINK C

ROLE WT ROLE WT ROLE WT

Numerical Oceanographic Model

Hydraulic Model

San Diego Bay

26 AUG 74
20 JUN 75
29 JAN 80

23452
22660
26406

Thesis

141363

S1526 Salas Römer

c.1 Comparison of numerical and hydraulic oceanographic prediction models..

26 AUG 74
20 JUN 75
29 JAN 80

23452
22660
26406

Th

S1

Thesis

141363

S1526 Salas Römer

c.1 Comparison of numerical and hydraulic oceanographic prediction models..

thesS1526
Comparison of numerical and hydraulic oc



3 2768 001 97694 7
DUDLEY KNOX LIBRARY